EFFECT OF CLIMATE CHANGE ON THE PRECIPITATION PATTERNS IN THE HOUSTON METROPOLITAN AREA

A Thesis

by

ZHENGCONG YIN

Submitted to the Office of Graduate and Professional Studies of
Texas A&M University
in partial fulfillment of the requirements for the degree of

MASTER OF SCIENCE

Chair of Committee,	Francisco Olivera
Committee Members,	Anthony T. Cahill
	Steven M. Quiring
Head of Department,	Ronald Adam Kaiser

December 2016

Major Subject: Water Management and Hydrological Science

ABSTRACT

Because extreme precipitation poses a potential threat to local water resource systems, this study predicts and analyzes future precipitation in the Houston area. The Modified Bartlett-Lewis Rectangular Pulse (MBLRP) model was utilized to generate stochastic precipitation based on source data. Observed precipitation of seven rainfall stations around the Houston area and daily precipitation data extracted from Global Circulation Model (GCM) were used as source data.

With respect to the statistics of precipitation, the MBLRP model reproduced the mean, variance and probability of zero rainfall well, but lag-1 autocorrelation coefficient was not reproduced well. With low frequency events, the MBLRP model tended to overestimate extreme precipitation. As for the duration curve, the MBLRP model performed well for reproducing precipitation events at probabilities larger than 1%, but it had a limited ability to reproduce the low frequency events. Compared to the MBLRP model, the GCM exhibited more uncertainty because of a tendency to systematically underestimate the amount of precipitation and annual hourly extreme value for different accumulation levels. The usage of the statistics relationship equations of observed precipitation for different accumulation levels introduced more uncertainty into the whole process, namely overestimation of precipitation. Among the three sources of uncertainty: the MBLRP method, the GCM, and the statistics relationship equations, the GCM, which represents the source of data, introduced more uncertainty into the prediction results.

Climate change has some impact on precipitation in the future in terms of changes in rainfall frequency and mean amount of rainfall. The duration curves indicate that the amount of future daily precipitation is larger than the present under the same probabilities. The annual hourly extreme precipitation largely depends on the local precipitation pattern and the selected model rather than the effect of climate change. Both the duration curve analysis and the frequency analysis show that the effect of climate change on precipitation is relatively small in the Houston area.

This study provides a framework for estimating the effect of climate change on precipitation, which can be applied to any area with historic data available.

DEDICATION

This thesis is dedicated to my supportive and loving family

and is in memory of my grandfather and grandmother.

ACKNOWLEDGEMENTS

Firstly, I would like to express my sincere gratitude to my adviser, Dr. Francisco Olivera, for his patience, support, and encouragement for my study and research. His guidance, attitude and enthusiasm teaches me a lot. I also gratefully acknowledge my committee members, Dr. Anthony T. Cahill, and Dr. Steven M. Quiring, for their suggestions and support to my research.

Secondly, I would like to thank my father, my mother and my whole family. Their support and encouragement helped me to overcome all the difficulties I met. I also would like to thank my girlfriend and her family for their support.

Last but not least, I would like to thank the Water Management and Hydrologic Science family for having amazing faculty and students. Finally, thanks to all my friends here and in China. Without their help, my research have never gone so smooth.

NOMENCLATURE

GCMs – General Circulation Models

GEV II – Generalized Extreme Value distribution of Type II

ISPSO – Isolated Speciation-Based Particle Swarm Optimization

MLBRP – Modified Bartlett-Lewis Rectangular Pulse Model

NCDC – National Climatic Data Center

RCP – Representative Concentration Pathway

TSHA – Texas State Historical Association

TABLE OF CONTENTS

Page

LIST OF FIGURES

Page

LIST OF TABLES

Page

1. INTRODUCTION

Precipitation plays an important role in hydrology and directly impacts the fields of agriculture and insurance, and the operation of water resources. Extremely high rainfall results in floods, and extremely low rainfall leads to drought. Therefore, prediction and analysis of precipitation are very important for water resource systems design. The resiliency and the vulnerability of water resource systems need to be evaluated in scenarios of extreme hydrologic events. However, predicting and analyzing extreme precipitation are not as easy as expected. Analysis of extreme precipitation requires historic time series data. Hence, uncertainties of both predicting methodology and sources of the historic data are involved in this process.

Rainfall prediction methods can be classified as statistical, stochastic, Artificial Neural Network or numerical prediction. The methodology that uses a stochastic model to generate rainfall time series has been applied to water management for decades (Fiering, 1967). They are widely used in the field of hydrology due to their capability to generate long-term precipitation time series. Generating long-term synthetic weather series is accomplished by models that can accurately simulate the observed properties of weather. Statistics of weather properties can be used for parameter calibration (Wilks and Wilby, 1999). However, several studies have pointed out that seasonality, region, and weather type have their own impacts on the prediction results. White, Franks, and McEvoy (2015) found that the forecasting of long-term extreme rainfall would benefit extended-range flood prediction, but the accuracy of current long-term, especially

subseasonal to seasonal rainfall prediction, needs improvement. Fowler, Kilsbv, and O'Connell (2000) developed a model that considers the regional weather type in order to simulate long-term hourly precipitation. However, their research illustrated that it would be better to take into account the variability of weather types and drought of various return periods. In order to take into account the effect of location and climate on precipitation, the parameters were calibrated by data from the 3,444 National Climate Data Center (NCDC) rain gauges (Kim, Olivera, and Cho, 2013). The Modified Bartlett-Lewis Rectangular Pulse (MBLRP) model used in this study is a Poisson cluster rainfall model. Its successful application to different rainfall characteristics in various locations is well documented (Isham et al., 1990; Verhoest et al., 1997). It has been proven that extreme rainfall can be reproduced by the MBLRP model at an hourly scale (Kim, Olivera, and Cho, 2013). However, the performance of the model at a sub-hourly time scale is poor when compared to an hourly time scale (Samuel, 1999).

In addition, under climate change conditions, more uncertainties are introduced, such as changes in precipitation patterns. Several studies have been conducted to evaluate the effect of climate change on precipitation. Pendergrass, Lehner, Sanderson, and Xu (2015) investigated the rate of change of extreme precipitation under four emission scenarios. The results showed that in most models extreme precipitation did not depend on an emissions scenario. Alexander, Scott, Mahoney and Barsugli (2013) used a regional climate model to simulate future summer precipitation in Colorado. They suggested that extreme precipitation events were difficult to detect and may not occur everywhere. The ecological effect of climate change in Puerto Rico was evaluated using

12 statistically downscaled models that were included in General Circulation Models (GCMs) (Khalyani et al., 2016). The results indicated that climate change would cause a loss of rain in a subtropical zone. Thus, the effect of climate change on precipitation varies by location. Mehrotra et al. (2003) pointed out that model selection causes uncertainty when using GCMs. They assessed future precipitation using multiple GCMs in India. The results showed that the outcomes of future precipitation were largely dependent on GCM model selection.

The present study provides a framework for estimating the effect of climate change on future precipitation. This framework can be applied to any area with historic data available. One source of data is observed rainfall station data, and the other one is GCMs. Similar to the previous studies, the parameters for the MBLRP method were calibrated by the local precipitation data to capture the characteristics of the regional and seasonal weather. 15-, 30-minute, 1-, 3-, 6-, 12-, and 24-hour accumulation intervals of stochastic precipitation were generated in order to obtain the sub-daily and daily precipitation events in response to climate change.

2. STUDY AREA AND DATA

2.1 Study Area

The study area consists of the metropolitan Houston area in Montgomery County, Harris County, Fort Bend County, and Galveston County. The climate of this area is classified as humid subtropical. The annual precipitation in this area is about 49.77 inches. The highest daily rainfall in the Houston area, which was recorded on October, 1994, was 14.35 inches (TSHA, 2016). On October 25, 1984, Houston Intercontinental Airport measured as much as 10 inches (USGS 1998). The Houston area has a total area of 601.7 square miles (1,558 km^2) — 579.4 square miles (1,501 km^2) of it is land, and 22.3 square miles (58 km^2) of it is water. Surface water in the Houston region consists of lakes, rivers, and an extensive system of bayous and manmade canals that are part of the rainwater runoff management system. Approximately 25%-30% of Harris County lies within the 100-year flood plain (Oguz et al., 2007).

2.2 Data

2.2.1 Observed rainfall station

The locations of rainfall stations were selected to be around the Houston area and were covered by the grid of the GCM. Seven stations that have 15-minute precipitation data available were selected to conduct the historic precipitation analysis (NCDC, 2014). The locations of each selected stations are displayed in Figure 1. The 15-minute precipitation data for the 1984-2009 period were obtained from these stations. All seven stations were used to conduct the duration curve analysis. COOP: 417594 rainfall station

(95.7552 ° W, 29.5838 ° N) was selected to conduct the frequency analysis of the annual peak precipitations, since it had more than 30 years' hourly rainfall data.

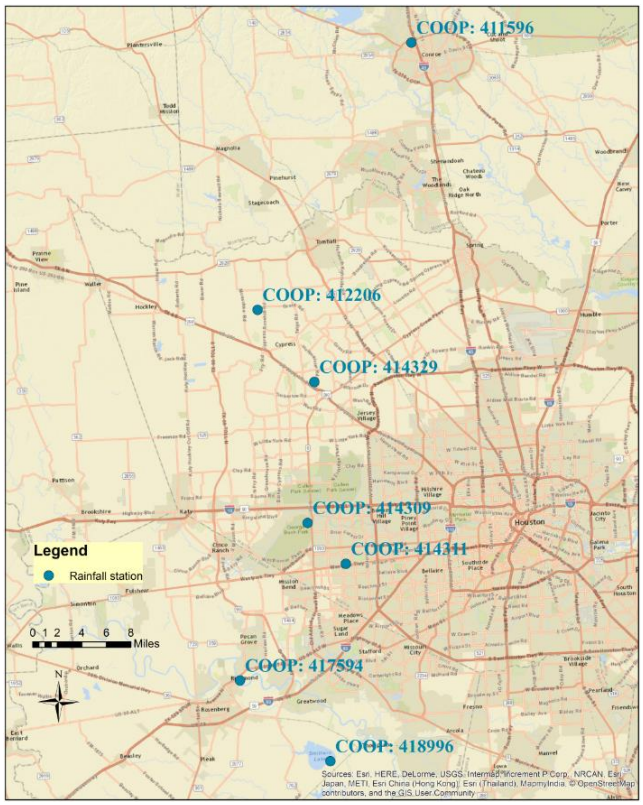

Figure 1 The locations of selected rainfall stations.

2.2.2 GCM

A GCM was used as the data source of past and future precipitation. The selected climate scenario of the GCM was RCP6.0. "RCP6.0 is a stabilization scenario in which total radiative forcing is stabilized shortly after 2100, without overshoot, by the application of a range of technologies and strategies for reducing greenhouse gas emissions" (Fujino et al. 2006; Hijioka et al. 2008). In this study, gfdl-cm3.1 model,

miroc-esm.1 model, and miroc-esm-chem.1 model were used to take into account the variance of different models. The average of annual precipitation increases as these three models projected in RCP6.0 scenario. However, it may be a limitation of the study that only three of the 13 models in scenario RCP6.0 were used.

3. METHODOLOGY

The purpose of this study is to estimate the effect of climate change on precipitation in the metropolitan Houston area. To achieve this goal, several tasks were accomplished.

3.1 Obtain Statistics of Precipitation Data

3.1.1 Observed precipitation

The 15-minute observed precipitation data in the 1984-2009 period were obtained from seven rainfall stations. The precipitation within one year contains the variability caused by seasonality. Because lumping one year of time series data into a single value could oversimplify the effect of seasonality, the time series were generated by aggregating different years' precipitation data that correspond to the same month to take into account the seasonality effect. Thus, the seven rainfall stations had 84 time series. In order to avoid the effects of missing values on the precipitation statistics, the missing values in the time series were processed as follows: (1) If the percentage of missing values of one month was larger than 10%, then the time series of the month were removed and (2) The missing value was replaced with the average of the two existing values before and after the missing value, if the percentage of missing values of one month were smaller than 10%. The assumption is that the processing of the missing values in the observed precipitation time series would not affect the characteristics of the statistics of precipitation. The duration of the remaining time series for each month and each station was summarized in Table 1. For each time series, the mean, variance, lag-1

autocorrelation coefficient, and probability of zero rainfall were calculated at 15-, and 30-minutes; 1-, 3-, 6-, 12-, and 24-hour accumulation levels. In total, there were 28 statistics for each month.

Table 1 The duration of the remaining time series for each month and each station

Station ID	**Station Name**	**Jan.**	**Feb.**	**Mar.**	**Apr.**	**May**	**Jun.**
COOP:411956	CONROE TX US	16	12	11	12	7	13
COOP:412206	CYPRESS TX US	5	4	6	6	5	3
COOP:414309	HOUSTON ADDICKS TX US	8	5	9	6	8	8
COOP:414311	HOUSTON ALIEF TX US	9	7	12	10	10	8
COOP:414329	HOUSTON SATSUMA TX US	4	3	4	3	1	3
COOP:417594	RICHMOND TX US	3	2	6	7	2	5
COOP:418996	THOMPSONS 3 WSW TX US	5	6	4	10	3	4
Station ID	**Station Name**	**Jul.**	**Aug.**	**Sep.**	**Oct.**	**Nov.**	**Dec.**
COOP:411956	CONROE TX US	16	18	16	14	10	13
COOP:412206	CYPRESS TX US	4	3	4	5	6	4
COOP:414309	HOUSTON ADDICKS TX US	9	8	7	10	13	8
COOP:414311	HOUSTON ALIEF TX US	8	8	11	10	10	8
COOP:414329	HOUSTON SATSUMA TX US	3	2	2	1	2	2
COOP:417594	RICHMOND TX US	7	8	1	2	5	1
COOP:418996	THOMPSONS 3 WSW TX US	8	8	4	8	6	3

The equations of the precipitation statistics were

$$\bar{P} = \frac{1}{j}\sum_{i=1}^{j} P_i \quad (1)$$

$$\mathrm{Var}(P) = \frac{1}{j-1}\sum_{i=1}^{j}(P_i - \bar{P})^2 \quad (2)$$

$$R(1) = \frac{1}{j-1} \frac{\sum_{i=1}^{j-1}(P_i - \bar{P})(P_{i+1} - \bar{P})}{\mathrm{Var}(P)} \quad (3)$$

$$P0 = \frac{(Number\ of\ P_i = 0)}{j} \quad (4)$$

where j is number of time intervals, i represents a certain accumulation interval, and P is the amount of precipitation. Once the statistics of the observed precipitation at seven accumulation levels were calculated, the relationship equations of these four statistics of the observed precipitation between 15-, and 30-minutes, 1-, 3-, 6-, and 12-hour accumulation intervals and the observed daily precipitation statistics were established. In total, 24 relationship equations (Table 2) were established (6 equations × 4 statistics).

Table 2 The relationship equations for the statistics of each accumulation levels based on daily precipitation statistics

Accumulation Level	**15-Minute**	**30-Minute**
Mean	$y = 0.0104x$ $R^2 = 1$	$y = 0.0208x$ $R^2 = 1$
Variance	$y = 0.0009x^{0.7078}$ $R^2 = 0.668$	$y = 0.0032x^{0.7718}$ $R^2 = 0.7565$
Lag-1	$y = -2.2952x^2 + 0.5985x + 0.5728$ $R^2 = 0.0327$	$y = -2.7727x^2 + 0.6306x + 0.4912$ $R^2 = 0.0561$
Probability of zero rainfall	$y = 0.9042e^{0.1008x}$ $R^2 = 0.2609$	$y = 0.8689e^{0.1413x}$ $R^2 = 0.3142$
Accumulation Level	**1-Hour**	**3-Hour**
Mean	$y = 0.0417x$ $R^2 = 1$	$y = 0.125x$ $R^2 = 1$
Variance	$y = 0.0106x^{0.8397}$ $R^2 = 0.8361$	$y = 0.0639x^{0.9364}$ $R^2 = 0.9263$
Lag-1	$y = -0.2177x^2 + 0.1262x + 0.4054$ $R^2 = 0.0034$	$y = 0.1556x^2 + 0.0688x + 0.2451$ $R^2 = 0.0054$
Probability of zero rainfall	$y = 0.8271e^{0.1913x}$ $R^2 = 0.3889$	$y = 0.728e^{0.3219x}$ $R^2 = 0.5904$

Table 2 Continued.

Accumulation Level	6-Hour	12-Hour
Mean	$y = 0.25x$ $R^2 = 1$	$y = 0.5x$ $R^2 = 1$
Variance	$y = 0.1707x^{0.9711}$ $R^2 = 0.9596$	$y = 0.407x^{0.9697}$ $R^2 = 0.971$
Lag-1	$y = -0.1554x^2 + 0.1799x + 0.1842$ $R^2 = 0.0168$	$y = -0.1726x^2 + 0.3297x + 0.1082$ $R^2 = 0.0685$
Probability of zero rainfall	$y = 0.6288e^{0.4714x}$ $R^2 = 0.7641$	$y = 0.4933e^{0.7147x}$ $R^2 = 0.9051$

where x represents the value of the statistic at the 24-hour accumulation level. And y represents the value of the statistic at the expected accumulation levels.

3.1.2 Current GCM precipitation

The current precipitation data were obtained from a GCM with the climate scenario of RCP6.0 and the selected three models. Seven daily precipitation data from 1950 to 2000, corresponding to each rainfall station, were extracted from the GCM individually. Each time series were processed by aggregating 51 years' rainfall data that corresponded to the same month to take into account the effect of seasonality. Then, the mean, variance, lag-1 autocorrelation coefficient, and probability of zero rainfall at 24-hour accumulation intervals were calculated. Since the time series of sub-daily past rainfall are not available, the statistics of the sub-daily were obtained using the statistics relationship equations (Table 2). Then, these four statistics of the current GCM precipitation at 15-, and 30-minutes, 1-, 3-, 6-, 12-, 24-hour accumulation levels were calculated with the assumption that the relationship for the statistics of the future precipitation remains the same as the observed one. In total, among the seven rainfall

stations, each station has seven accumulation levels, and four statistics were calculated for each accumulation level under each model.

3.1.3 Future GCM precipitation

Future Daily Precipitation data were obtained from GCMs. The climate scenario and the selected three models were the same as what was used for the current GCM precipitation. Seven daily precipitation from 2040 to 2099, corresponding to each rainfall station, were extracted from the GCM individually. The principle of calculating the statistics of the current GCM precipitation was applied to get the statistics of future precipitation. Like current precipitation, 196 statistics of GCM future precipitation were calculated for each model (7 rainfall stations × 4 statistics × 7 accumulation levels).

3.2 Parameter Calibration of the MLBRP Model

In this study, the MBLRP model (Rodriguez-Iturbe et al., 1988) was selected as the stochastic rainfall generator. It is widely used (Onof et al., 2000; Koutsoyiannis and Onof, 2001) due to its robust model assumptions that are based on physical processes of rainfall occurrences (Olsson and Burlando, 2002). In order to generate the simulated precipitation time series, the MLBRP simulator needs six input parameters: λ, ν, α, μ, $\phi = \gamma/\eta$, and $\kappa = \beta/\eta$. These six input parameters were obtained from solving four statistics equations of mean, variance, probability of zero rainfall, and lag-1 autocorrelation coefficient (Rodriguez-Iturbe et al., 1988), at 15-, and 30-minutes, 1-, 3-, 6-, 12-, and 24-hour accumulation levels. The equations of these four statistics at a certain accumulation T are:

$$\mathrm{E}\left[Y_t^{(T)}\right] = \lambda\mu\mu_c\frac{\nu}{\alpha-1}T \quad (5)$$

$$\mathrm{Var}\left[Y_t^{(T)}\right] = \frac{2\nu^{2-\alpha}T}{\alpha-2}\left(\mathrm{k}_1 - \frac{\mathrm{k}_2}{\phi}\right) - \frac{2\nu^{3-\alpha}}{(\alpha-2)(\alpha-3)}\left(\mathrm{k}_1 - \frac{\mathrm{k}_2}{\phi^2}\right) + \frac{2}{(\alpha-2)(\alpha-3)}\left[\mathrm{k}_1(T+\nu)^{3-\alpha} - \frac{k^2}{\phi^2}(\phi T+\nu)^{3-\alpha}\right] \quad (6)$$

$$\mathrm{Cov}\left[Y_t^{(T)}, Y_{t+s}^{(T)}\right] = \frac{\mathrm{k}_1}{(\alpha-2)(\alpha-3)}\{[T(s-1)+\nu]^{3-\alpha} + [T(s+1)+\nu]^{3-\alpha} - 2(Ts+\nu)^{3-\alpha}\} + \frac{\mathrm{k}_2}{\phi^2(\alpha-2)(\alpha-3)}\{2(\phi Ts+\nu)^{3-\alpha} - [\phi T(s-1)+\nu]^{3-\alpha} + [\phi T(s+1)+\nu]^{3-\alpha}\} \quad (7)$$

$$\mathrm{P}(0) = exp\left\{-\lambda T - \frac{\lambda\nu}{\phi(\alpha-1)}\left[1 + \phi(\phi+\kappa) - \frac{1}{4}\phi(\phi+\kappa)(4\phi+\kappa) + \frac{\phi(\phi+\kappa)\left(4\kappa^2+27\phi\kappa+72\phi^2\right)}{72}\right] + \frac{\lambda\nu}{(4\phi+\kappa)(\alpha-1)}\left(1-\kappa-\phi+\frac{3}{2}\phi\kappa+\phi^2+\frac{\kappa^2}{2}\right) + \frac{\lambda\nu}{(\phi+\kappa)(\alpha-1)}\left[\frac{\nu}{\nu+(\phi+\kappa)T}\right]^{\alpha-1}\frac{\kappa}{\phi}\left(1-\kappa-\phi+\frac{3}{2}\phi\kappa+\phi^2+\frac{\kappa^2}{2}\right)\right\} \quad (8)$$

$$\mathrm{k}_1 = \left(2\lambda\mu^2\mu_c + \frac{\lambda\mu^2\mu_c\kappa}{\phi^2-1}\right)\left(\frac{\nu^\alpha}{\alpha-1}\right) \quad (9)$$

$$\mathrm{k}_2 = \left(\frac{\lambda\mu^2\mu_c\kappa}{\phi^2-1}\right)\left(\frac{\nu^\alpha}{\alpha-1}\right) \quad (10)$$

$$\mu_c = 1 + \frac{\kappa}{\phi} \quad (11)$$

where $Y_t^{(T)}$ is the time series of precipitation at a certain accumulation level T and s is the lag time for an accumulation level. Given this highly non-linear equations set with more unknowns than the number of statistics equations, the solution cannot be found using the substitution method. In addition, it is difficult to get an accurate solution. The best solution is the one that minimizes the discrepancy between the statistics of the observed and simulated rainfall time series. The objective function (12) is employed to

help find the minimal discrepancy between the statistics of the observed and simulated rainfall time series:

$$\sum_{k=1}^{n} W_k \left[1 - \frac{F_k(\vec{\theta})}{f_k}\right]^2 \quad (12)$$

where $\vec{\theta}$ is the vector that contains the model's parameters, n is the number of rainfall statistics needs to be matched, F_k is the kth statistic of the MBLRP simulated rainfall time series, f_k is the kth statistic of the observed rainfall time series, and W_k is the weight factor of the kth statistic. An algorithm that is good at iteratively finding the solution and can minimize the objective function (12) is needed. The Isolated Speciation-Based Particle Swarm Optimization algorithm, which shows a more reliable capability of finding true minima through low objective function values, was used in this study (Cho, Kim, Olivera, and Guikema 2011). The weight of each statistic was equal initially but was adjusted by comparing the observed precipitation to the MBLRP simulation results based on these observed data. Kim, Olivera, and Cho (2013) found it difficult for the MLBRP model to reproduce the lag-1 autocorrelation coefficient. Thus, the lag-1 autocorrelation coefficient was assigned the smallest weight. They also found that the weight of each statistic could be determined by the interpolation of the simulated results. In this study, the weight was determined by minimizing the difference between the simulated result and the observed result. Given the importance of mean, it was assigned the highest weight. Increasing the weight of probability of zero rainfall would cause loss of fit for mean and variance. Therefore, the weights for mean, variance and Probability of zero were adjusted recursively by the difference of the simulated result

and the observed result. The weight of each statistics at different accumulation levels can be seen in Table 3.

Table 3 The weight of four statistics

Statistics	**Weight**
Mean	30.4
Variance	16.8
Lag-1	1
Probability of Zero Rainfall	18

The solutions were evaluated by the difference between the observed statistic values and the values calculated with the statistics equations (5) through (8) for the parameters. Mean and variance were plotted, since they were important in terms of determining extreme value. Each plot contains 84 paired points (7 stations × 12 months), which means there are 84 sets of parameters' solutions.

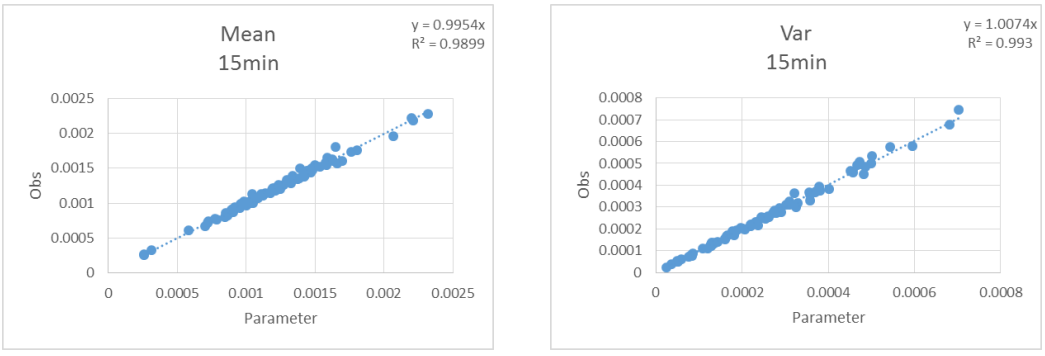

Figure 2 Mean and variance of the observed precipitation vs. those calculated from each set of parameters by precipitation statistics equations.

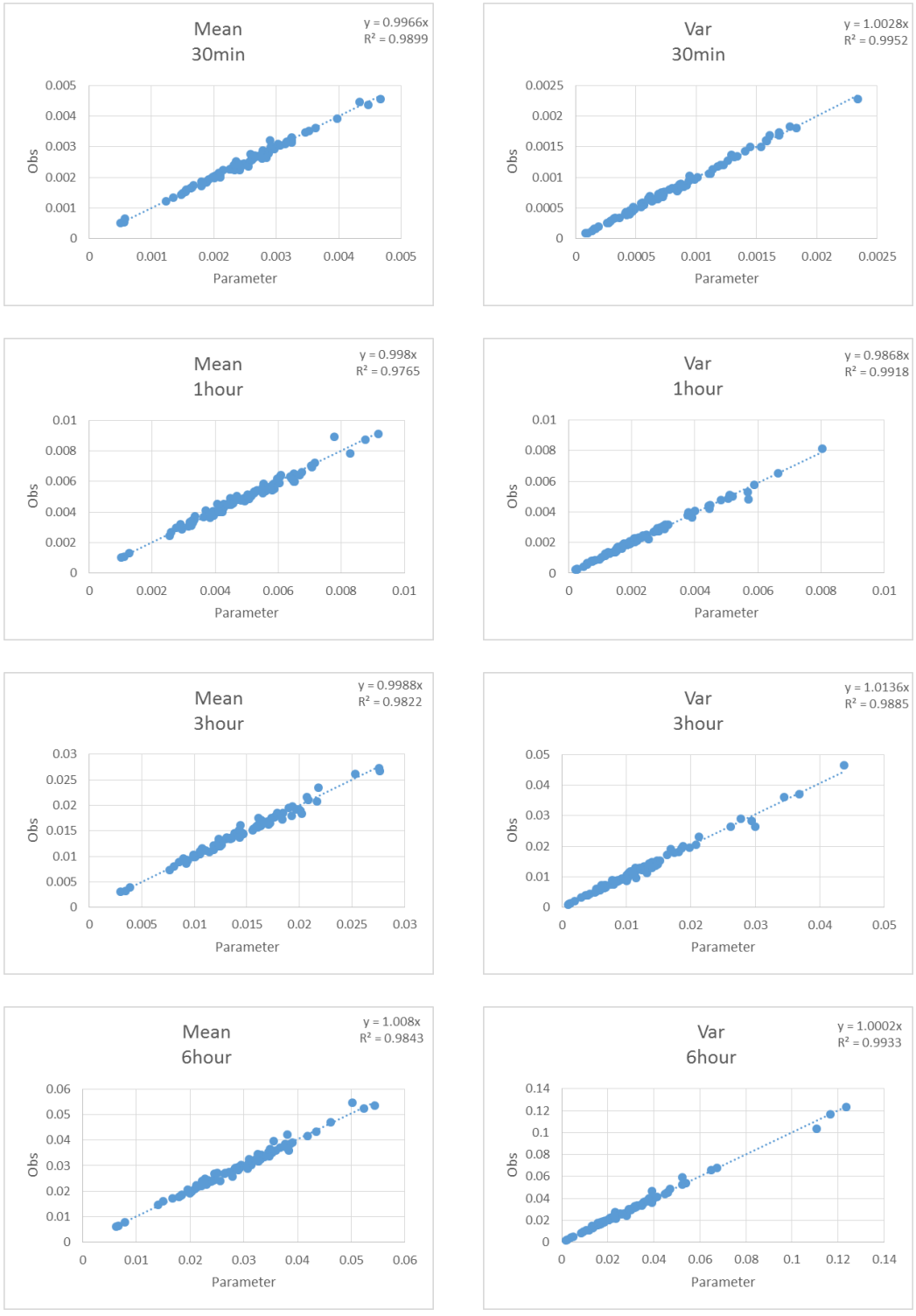

Figure 2 Continued.

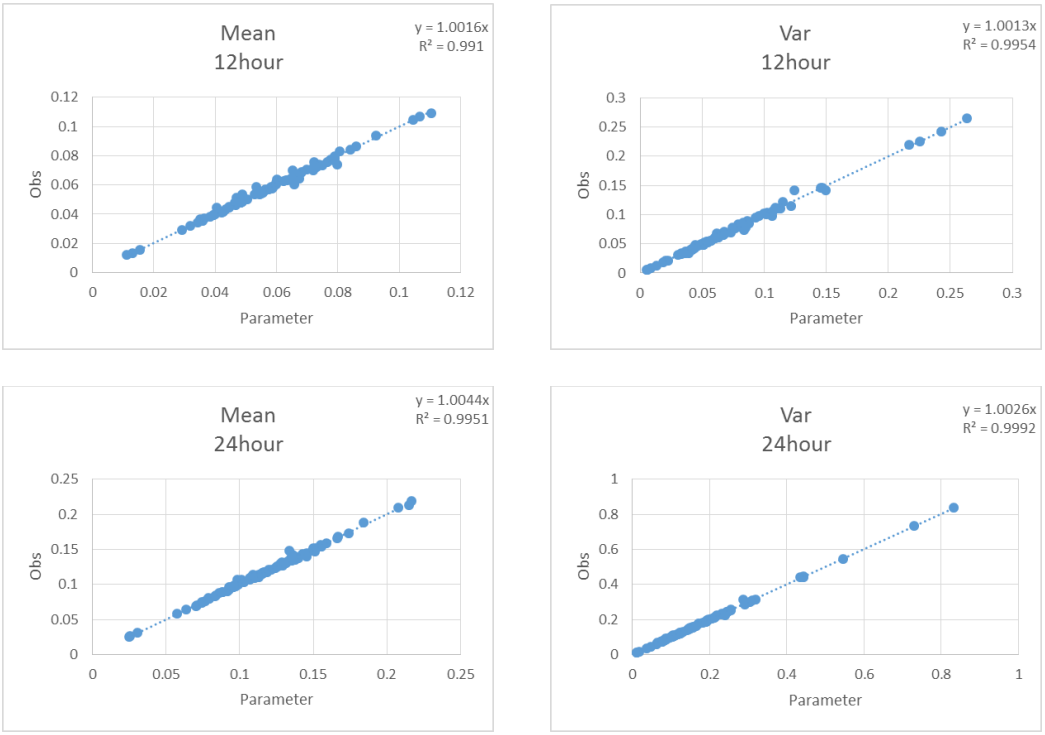

Figure 2 Continued.

From the above plots, the mismatched errors of mean and variance are relatively small. At each accumulation level, the slopes of the regression equation were around 1. Given the importance of mean and variance for the extreme precipitation, the solution of each set of parameters was considered acceptable.

3.3 MBLRP Parameters Conversion

Before each set of parameters can be used as input for the MBLRP simulator, it needs to be converted based on its accumulation interval (T). λ [1/T] is the expected number of storms that arrive in the accumulation interval. 1/ γ [T] is the expected duration of storm activity. μ [L/T] is the expected rain cell intensity in depth per

accumulation interval. β [1/T] is the expected number of rain cells within the storm duration per accumulation interval. 1/η [T] is the expected duration of the rain cells in the accumulation interval. t_1 represents the accumulation interval used for calculating the parameter, t_2 represents the desired accumulation interval, parameters with subscript (t_1) represent the parameters after calibration, and parameters with subscript (t_2) represent the parameters after unit conversion. In order to generate simulated precipitation at a certain accumulation interval, the value of each parameter needs to be converted to:

$$\lambda_{(t_2)} = \lambda_{(t_1)} \times \left(\frac{t_2}{t_1}\right) \quad (13)$$

$$\alpha_{(t_2)} = \alpha_{(t_1)} \quad (14)$$

$$\nu_{(t_2)} = \frac{\nu_{(t_1)}}{\frac{t_2}{t_1}} \quad (15)$$

$$\mu_{(t_2)} = \mu_{(t_1)} \times \left(\frac{t_2}{t_1}\right) \quad (16)$$

$$\phi_{(t_2)} = \phi_{(t_1)} \quad (17)$$

$$\kappa_{(t_2)} = \kappa_{(t_1)} \quad (18)$$

3.4 MBLRP Simulation Performance Evaluation

The simulated rainfall time series were obtained using the MBLRP simulator (D Kim, 2009) with the six parameters. In this study, the simulation length was 200 years. With this length, the statistics of the MLBRP precipitation match the observed precipitation statistics. Once the simulated rainfall time series were obtained, the mean,

variance, probability of zero rainfall, and lag-1 autocorrelation coefficient at 15-, 30-minute, 1-, 3-, 6-, 12-, and 24-hour accumulation levels could be calculated. The performance of the MBLRP method was evaluated by comparing the values calculated in equations (5) through (8) using parameters values and the values calculated from the MBLRP method.

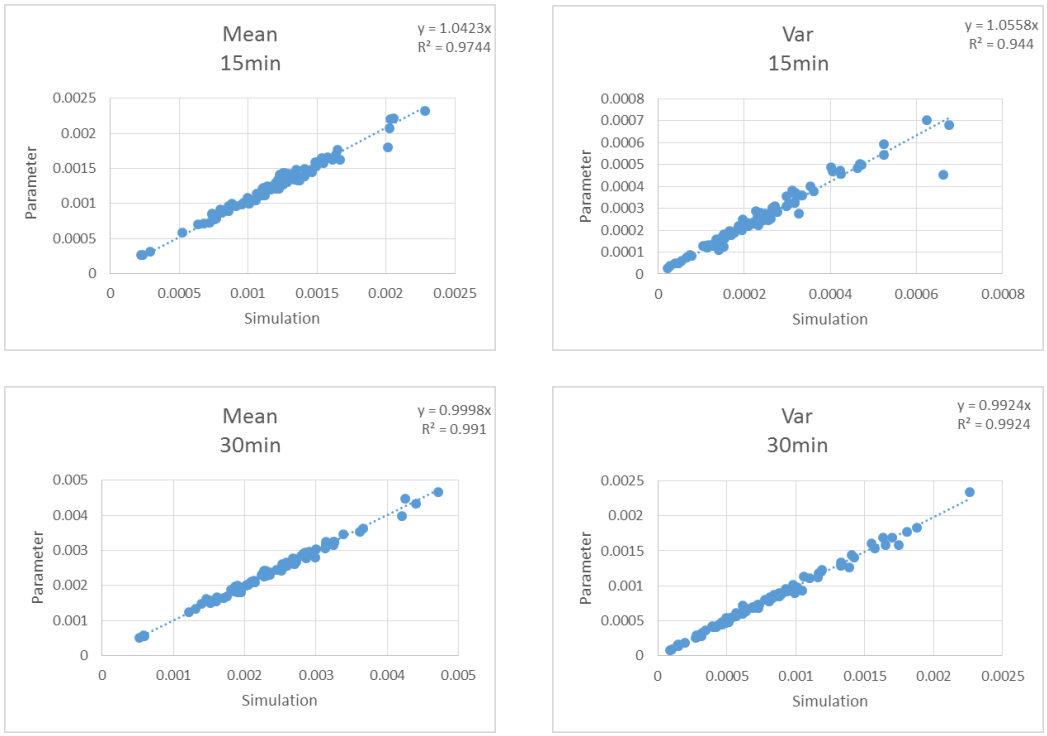

Figure 3 Mean and variance of calculated from each set of parameters vs. those calculated from each set of parameters by the MBLRP model.

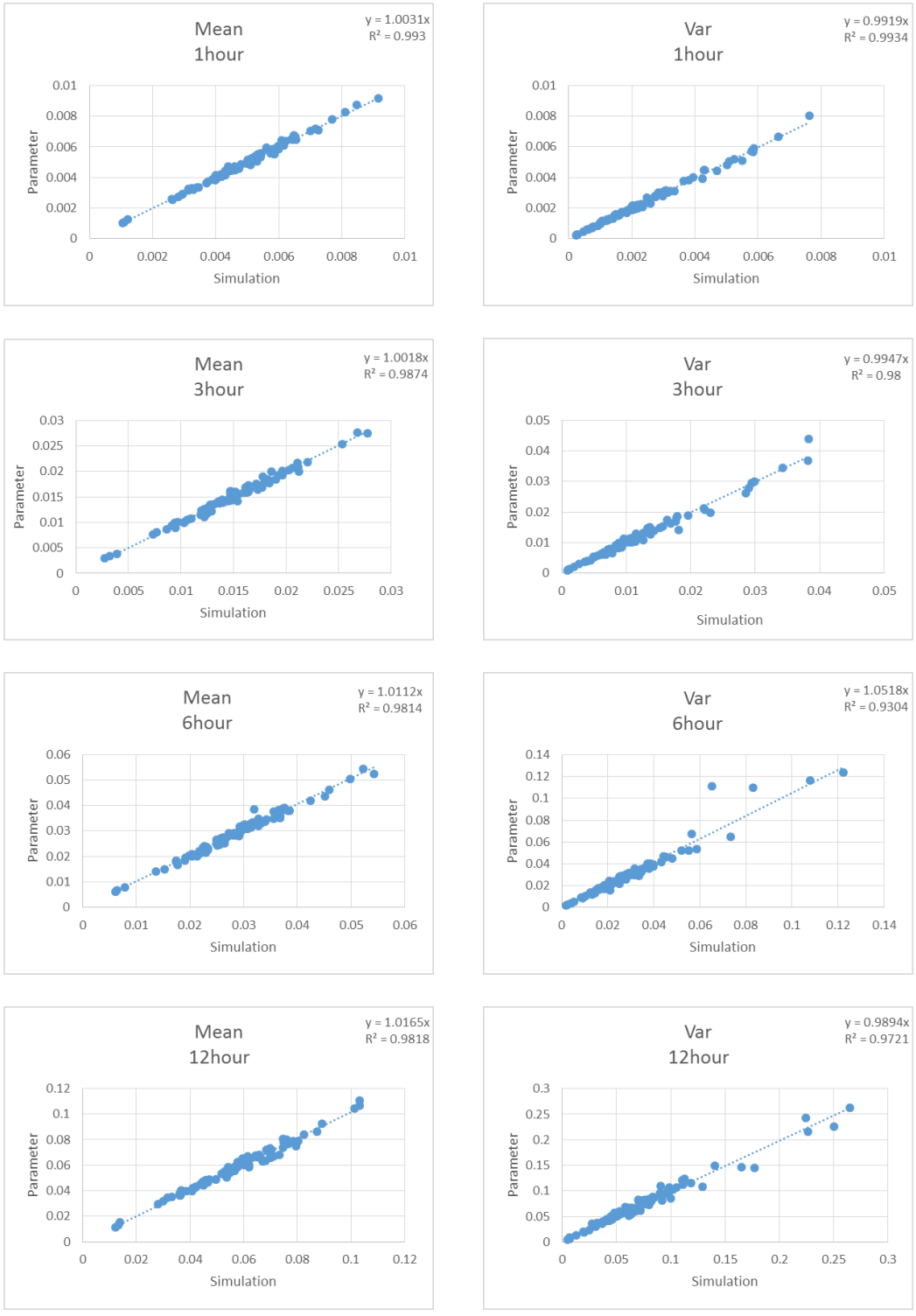

Figure 3 Continued.

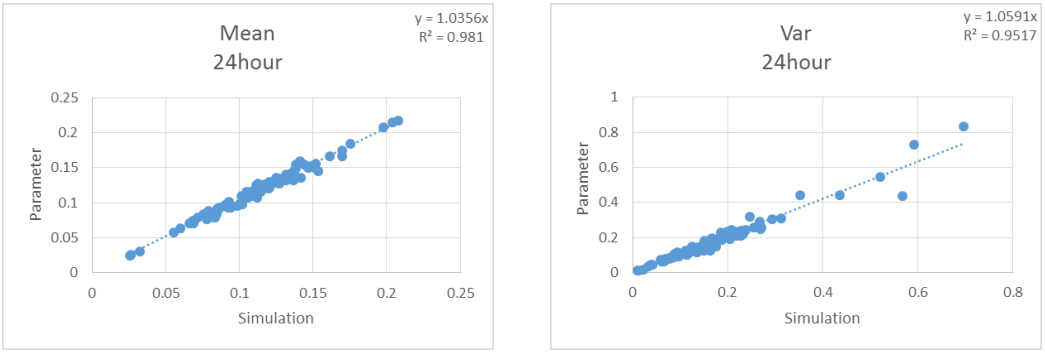

Figure 3 Continued.

The plots in Figure 3 show that the MBLRP method reproduced the mean well. Despite some outliers in the variance, the majority of variance was reproduced well. Hence, the accuracy of the MBLRP stochastic precipitation time series largely depends on the solution of a parameters set. The MBLRP simulation results were evaluated by comparing the observed time series to the simulated one. The comparison of mean and the comparison of variance were plotted. As a reference:

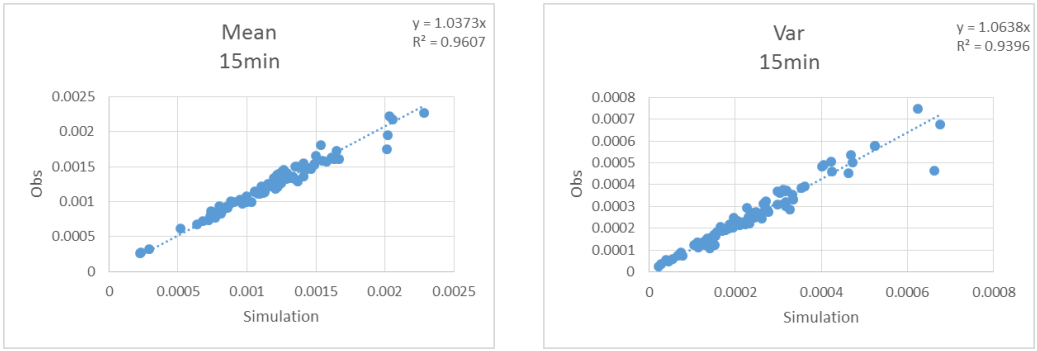

Figure 4 Mean and variance of the observed precipitation vs. those calculated from each set of parameters by the MBLRP model.

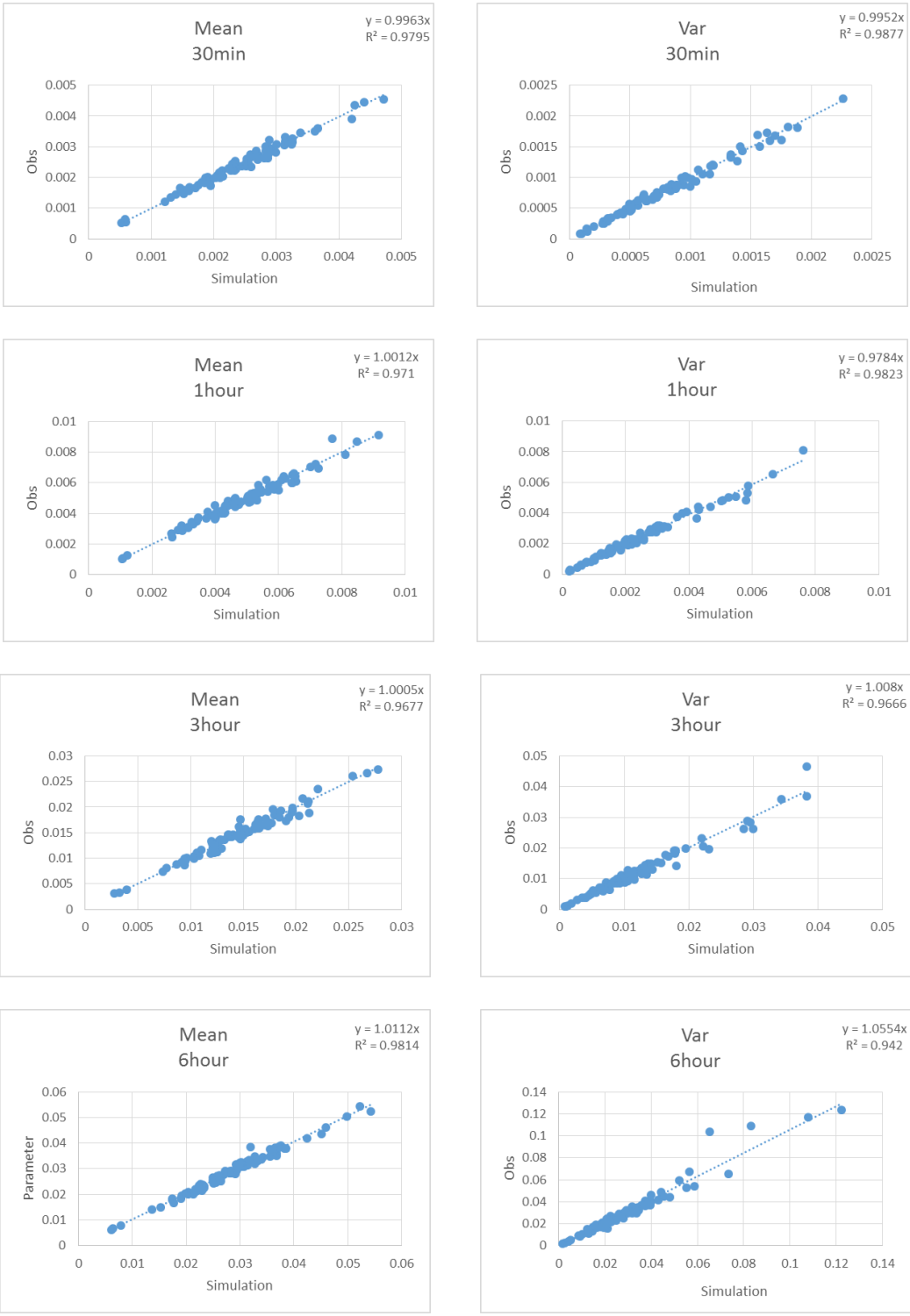

Figure 4 Continued.

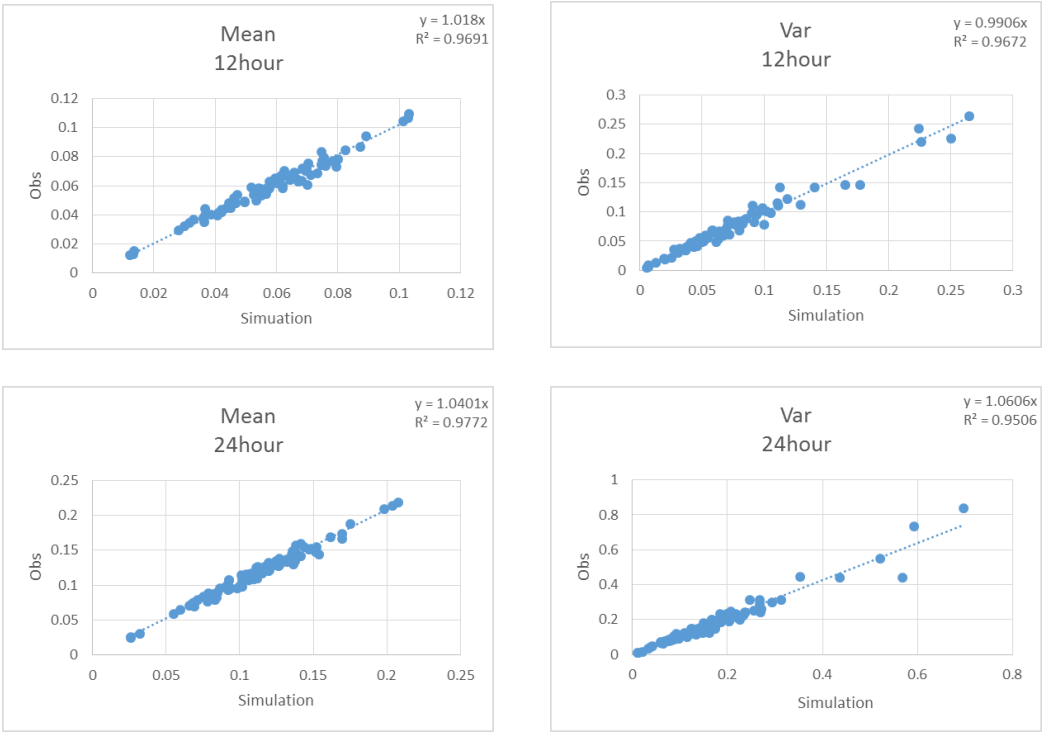

Figure 4 Continued.

From the above plots in Figure 4, the MBLRP method is capable of matching the statistics with a simulation length of 200 years. The outliers for the variance in some plots were in accordance with the precipitation time series, which has a low probability of zero rainfall and a large mean of precipitation. This reflects the limitation of the MBLRP method on reproducing precipitation for a relatively dry period. Even though there were some outliers on the plots for the variance, which lead to overestimation of precipitation for some months' time series, its impact on the whole time series was relatively limited. To better capture the characteristics of precipitation, more efforts may be needed to improve the MBLRP model, which are beyond the scope of this study.

3.5 Duration Curve Analysis

A duration curve was plotted to analyze the frequency of precipitation events. It describes the exceedance probability for a certain amount of precipitation. To calculate the exceedance probability, precipitation values in a time series first needed to be sorted in descending order. Then, the exceedance probability (P) was calculated based on the following equation:

$$\mathrm{P} = \frac{m}{n+1} \quad (19)$$

where m is the rank of the precipitation amount, m = 1, the largest possible value, and n is the total number of precipitation values. Therefore, in a time series, each amount of precipitation has its own probability (P). A curve was plotted by pairing a value with its probability. Among seven accumulation intervals, each accumulation interval contains four time series of precipitation: (1) the observed precipitation, (2) the MBLRP simulated precipitation based on the observed data, (3) the MBLRP simulated precipitation based on GCM current data, and (4) the MBLRP simulated precipitation based on GCM future data. For the observed precipitation, the time series was directly generated from the observed data. For the MBLRP simulated precipitation, the time series were generated based on different sources of data. Once the time series were obtained, the amount of precipitation was ranked from largest to smallest. Then, the probability of each amount of precipitation was calculated using equation (19). After calculating the probability of each amount of precipitation in the time series, the amount of precipitation and the probability was paired to generate the curve. Then, in each plot,

there were four duration curves for four time series. Each curve contains all months of the 200-year simulated timespan. The horizontal axis was plotted in the logarithmic scale to better display each curve. The probability ranged from 0.1% to 10%. Figure 5 shows the duration curves of COOP: 414311 rainfall station for the seven accumulation intervals.

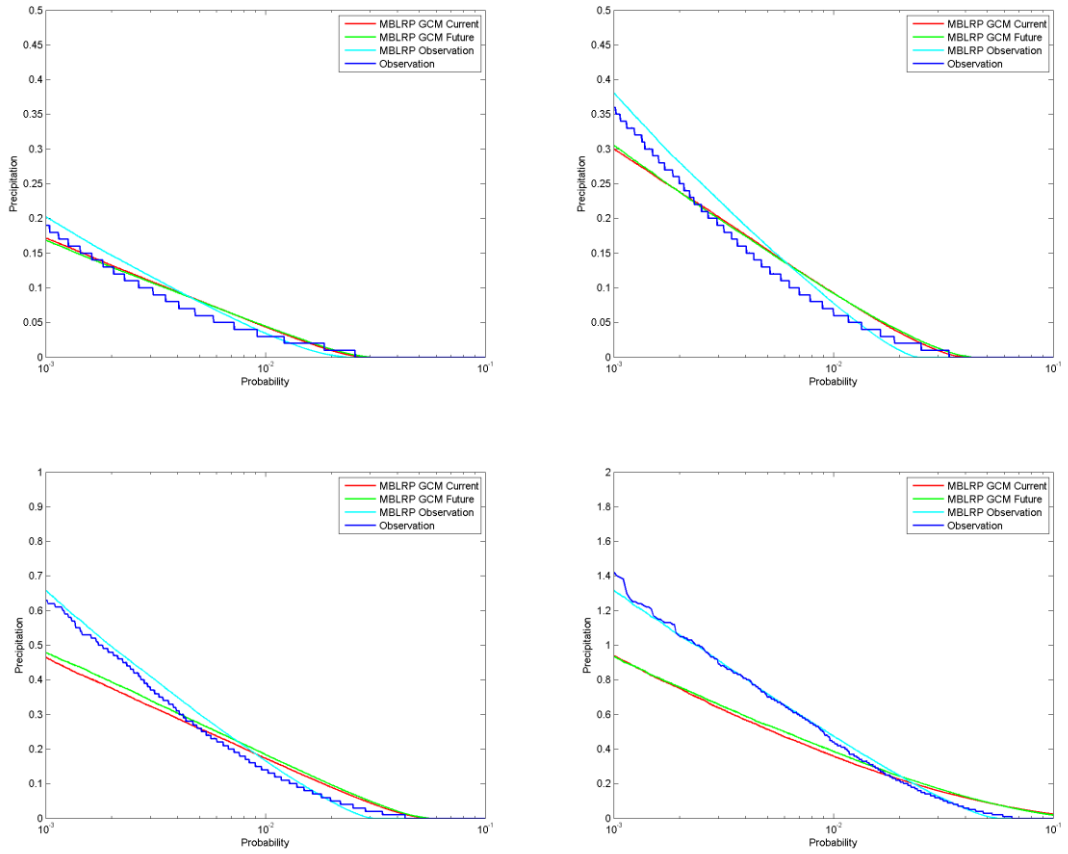

Figure 5 Duration curves of COOP: 414311 rainfall station for 7 accumulation levels' precipitation. From left to right, top to bottom, 15-, 30-minute, 1-, 3-, 6-, 12-, 24-hour accumulation levels.

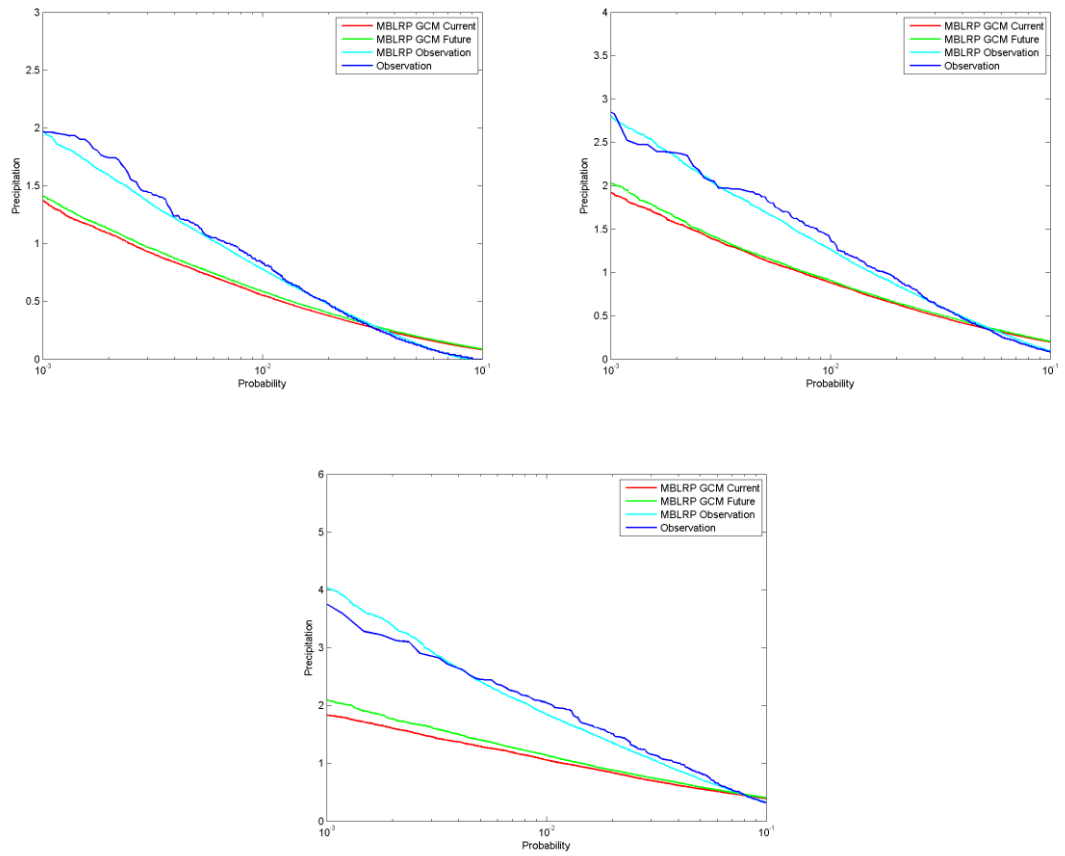

Figure 5 Continued.

In total, there were seven plots representing seven different accumulation intervals for each of the seven stations.

3.6 Frequency Analysis of Extreme Precipitation Values

The frequency analysis of hourly extreme rainfall was conducted to analyze the extreme precipitation amount for a certain return period. In this study, the return periods were 2, 5, 10, 25, 50, and 100 years to capture relatively high-frequency events and relatively low-frequency events.

3.6.1 Annual hourly peak precipitation value

The annual hourly peak precipitation value is the maximum value in a one-year time series of hourly precipitation. In this study, there were four different time series. One of them was the observation data of the COOP: 417594 rainfall station. This rainfall station was selected because it had more than 30 years of hourly precipitation records, which is statistically significant. The observed time series ranged from 1968-2009. The remaining time series were the MBLRP simulated precipitation series based on the observed data, the MBLRP simulated precipitation series based on GCM current data, and the MBLRP simulated precipitation series based on GCM future data. The largest value of each year was selected from this time series to obtain annual peak values. Therefore, for the observed data, since the length of time series was 42 years, there were 42 peak values. For all MBLRP stochastically generated time series, since the length of the time series was 200 years, there were 200 peak values.

3.6.2 Distribution and frequency analysis

To determine the extreme precipitation amount for a certain return period, a distribution that fits these peak values is needed. Koutsoyiannis (2004) suggested that the Generalized Extreme Value distribution of type II (GEV II) is better for describing the real behavior of rainfall maxima distribution than the Gumbel distribution. Thus, the goodness of fit test was used to verify the fitting for these two distributions. After the maximum value of each year was selected to consist of a time series of peak values. Each series of peak values was used to fit the GEV II distribution and the Gumbel

distribution. Then, the Chi-square test was conducted to measure how well the selected distribution fits the data (Table 4).

Table 4 The result of Chi-square test for the GEV II distribution and the Gumbel distribution

Time Series	**GEV**	**Gumbel**
Observation	2.3302	6.7366
MBLRP Observation	10.096	33.205
MBLRP GCM Current	4.8927	32.251
MBLRP GCM Future	9.4549	22.201

The values in Table 4 represent the goodness of fit for a particular distribution. With the increasing value, the goodness of fit for this distribution decreased. The test results showed that the GEV II distribution was better than the Gumbel distribution for each series. Thus, the GEV II distribution was utilized to fit annual peak values series. After determining the best distribution to describe the peak values, the peak value for a certain year return period could be calculated. The probability of a T-year return period event happening (p) is:

$$\mathrm{p} = \frac{1}{T} \quad (20)$$

Let the upper case letter X denote rainfall amount, and the lower case letter x denote a possible value of X. $\mathrm{Fx}(x)$ is the nonexceedance probability for the value x.

$$\mathrm{Fx}(x) = 1 - \mathrm{p} \quad (21)$$

Thus, precipitation with a return period of 2-, 5-, 10-, 25-, 50-, and 100-years is in accordance with the GEV II distribution with probability larger than 0.5, 0.8, 0.9, 0.96,

0.98, and 0.99, respectively. Four curves were plotted to make a comparison of (1) the observed data and the MBLRP simulated precipitation based on the observed data, (2) the MBLRP simulated precipitation based on the observed data and the MBLRP simulated precipitation based on the GCM current data, and (3) the MBLRP simulated precipitations based on the GCM current data and the GCM future data.

4. RESULTS AND DISCUSSIONS

4.1 Duration Curve Analysis

The duration curve is expected to reveal the likelihood of the precipitation exceeding a given value. The accuracy of the duration curve needs to be evaluated, since a lot of uncertainty will be generated in the process of obtaining stochastic precipitation. In this study, there are three sources of uncertainty: (1) the MBLRP method, (2) the GCM, and (3) the statistics relationship equations.

4.1.1 Uncertainty of the MBLRP method

In the plot, the MBLRP observed curve was obtained by using the MBLRP method based on the observed precipitation. Thus, the comparison of the MBLRP observed curve and the observation curve reflects the uncertainty of the MBLRP method.

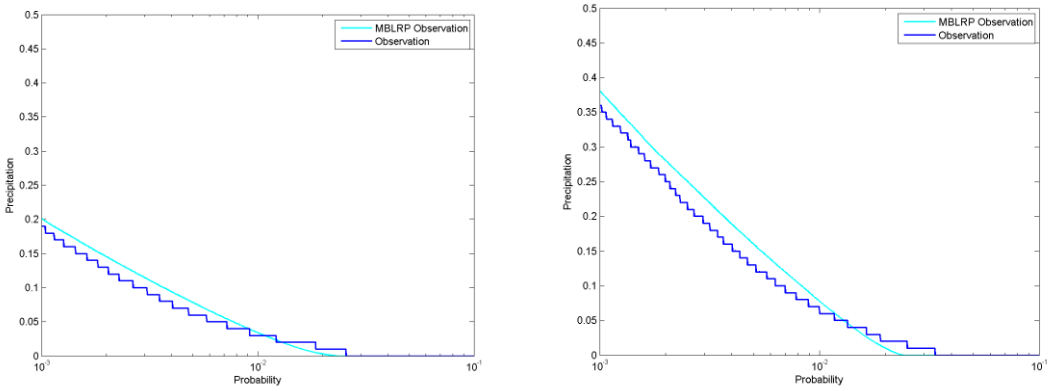

Figure 6 Duration curves of the stochastic precipitation based on the observed data and the observed precipitation for COOP: 414311 rainfall station at different accumulation levels with gfdl-cm 3.1 model. From left to right, top to bottom, 15-, 30-minute, 1-, 3-, 6-, 12-, and 24-hour accumulation levels.

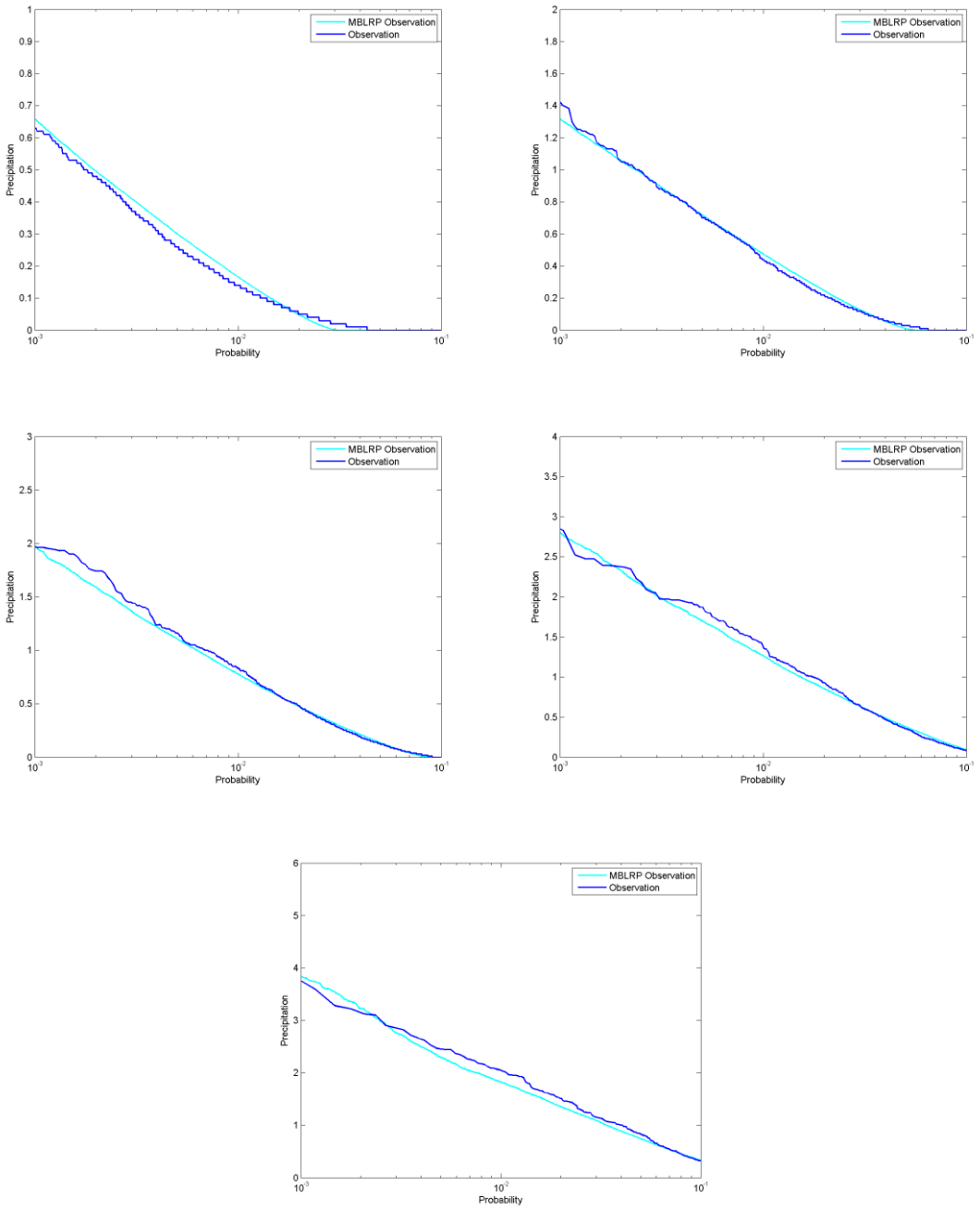

Figure 6 Continued.

Given the fact that the MBLRP method performed well in terms of reproducing the statistics of mean and variance, the plots of the duration curve show that the MBLRP method is capable of reproducing precipitation time series within the probability ranges from 0.1% to 10% well. For each rainfall station, it was noticed that with an increased accumulation level, the difference between the MBLRP observed curve and the observation curve decreased for probabilities larger than 1%. For 3-hour and 6-hour accumulation level's precipitation, these two curves have minimal differences. However, for accumulation levels smaller than one hour, it was found that these two curves do not match well. This reflects the MBLRP method's limitation in reproducing sub-hourly precipitation time series. It was found that these two curves tended to differ from each other when the probability was less than 1% at 7 different accumulation levels. This reflects the limitation of the MBLRP method to reproduce low-frequency events. This situation was observed from COOP: 414311 rainfall station, which was similar to the rest rainfall stations.

4.1.2 Uncertainties of GCMs and the statistics relationship equations

Uncertainty of the GCM existed in the MBLRP GCM current curve for the 24-hour accumulation level, since the precipitation time series was generated based on the data extracted from the GCM.

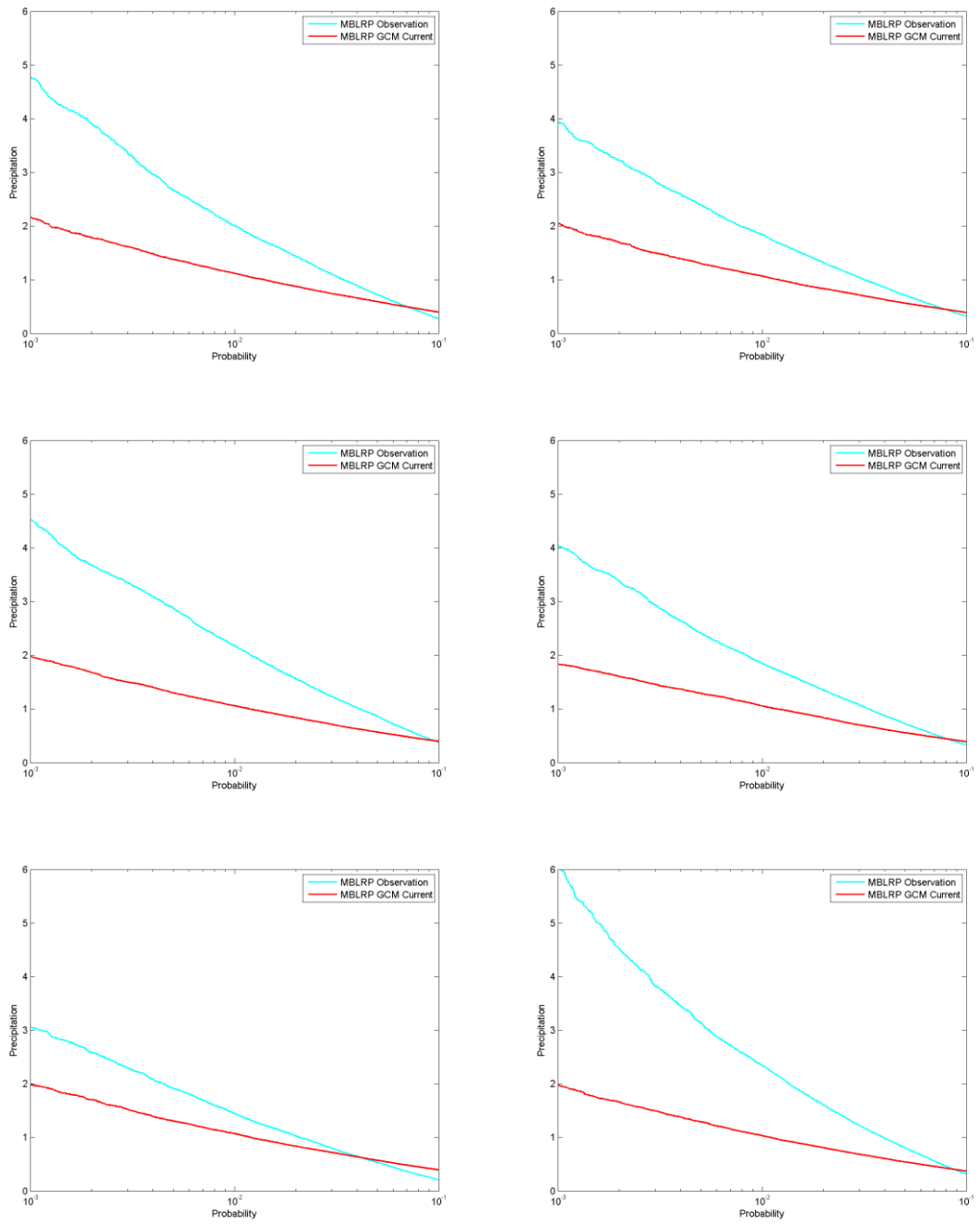

Figure 7 Duration curves of the stochastic precipitation based on the observed data and GCMs past data for different rainfall stations with gfdl-cm 3.1 model. From the top to bottom and left to right, COOP: 411956, COOP: 412206, COOP: 414309, COOP: 414311, COOP: 414329, COOP: 417594, COOP: 418996.

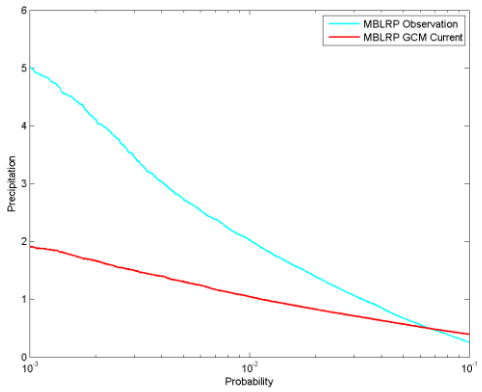

Figure 7 Continued.

Figure 7 shows that the stochastic precipitation based on GCMs current data for gfdl-cm3.1 model was systematically lower than the precipitation based on observed data. It also was observed from the rest two GCM models. This shows that the three GCMs tend to underestimate daily precipitations in the Houston area, especially for low-frequency precipitation events. It's noticed that the observation data come from the rainfall stations. The GCM data was extracted from the downscaled model for a grid which has a spatial resolution is about 12 kilometers × 12kilometers. Therefore, the difference between the GCM data and the observed data may contain the error caused by spatial scale.

Besides the uncertainty of the GCM, the MBLRP GCM current curves for the six sub-daily accumulation levels also contain uncertainty of statistics relationship equations because the time series of sub-daily precipitation was not available in GCMs. The duration curves of the COOP: 414311 rainfall station for 12-hour and 24-hour accumulation levels' precipitation are plotted in Figure 8.

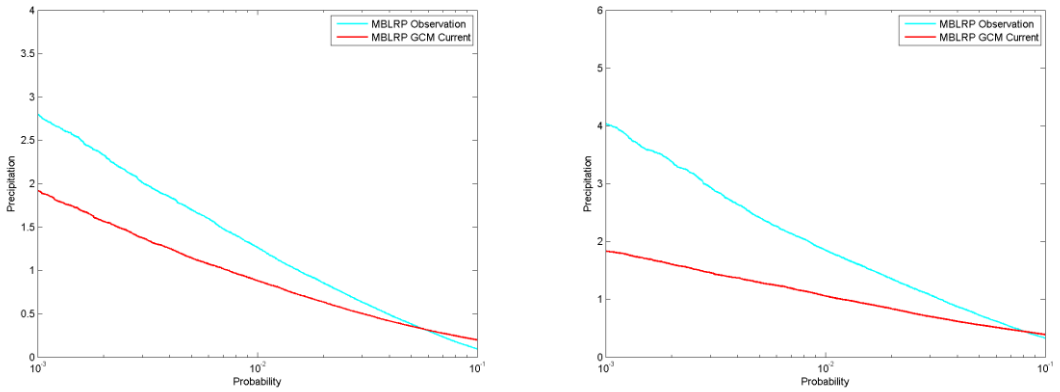

Figure 8 Duration curves of COOP: 414311 rainfall station for 12-hour (left) and 24-hour (right) accumulation levels' precipitation time series with gfdl-cm 3.1 model.

With the usage of the statistics relationship equations, the comparison of duration curves of precipitation time series at the 12-hour accumulation level and the 24-hour accumulation level shows that the difference between the stochastic precipitation based on the observed data and the observed data decreased. Hence, the statistics relationship equations tend to overestimate the precipitation, especially for the low frequency precipitation events.

4.1.3 Effect of climate change

Both the MBLRP GCM current duration curve and the MBLRP GCM future duration curves contain the same uncertainties, since they are generated by the same method based on GCM precipitation data. The only difference between these two curves is the climate scenario of its precipitation data. Thus, the difference of these two curves indicates the effect of climate change on precipitation. From the plots in Figure 9, the curve generated from GCM current data was almost overlapped with one generated by

GCM future data. It also was observed from the rest rainfall stations, which indicates the effect of climate on precipitation is illegible under the selected emissions scenario. The difference of the two curves becomes most significant at the duration of 24 hours, which illustrates that the effect of climate change on the precipitation events happened within one day. The curve for future precipitation is above the curve for past precipitation. This means given the same probability, the amount of future daily precipitation is larger than the past. Likewise, it was also observed for the rest rainfall stations. Thus, this result indicates that precipitation in the future becomes more frequent than past. As reference:

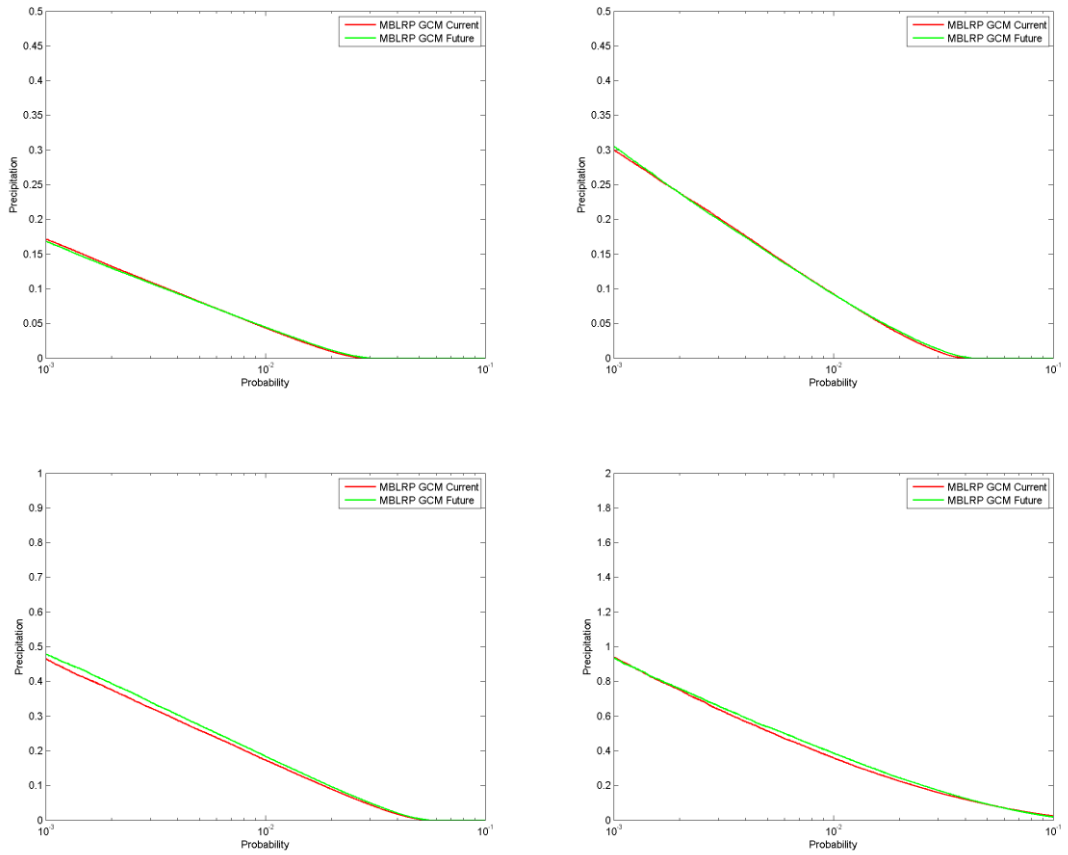

Figure 9 Duration curves of COOP: 414311 rainfall station for GCM past precipitation and GCM future precipitation with gfdl-cm 3.1 model. From left to right, top to bottom, 15-, 30-minute, 1-, 3-, 6-, 12-, 24-hour accumulation levels.

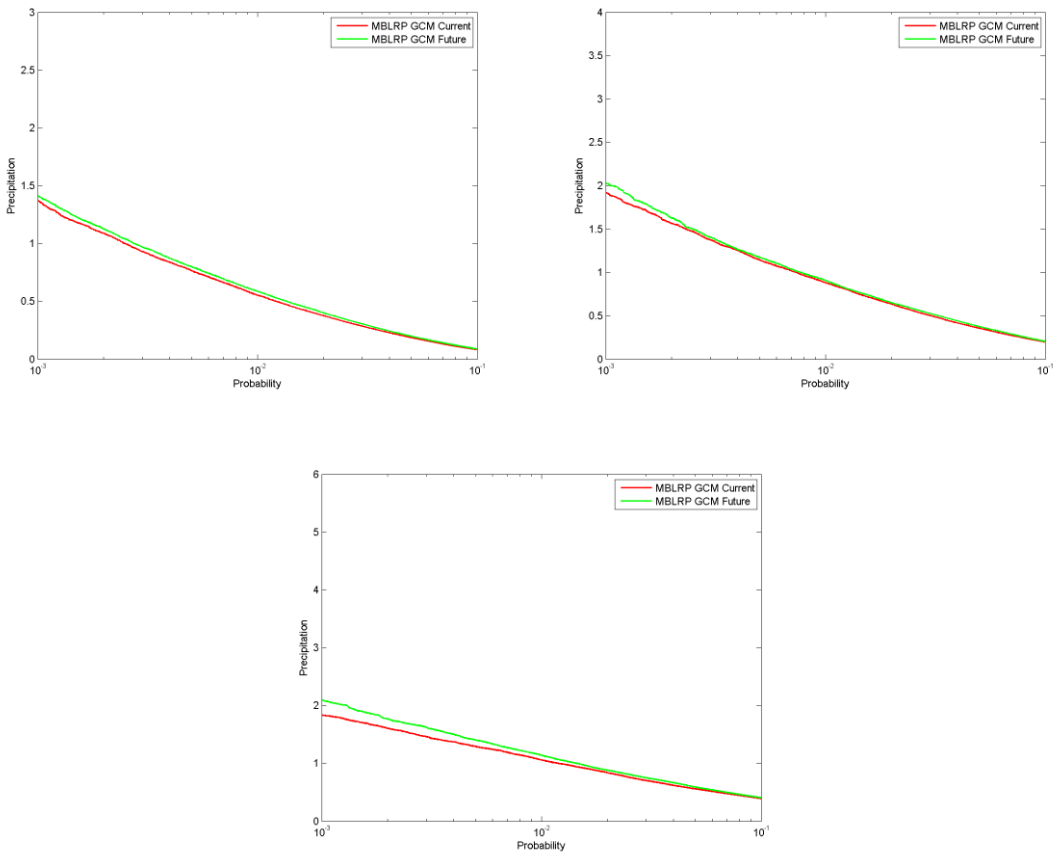

Figure 9 Continued.

4.2 Frequency Analysis of Extreme Precipitation

Each curve in the frequency analysis plots contains the same uncertainties as the duration curve, because the method used to generate the precipitation time series is the same. The uncertainties are coming from: (1) the MBLRP method, (2) the GCM, and (3) the statistics relationship equations.

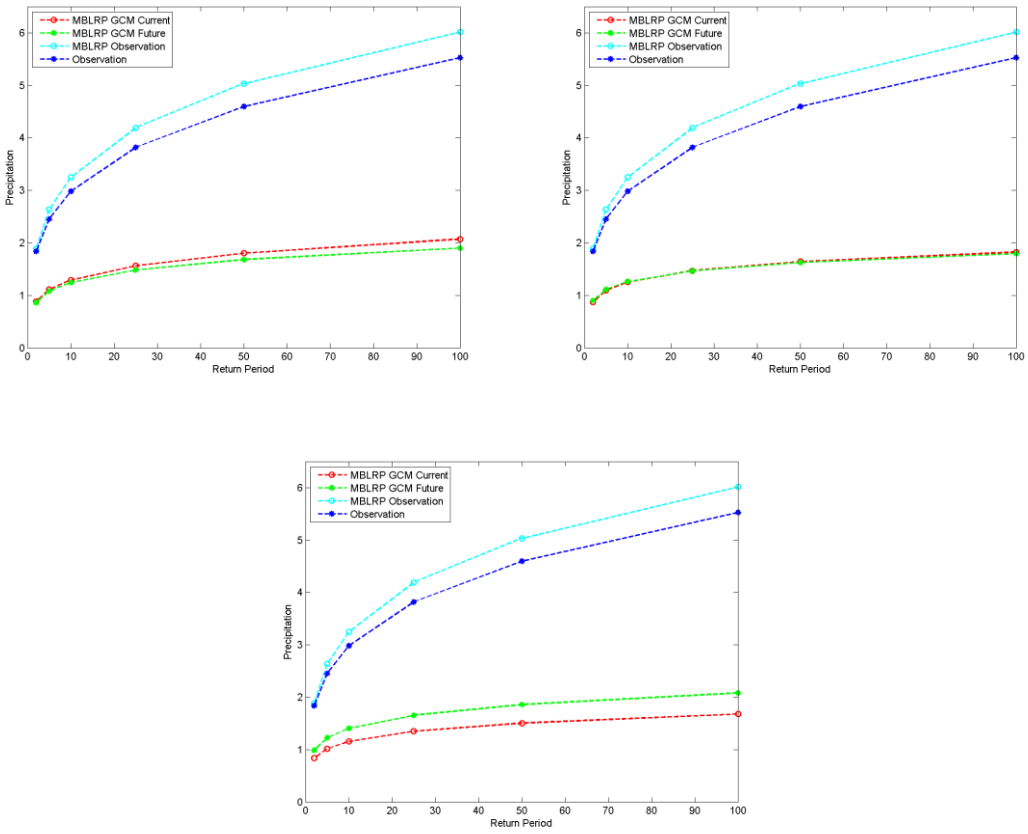

Figure 10 Annual hourly extreme precipitation for the return periods of 2-, 5-, 10-, 25-, 50-, and 100-years of Rainfall station 417594. From left to right, top to bottom, gfdl-cm 3.1 model, miroc-esm.1 model, and miroc-esm-chem.1 model.

4.2.1 Uncertainty of the MBLRP method

Comparing the observation curve to the MBLRP curve reflects the performance of the MBLRP method. The extreme values of 2-year and 5-year return periods are similar. However, the differences of annual hourly peak values at 10-year, 25-year, 50-year, and 100-year return periods become more significant. This shows that the MBLRP method tends to overestimate the extreme values, especially for low frequency extreme values, and confirms what has been observed in duration curve.

4.2.2 Uncertainties of GCMs and the statistics relationship equations

Hourly precipitation was generated with the help of the statistics relationship equations. Comparing the MBLRP GCM current curve to the observation curve reflects the uncertainties of GCM and the statistics relationship equations. Similar to the duration curve, the peak value that was generated based on GCM precipitation and the statistics relationship equations was underestimated. Like the duration curve analysis, GCM and the statistics relationship equations reflect a large uncertainty caused by the MBLRP method and the spatial scale mismatch. The frequency analysis was only conducted on the hourly precipitation time series, hence the evaluation of GCMs was not reasonable.

4.2.3 Effect of climate change

Comparison of the GCMs current curve and the GCMs future curve shows the effect of climate change on extreme precipitation. The effect of climate change varies from model to model. Overall, the effect of climate change is relatively small in the Houston area. The peak values at the 2-year, 5-year, 10-year, and 25-year return periods in future were relatively higher than current. It could be explained by the effect of climate change on precipitation. At the 50-year and 100-year return period, the extreme value became smaller than the current extreme value, which may be explained by the location of the Houston area in the zone of subtropical drying, in which precipitation is expected to decline in future. Similar to the plots of the duration curve, the effect of climate is smaller than the difference resulted from the uncertainties of the MBLRP method and GCM. On the one hand, it confirms that climate change does not influence the duration curve too much. On the other hand, it also illustrates that the factor of

climate change is relatively smaller than the factors of the MBLRP method and GCM, in terms of the accuracy of estimation results. These plots also indicates the effect of climate change was projected differently by models in GCMs.

5. CONCLUSIONS

Both flooding caused by extremely high precipitation and drought resulting from extremely low rainfall have a huge impact on agricultural, industrial and social fields. The purpose of estimating the effect of climate change on precipitation is to provide the hydrologist, policy maker, and all citizens with the information that could help them to make better decisions for the potential hydrologic risk.

The key part of estimating the effect of climate change on precipitation is to generate a time series of precipitation in a future climate scenario. In this study, the MBLRP model was used to generate stochastic precipitation time series based on source data. Three GCM was used as a data source to provide current and future precipitation data. Since all models are simplifications of reality, the use of the MBLRP model and GCM brings uncertainty to the prediction results. Climate change could affect precipitation patterns, eventually including extreme precipitation. All factors have to be evaluated in order to evaluate the accuracy of the estimation results.

Comparison of the statistics shows that for a 200-year time series, mean and variance were reproduced well by the MBLRP model. The accuracy of the MBLRP model largely depends on the solution of six parameters. The duration curve shows that the MBLRP method is limited in its ability to reproduce precipitation with frequency lower than 1% or for accumulation levels shorter than one hour. As accumulation levels increase, especially for 3-hour and 6-hour accumulation levels, the MBLRP model would have a better performance of generating stochastic precipitation. The study of an

algorithm for solving six parameters and improving the MBLRP model is beyond the scope of this study and could be future work.

Compared with the observed data, the GCM largely and systematically underestimated the precipitation, which shows a large source of uncertainty from the MBLRP method. It is noticed that this source of uncertainty also caused by the difference on spatial resolution. Further, only three model out of 13 models in RCP6.0 were selected from the GCMs, it is difficult and unreasonable to use this study to evaluate the uncertainty of all GCMs. In order to evaluate GCMs as a whole, all models must be taken into account. Also, the statistics relationship equations tend to overestimate the precipitation. Climate change did have some impact on precipitation in terms of changing frequency of rainfall and the mean amount of rainfall. However, both the duration curve analysis and the frequency analysis indicate that the effect of climate change on future precipitation is relatively small in the Houston area. The duration curve of future precipitation tends to be above the current one, which means that for the same probability, the amount of future daily precipitation is larger than the current precipitation. The predicted annual hourly extreme precipitation tends to be lower than the present due to the climate of the Houston area.

The methodology presented in this study provides a framework for estimating the effect of climate change on precipitation. Among the three uncertainties, the uncertainty of the MBLRP model has a smaller impact on the results. The source of GCM data and the mismatched spatial resolution introduced more uncertainty into the estimation

results. From the result of the selected three models in RCP6.0, the effect of climate change on precipitation is limited in the Houston area.

REFERENCES

Alexander, M. A., Scott, J. D., Mahoney, K., and Barsugli, J. 2013. "Greenhouse gas-induced changes in summer precipitation over Colorado in NARCCAP regional climate models." Journal of Climate 26, no. 21: 8690-8697.

Cho, H., Kim, D., Olivera, F., and Guikema. S. D. 2011. "Discrete Optimization: Enhanced speciation in particle swarm optimization for multi-modal problems." European Journal of Operational Research 213, 15-23.

Fiering, M. B. 1967. Streamflow Synthesis. Harvard University Press, Cambridge, Massachussets.

Fowler, H. J., Kilsby, C. G., O'Connell, P. E. 2000. "A stochastic rainfall model for the assessment of regional water resource systems under changed climatic condition." Hydrology and Earth System Sciences 4, no.2: 263-281.

Fujino, J., Nair, R., Kainuma, M., Masui, T., and Matsuoka, Y. 2006. "Multigas mitigation analysis on stabilization scenarios using aim global model." The Energy Journal, no.3:343–354.

Hijioka, Y., Matsuoka, Y., Nishimoto, H., Masui, T., and Kainuma, M. 2008. "Global GHG emission scenarios under GHG concentration stabilization targets." Journal of Global Environmental Engineering 13, 97–108.

Isham, S., D. Entekhabi, and R. L. Bras. 1990. "Parameter estimation and sensitivity analysis for the modified Bartlett-Lewis rectangular pulses model of rainfall." Journal of Geophysical Research 95, no.3: 2093-2100.

Khalyani, A. H., Gould, W. A., Harmsen, E., Terando, A., Quinones, M. and Collazo, J. A. 2016. "Climate change implications for tropical islands: interpolating and interpreting statistically downscaled GCM projections for management and planning." Journal of Applied Meteorology & Climatology 55, no. 2: 265-282.

Kim, D., Olivera, F., Cho, H., and Socolofsky, S. A. 2013. "Regionalization of the modified Bartlett-Lewis rectangular pulse stochastic rainfall model." Terrestrial, Atmospheric & Oceanic Sciences 24, no. 3: 421-436.

Koutsoyiannis, D. 2004. "Statistics of extremes and estimation of extreme rainfall: I. Theoretical investigation." Hydrological Sciences Journal 49, no. 4: 575-590.

Mehrotra, R., Sharma, A., Nagesh Kumar, D., and Reshmidevi, T. V. 2013. "Assessing future rainfall projections using multiple GCMs and a multi-site stochastic downscaling model." Journal of Hydrology 488, 84-100.

Oguz, H., Klein, A.G. and Srinivasan, R., 2007. "Using the SLEUTH urban growth model to simulate the impacts of future policy scenarios on urban land use in the Houston-Galveston-Brazoria CMSA." Research Journal of Social Sciences 2, no.1: 72-82.

Onof, C., Chandler, R. E., Kakou, A., Northrop, P., Wheater, H. S., and Isham, V. 2000. "Rainfall modelling using Poisson-cluster processes: a review of developments." Stochastic Environmental Research & Risk Assessment 14, no. 6: 384.

Pendergrass, A.G., Lehner, F., Sanderson, B. M., and Xu, Y. 2015. "Does extreme precipitation intensity depend on the emissions scenario?" Geophysical Research Letters 42, no. 20: 8767-8774.

Samuel, C. 1999. Stochastic rainfall modelling of convective storms in Walnut Gulch, Arizona. PhD Thesis, Imperial College London.

Smithers, J., Schulze, R., and Pegram, G. 1999. "Predicting short duration design storms in South Africa using inadequate data, hydrological extremes: understanding, predicting, mitigating." Proceedings of the IUGG 99, Symposium HS1, Birmingham, UK.

Texas State Historical Association. (2016) "Texas Temperature, Freeze, Growing Season and Precipitation Records by County." Retrieved 02/01/2016, from https://texasalmanac.com/sites/default/files/images/almanac-feature/countyweatherA.pdf.

United States Geological Survey. (1998) "Extreme Precipitation Depth for Texas, Excluding the Trans-Pecos Region" Retrieved 02/02/2016, from http://pubs.usgs.gov/wri/wri984099/pdf/wri98-4099.pdf.

Verhoest, N., P. A. Troch, and F. P. De Troch. 1997. "On the applicability of Bartlett-Lewis rectangular pulses models in the modeling of design storms at a point." Journal of Hydrology 202, no.1: 108-120.

White, C. J., Franks, S. W., and McEvoy, D. 2015. "Using subseasonal-to-seasonal (S2S) extreme rainfall forecasts for extended-range flood prediction in

Australia." Proceedings of the International Association of Hydrological Sciences (PIAHS) 370, 229-234.

Wilks, D., and Wilby, R. (1999). "The weather generation game: a review of stochastic weather models." Progress in Physical Geography 23, no.3: 329-357.

APPENDIX A. DURATION CURVE

Gfdl-cm-3.1 model

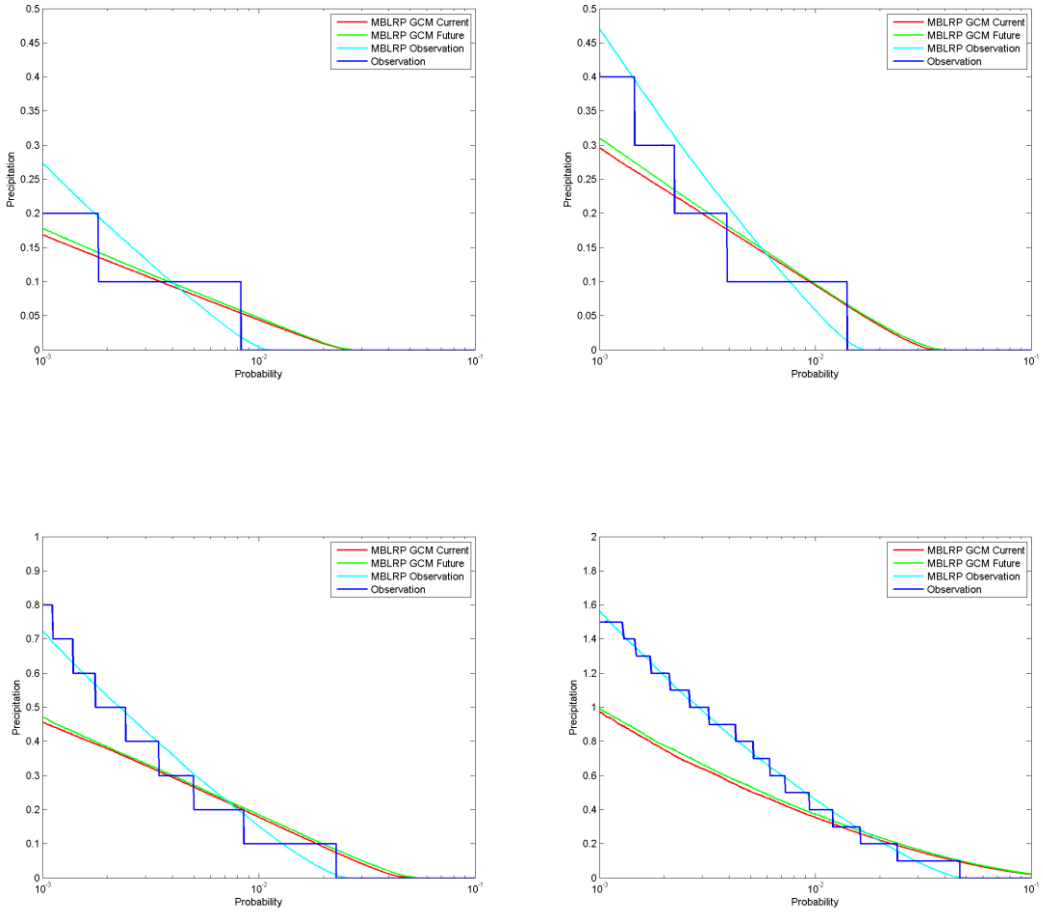

Duration curves of COOP: 411956 rainfall station for different accumulation levels' precipitation. From the top to bottom and left to right, 15-, 30-minute, 1-, and 3-hour levels.

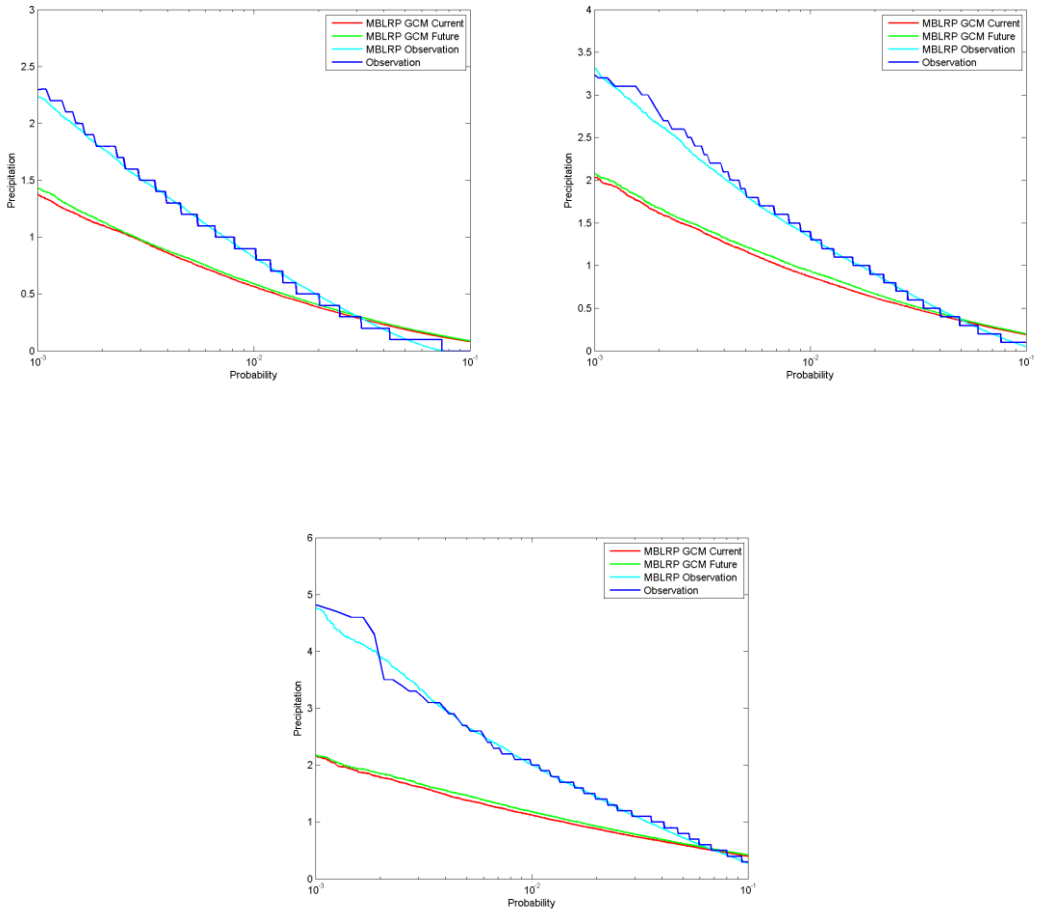

Duration curves of COOP: 411956 rainfall station for different accumulation levels' precipitation. From the top to bottom and left to right, 6-, 12-, and 24-hour levels.

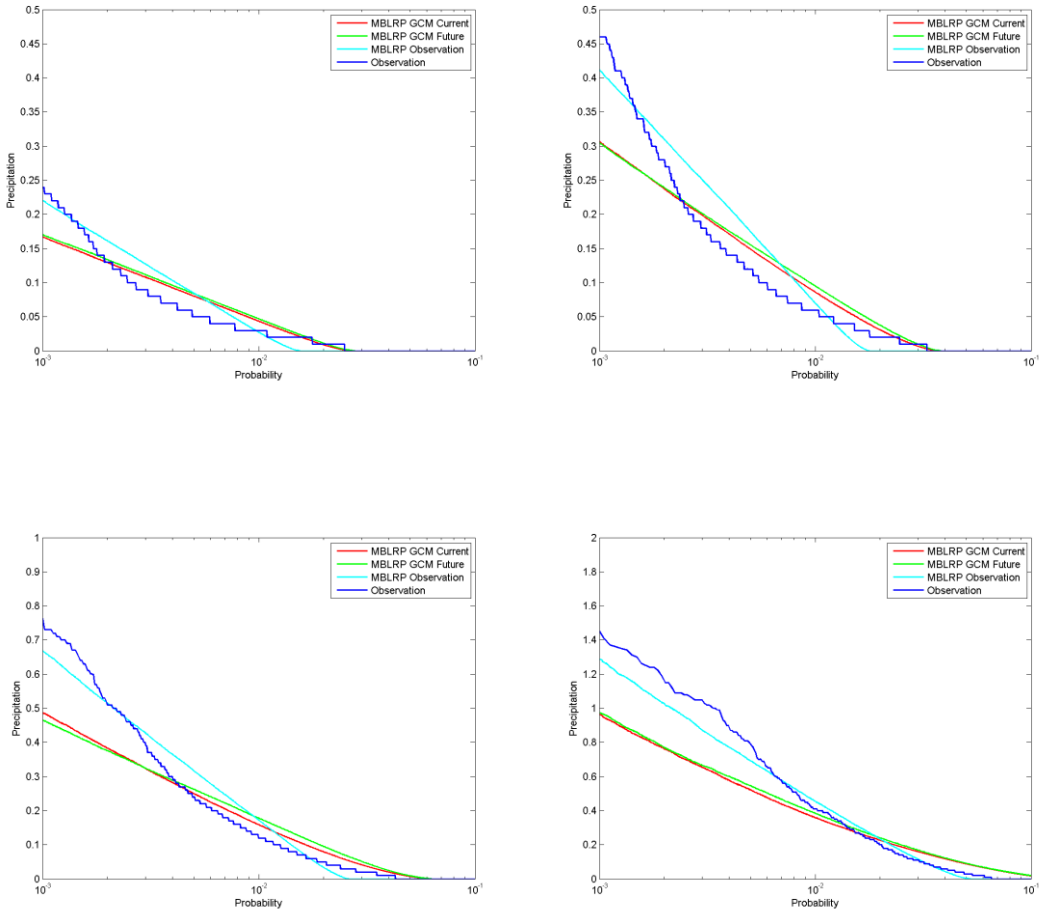

Duration curves of COOP: 412206 rainfall station for different accumulation levels' precipitation. From the top to bottom and left to right, 15-, 30-minute, 1-, and 3-hour levels.

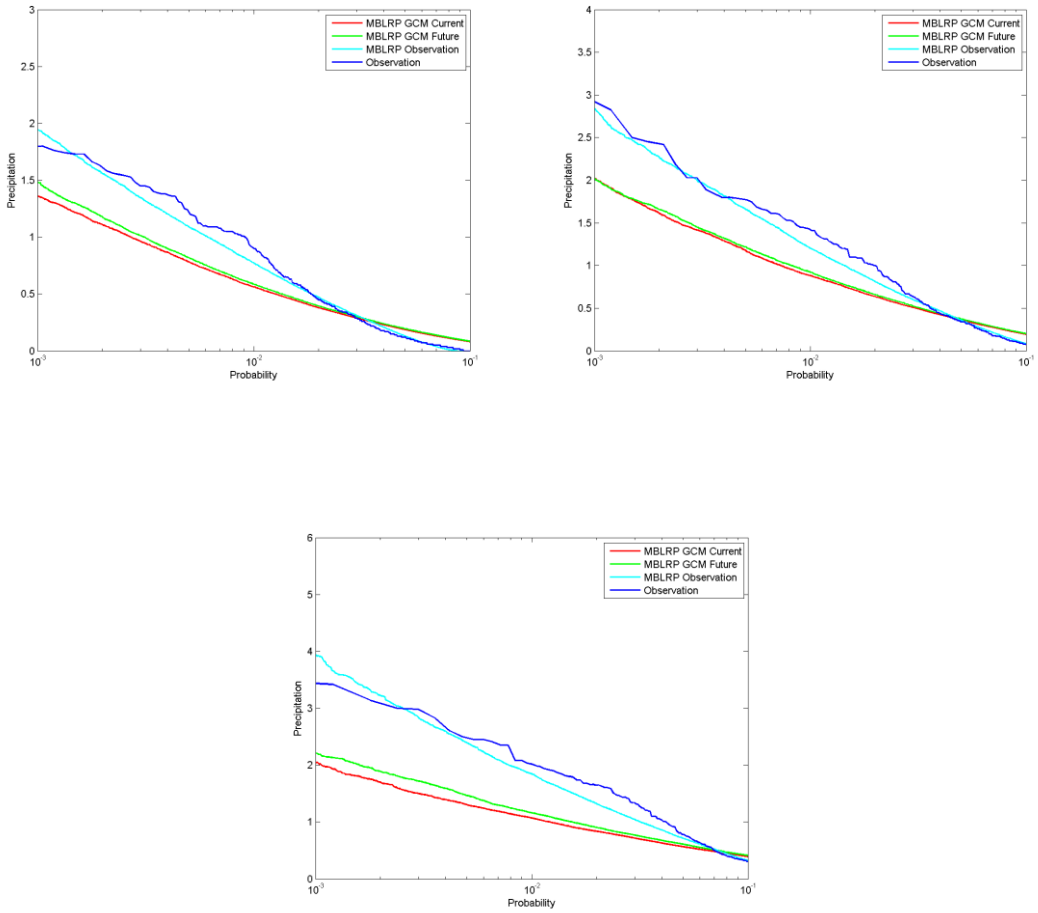

Duration curves of COOP: 412206 rainfall station for different accumulation levels' precipitation. From the top to bottom and left to right, 6-, 12-, and 24-hour levels.

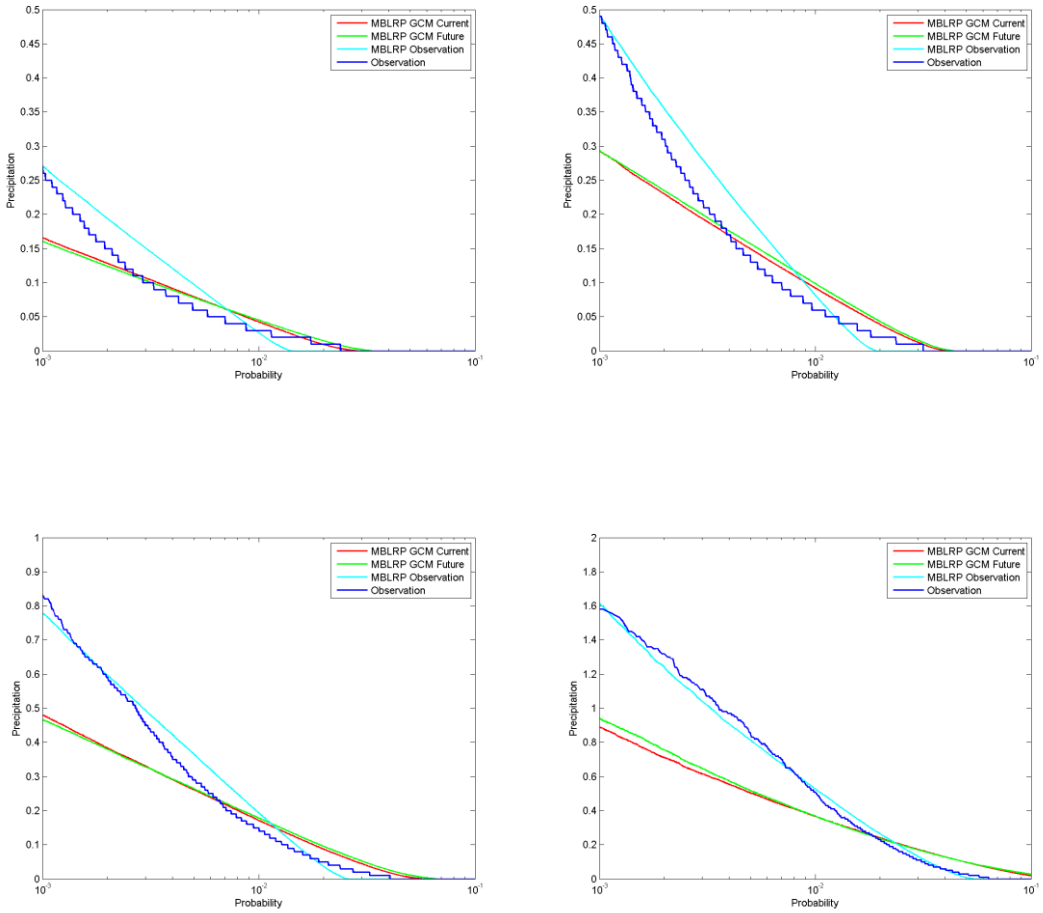

Duration curves of COOP: 414309 rainfall station for different accumulation levels' precipitation. From the top to bottom and left to right, 15-, 30-, 1-, and 3-hour levels.

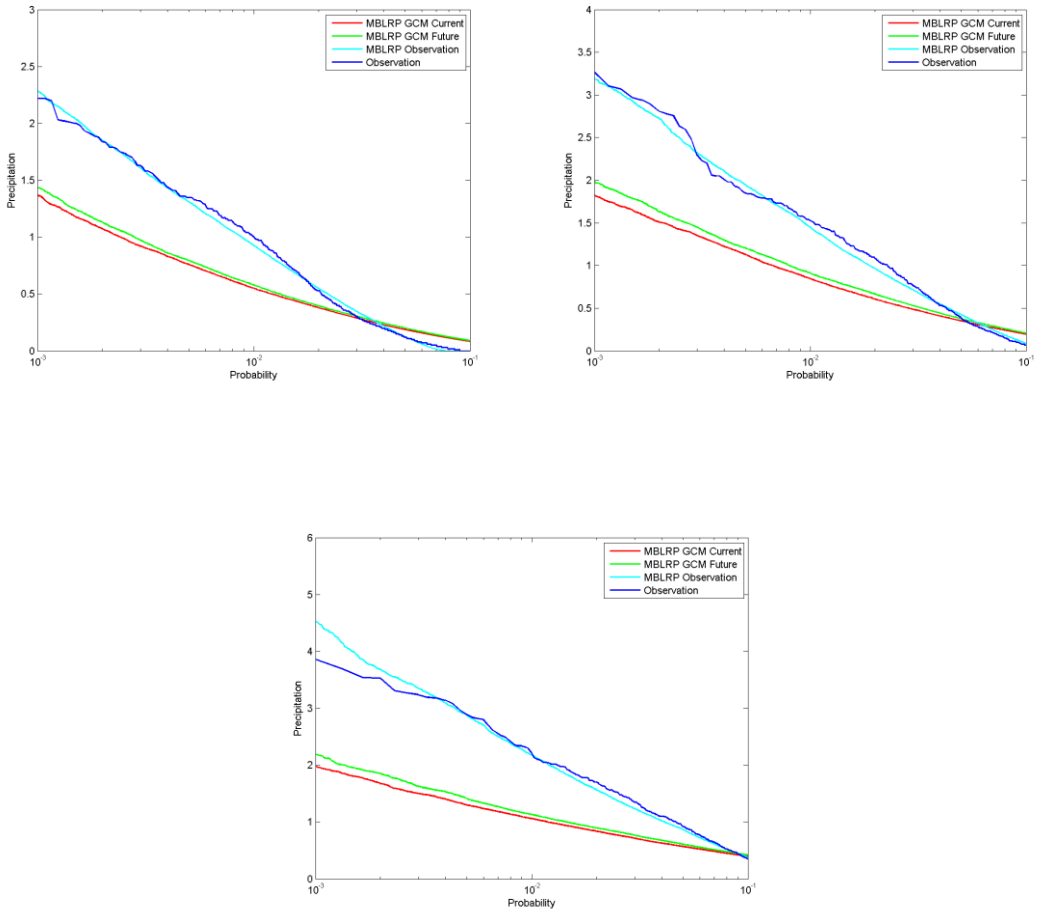

Duration curves of COOP: 414309 rainfall station for different accumulation levels' precipitation. From the top to bottom and left to right, 6-, 12-, and 24-hour levels.

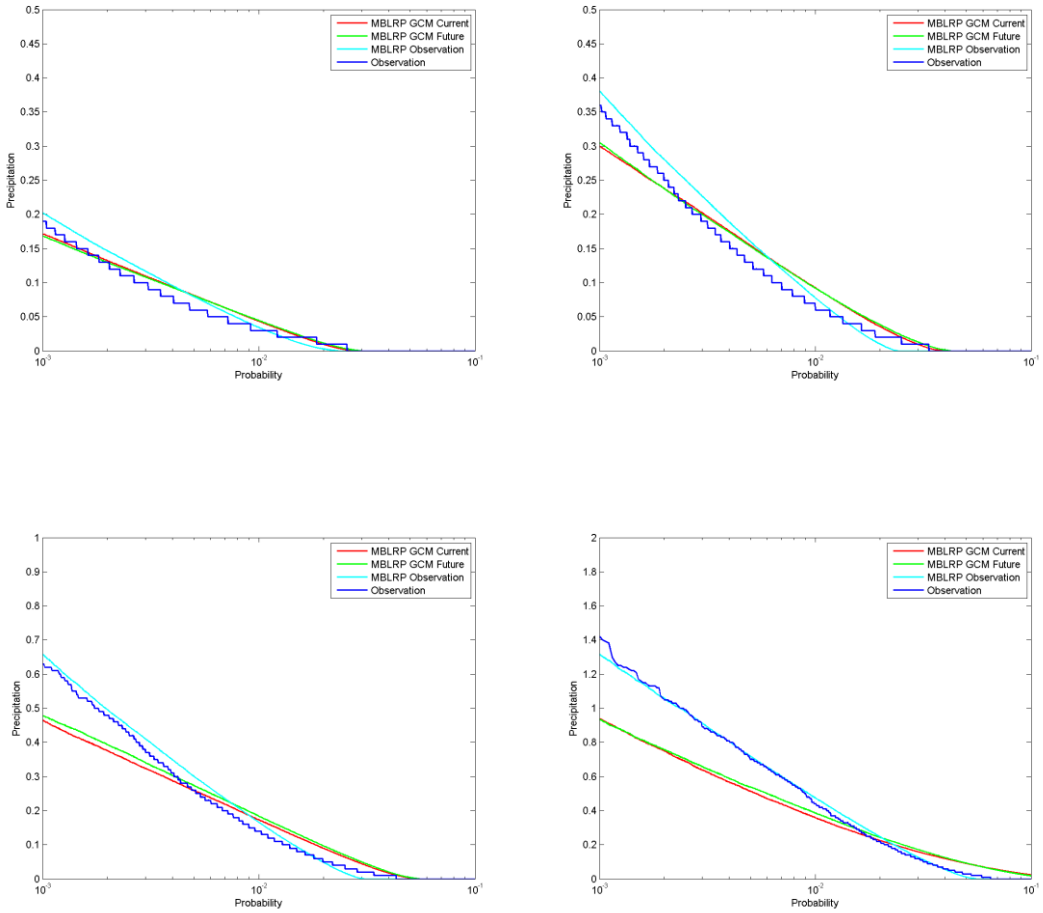

Duration curves of COOP: 414311 rainfall station for different accumulation levels' precipitation. From the top to bottom and left to right, 15-, 30-, 1-, and 3-hour levels.

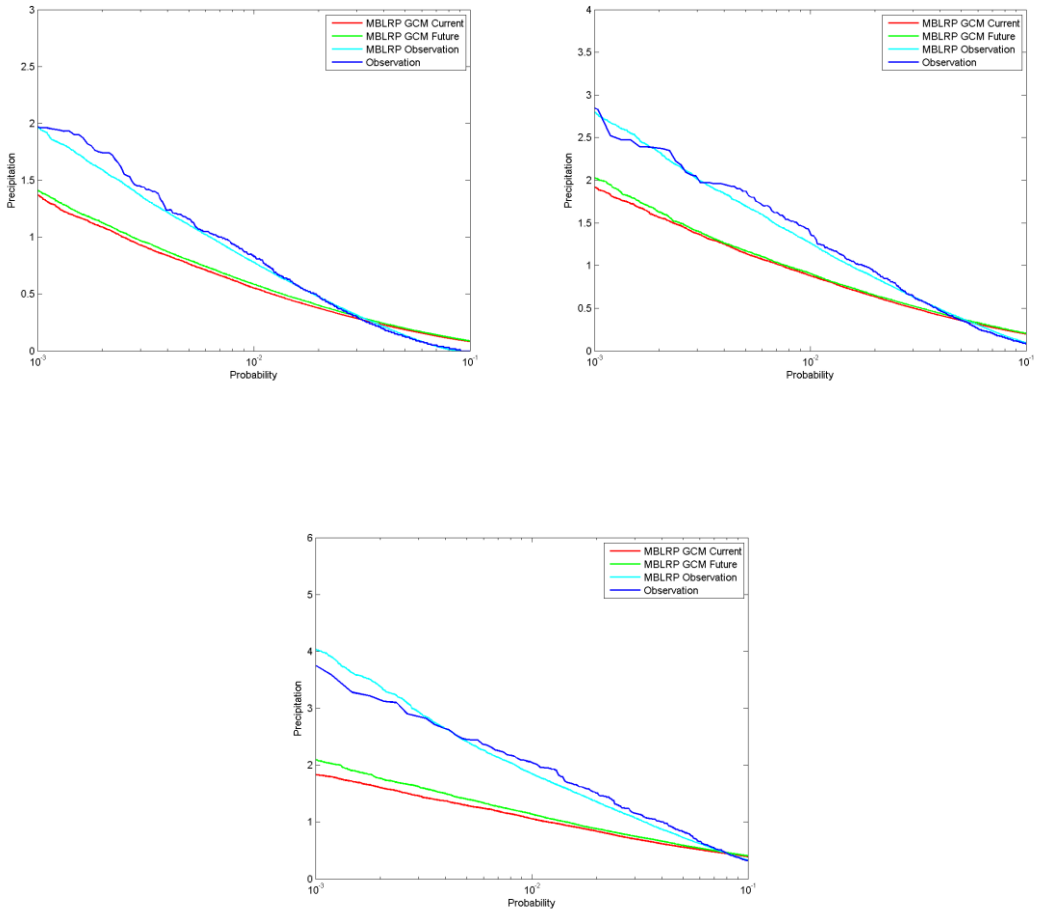

Duration curves of COOP: 414311 rainfall station for different accumulation levels' precipitation. From the top to bottom and left to right, 6-, 12-, and 24-hour levels.

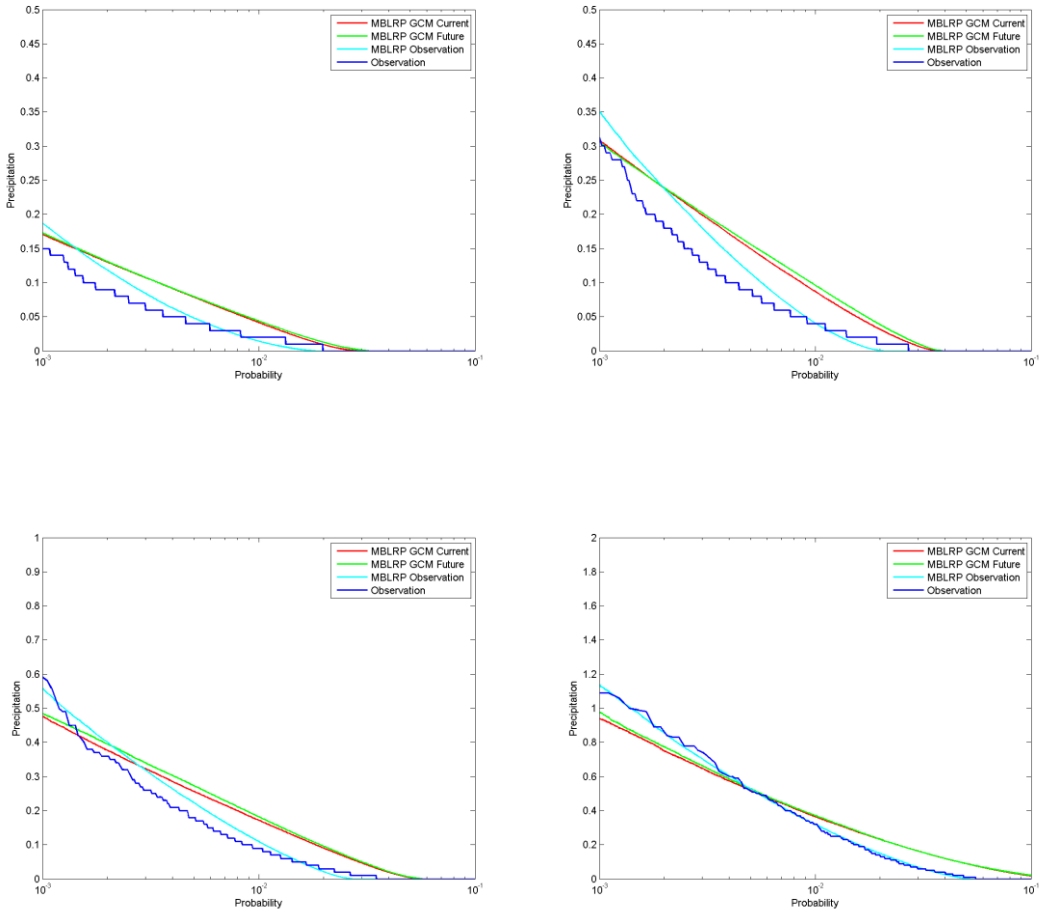

Duration curves of COOP: 414329 rainfall station for different accumulation levels' precipitation. From the top to bottom and left to right, 15-, 30-, 1-, and 3-hour levels.

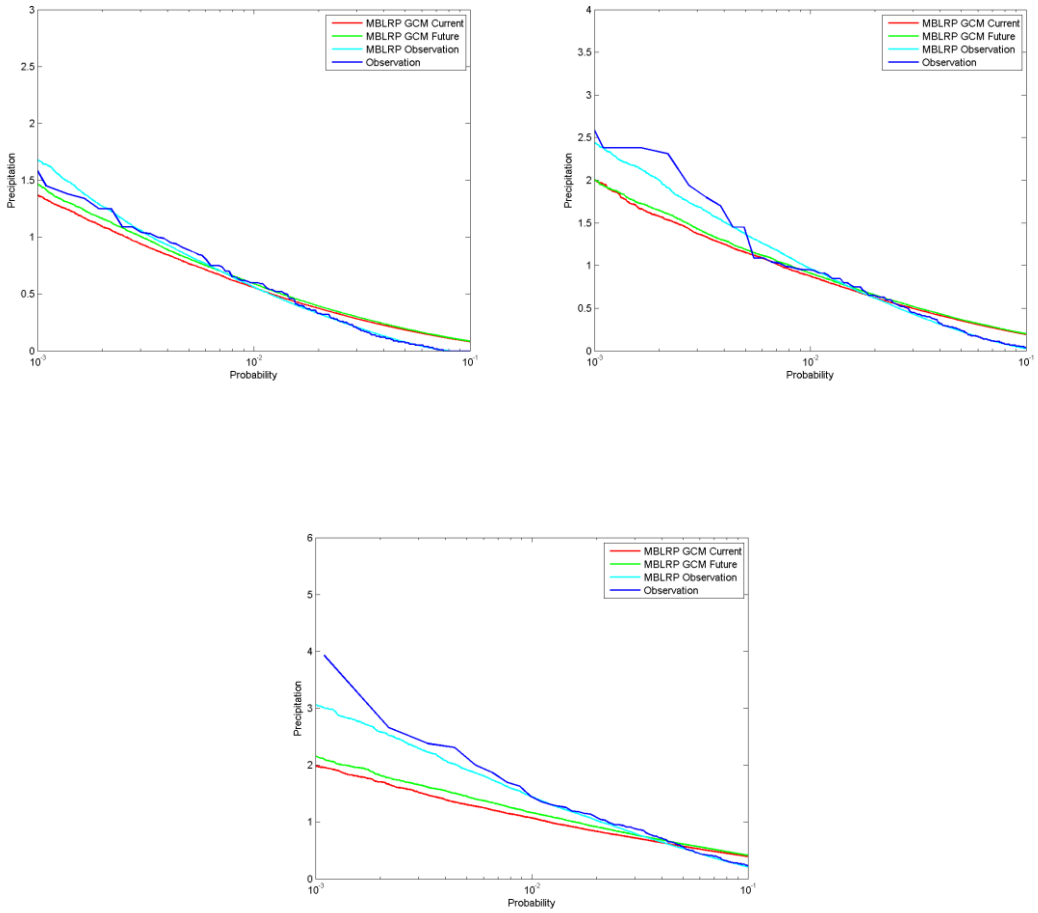

Duration curves of COOP: 414329 rainfall station for different accumulation levels' precipitation. From the top to bottom and left to right, 6-, 12-, and 24-hour levels.

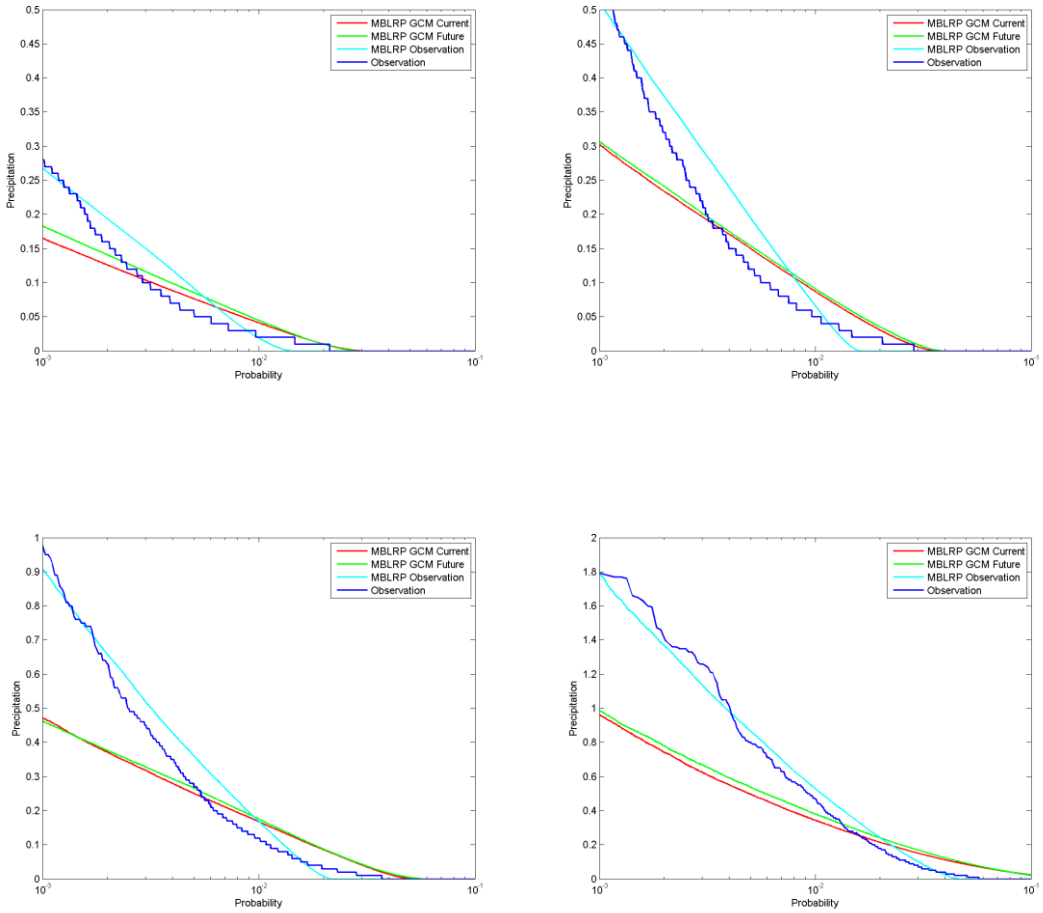

Duration curves of COOP: 417594 rainfall station for different accumulation levels' precipitation. From the top to bottom and left to right, 15-, 30-minute, 1-, and 3-hour levels.

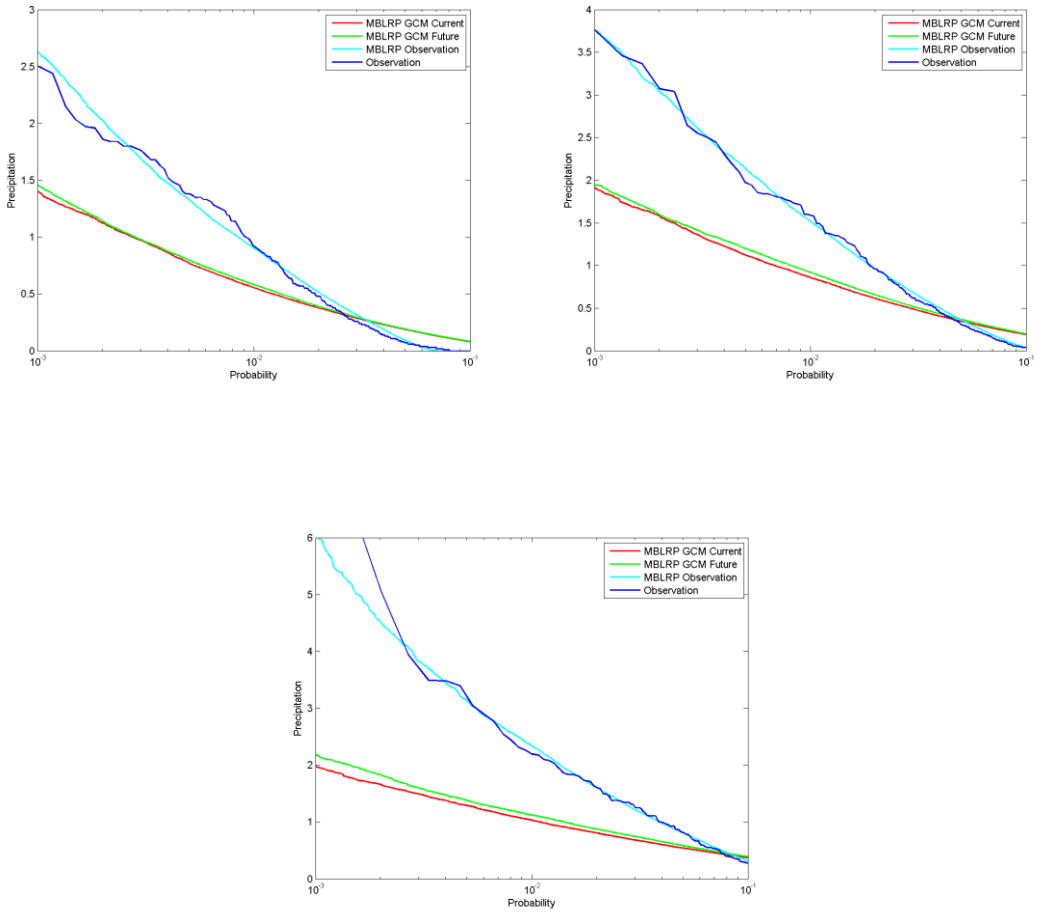

Duration curves of COOP: 417594 rainfall station for different accumulation levels' precipitation. From the top to bottom and left to right, 6-, 12-, and 24-hour levels.

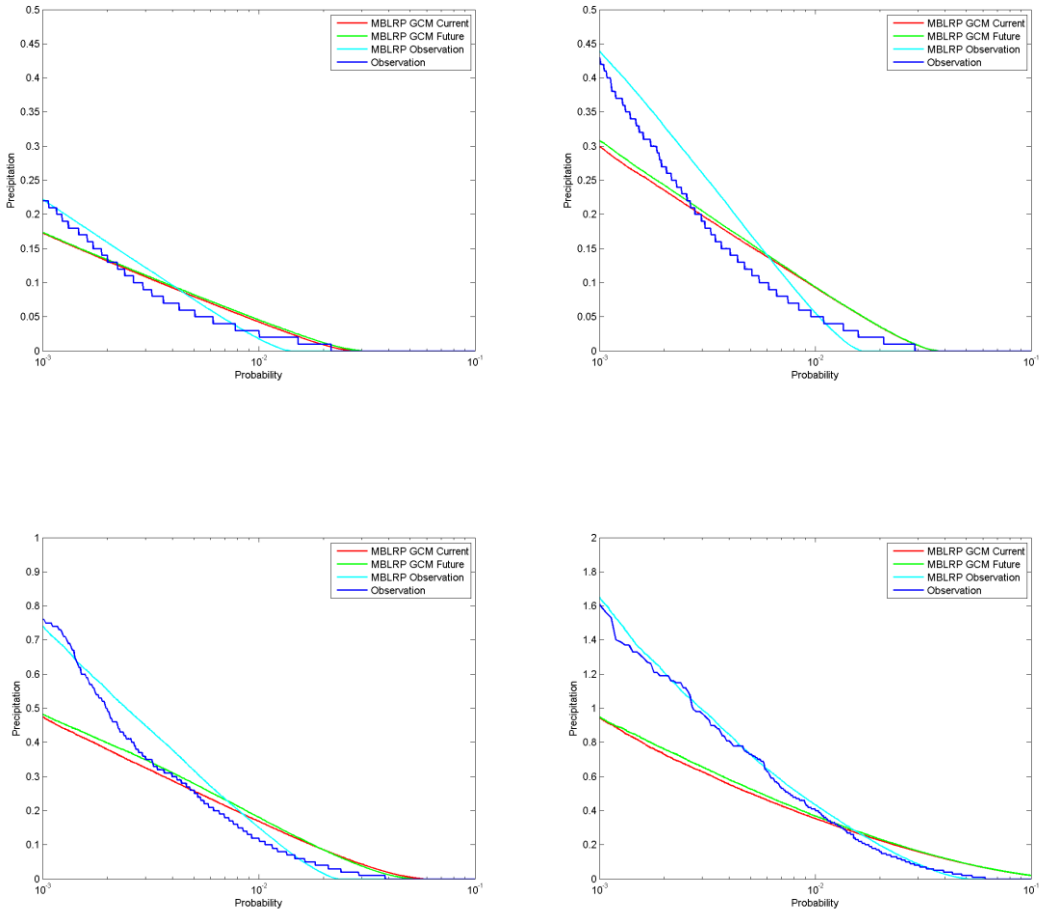

Duration curves of COOP: 418996 rainfall station for different accumulation levels' precipitation. From the top to bottom and left to right, 15-, 30-minute, 1-, and 3-hour levels.

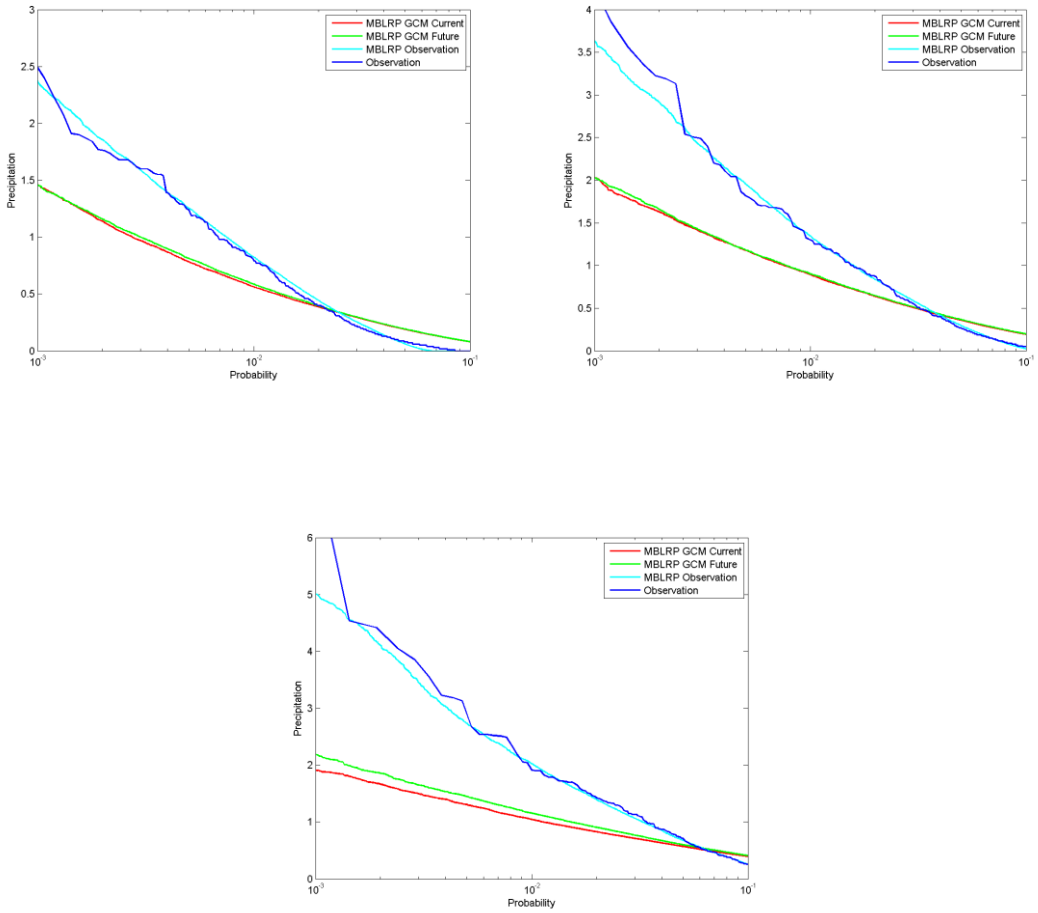

Duration curves of COOP: 418996 rainfall station for different accumulation levels' precipitation. From the top to bottom and left to right, 6-, 12-, and 24-hour levels.

Miroc-esm.1 model:

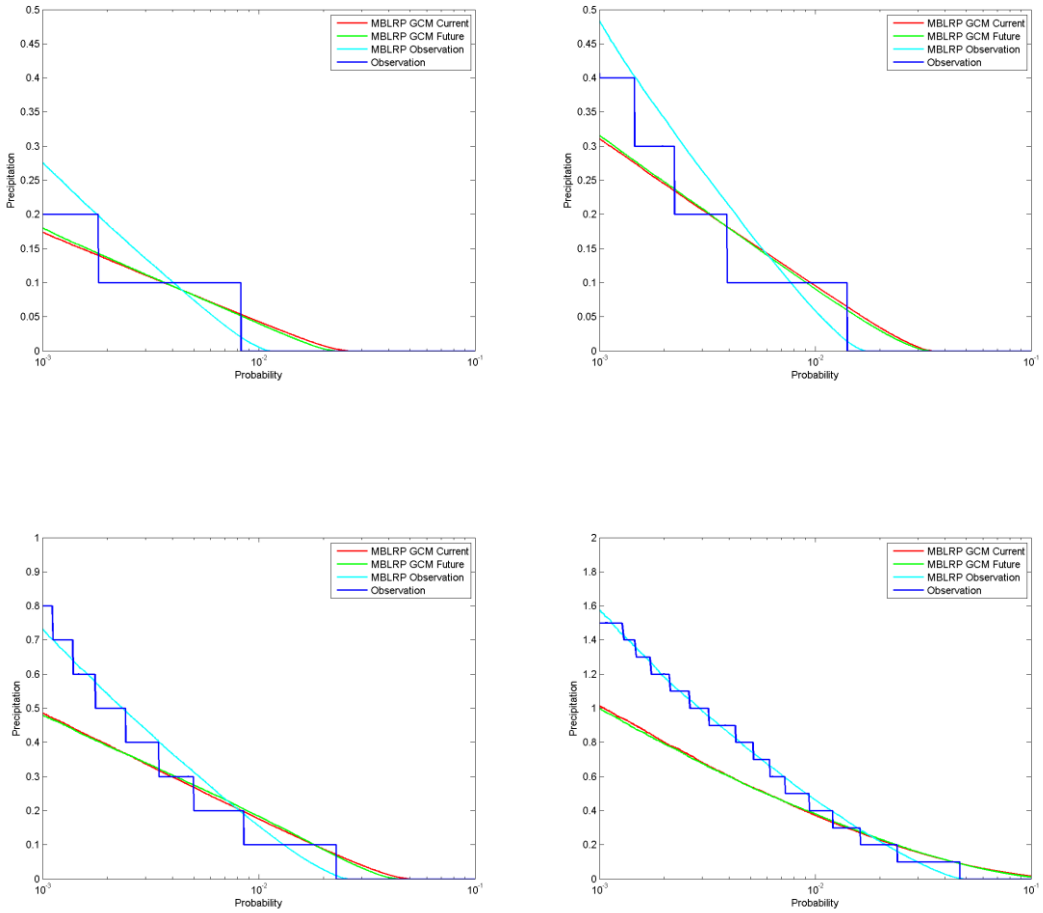

Duration curves of COOP: 411956 rainfall station for different accumulation levels' precipitation. From the top to bottom and left to right, 15-, 30-minute, 1-, and 3-hour levels.

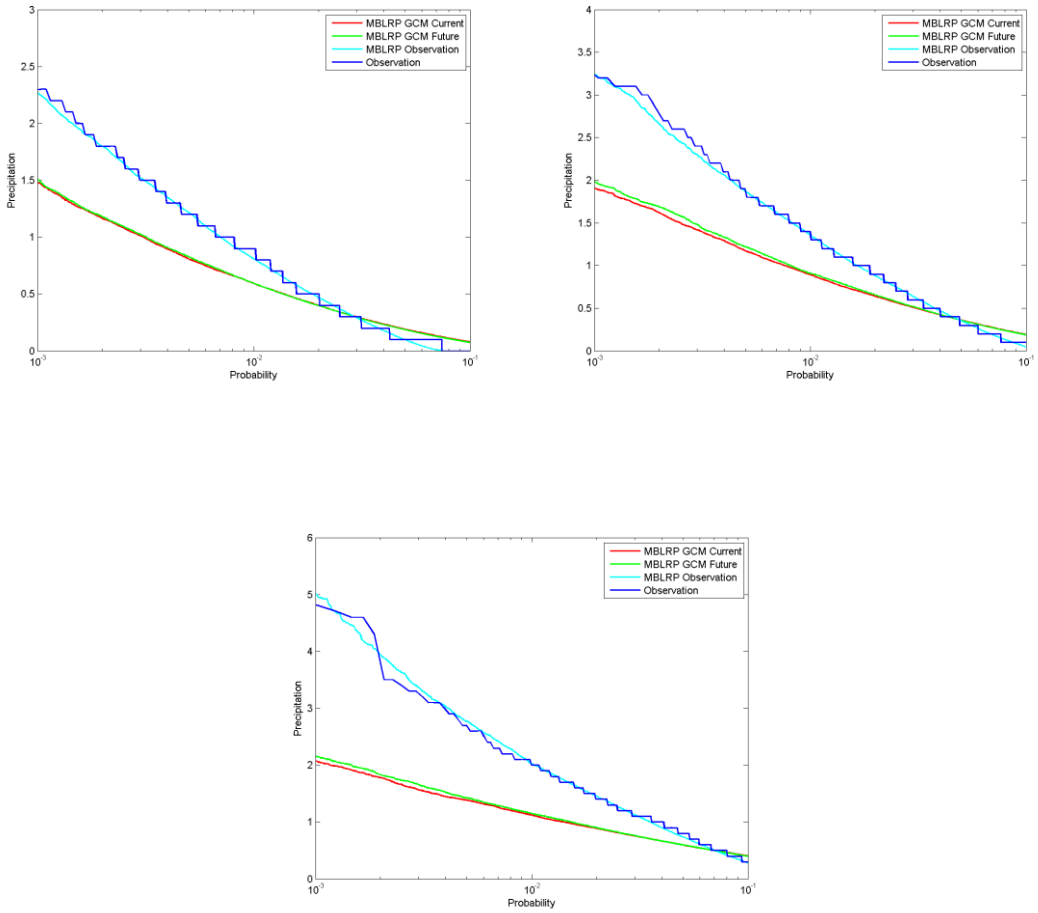

Duration curves of COOP: 411956 rainfall station for different accumulation levels' precipitation. From the top to bottom and left to right, 6-, 12-, and 24-hour levels.

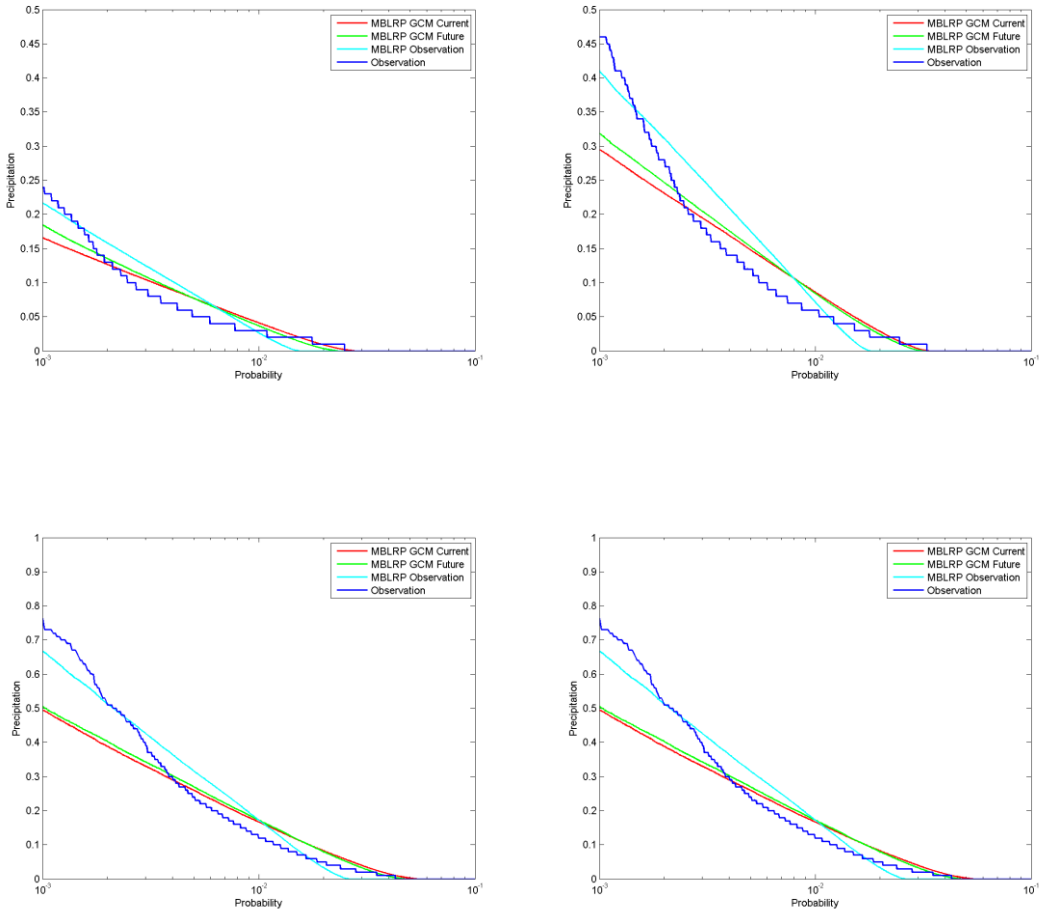

Duration curves of COOP: 412206 rainfall station for different accumulation levels' precipitation. From the top to bottom and left to right, 15-, 30-minute, 1-, and 3-hour levels.

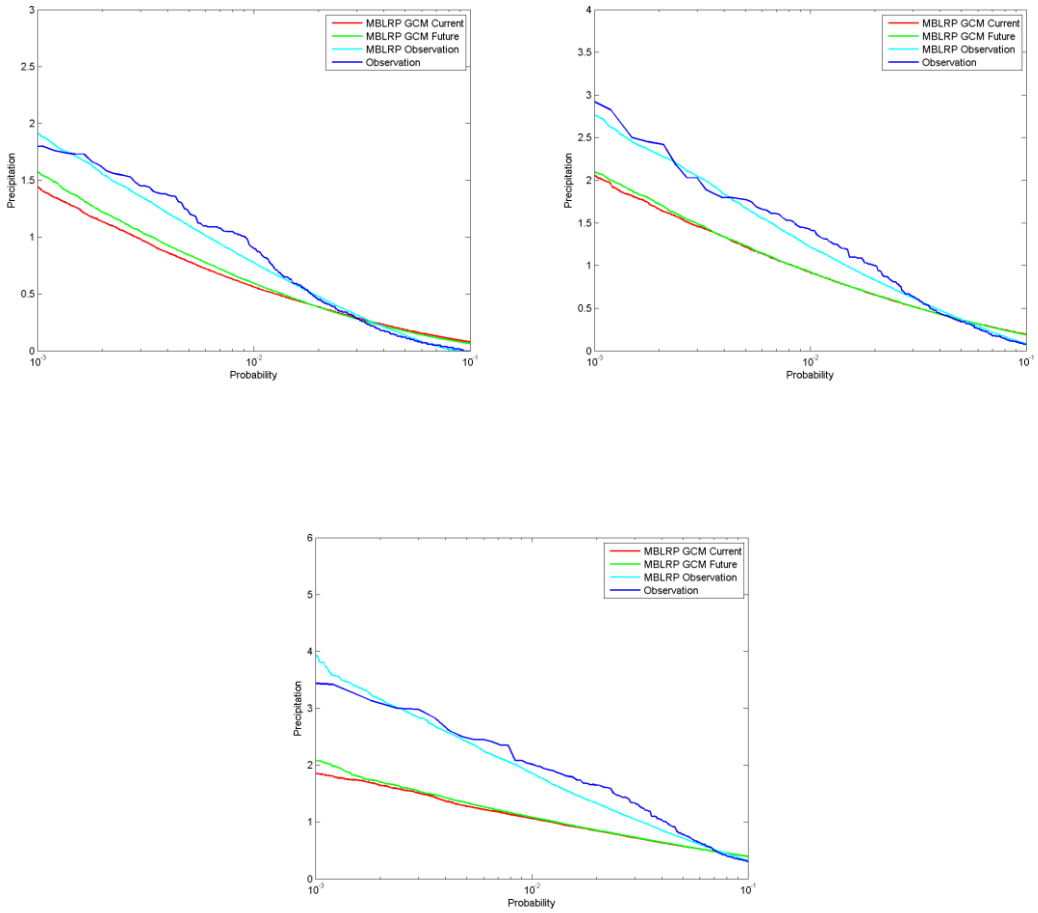

Duration curves of COOP: 412206 rainfall station for different accumulation levels' precipitation. From the top to bottom and left to right, 6-, 12-, and 24-hour levels.

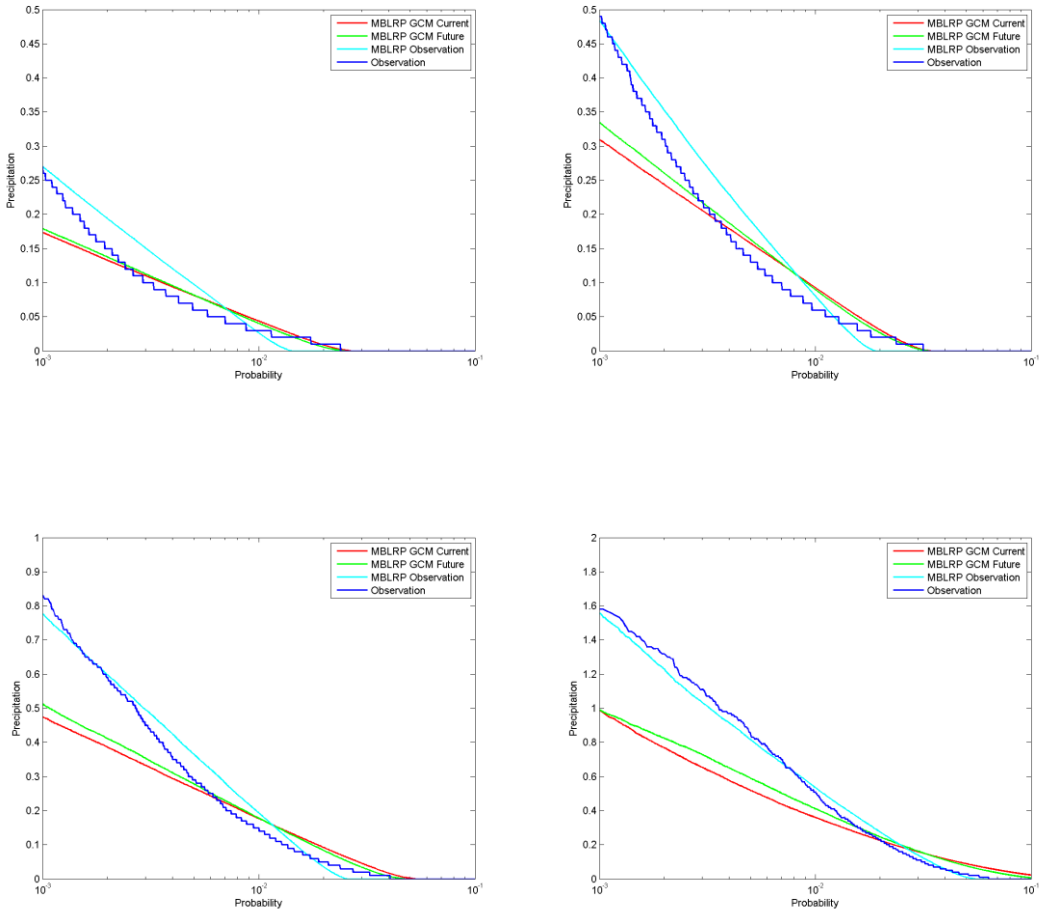

Duration curves of COOP: 414309 rainfall station for different accumulation levels' precipitation. From the top to bottom and left to right, 15-, 30-, 1-, and 3-hour levels.

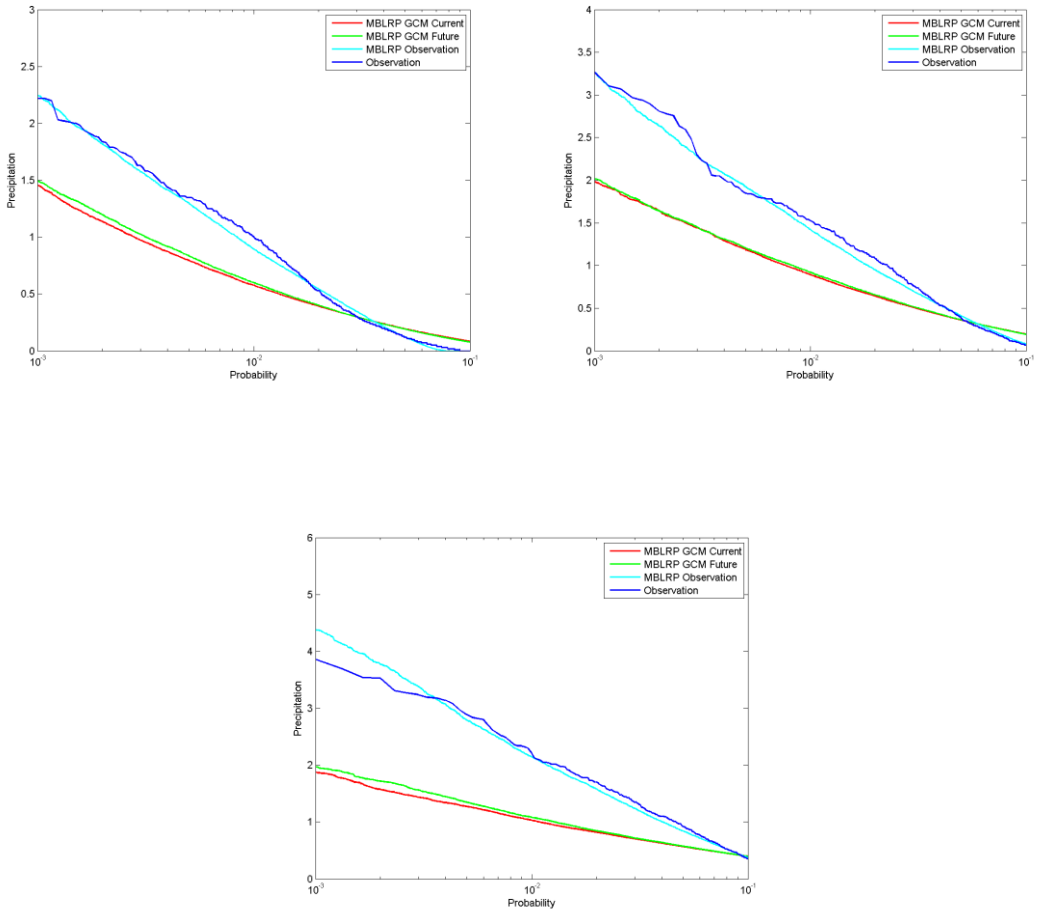

Duration curves of COOP: 414309 rainfall station for different accumulation levels' precipitation. From the top to bottom and left to right, 6-, 12-, and 24-hour levels.

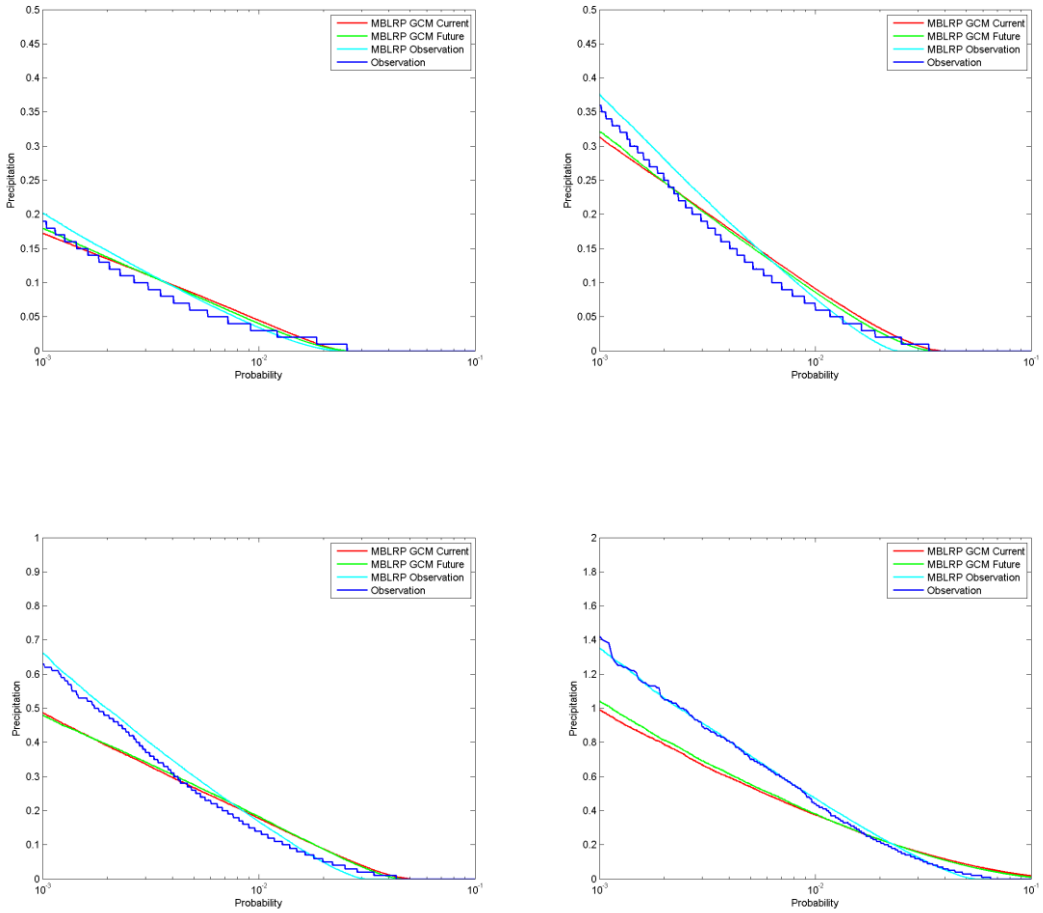

Duration curves of COOP: 414311 rainfall station for different accumulation levels' precipitation. From the top to bottom and left to right, 15-, 30-, 1-, and 3-hour levels.

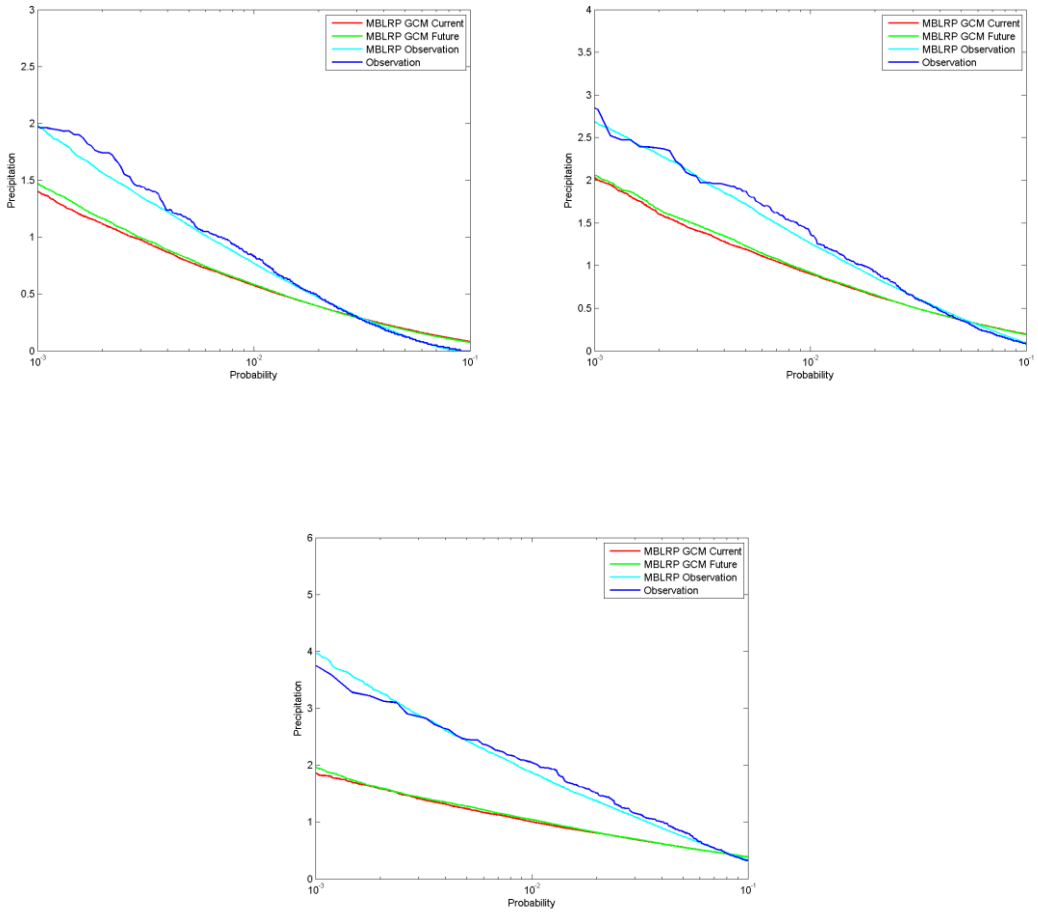

Duration curves of COOP: 414311 rainfall station for different accumulation levels' precipitation. From the top to bottom and left to right, 6-, 12-, and 24-hour levels.

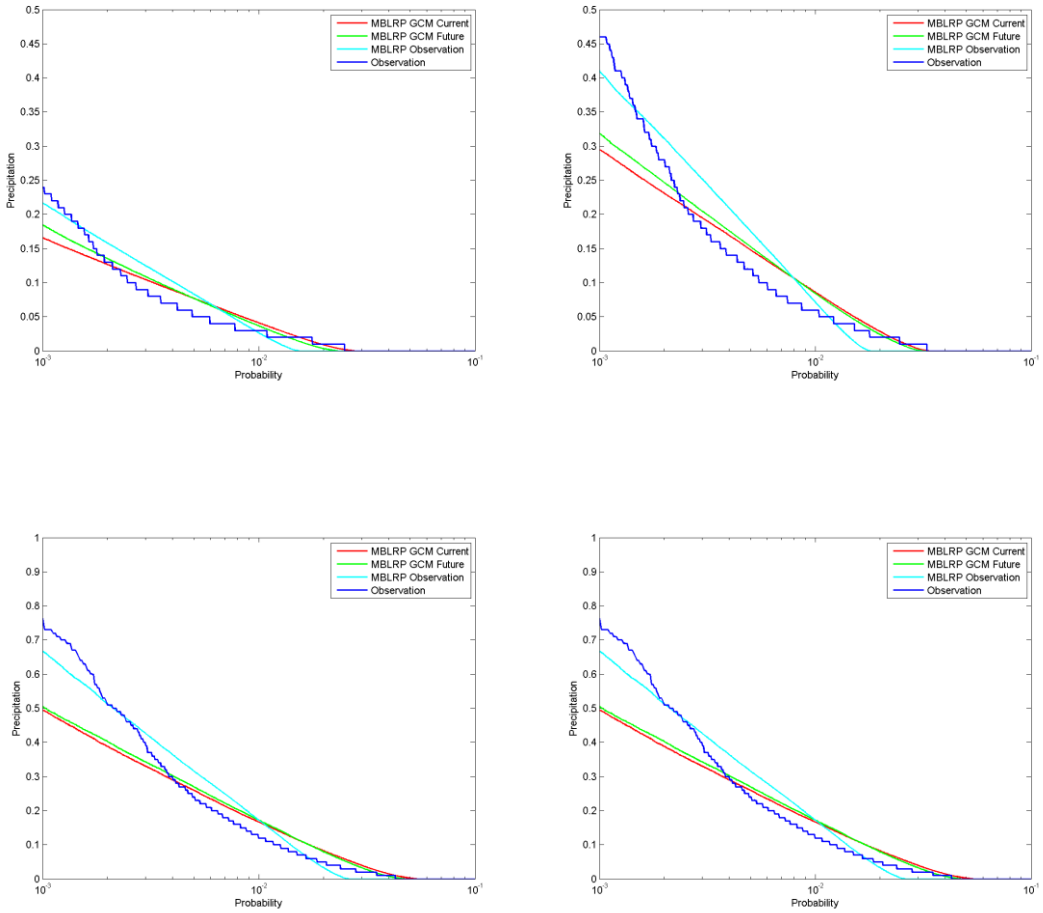

Duration curves of COOP: 414329 rainfall station for different accumulation levels' precipitation. From the top to bottom and left to right, 15-, 30-minute, 1-, and 3-hour levels.

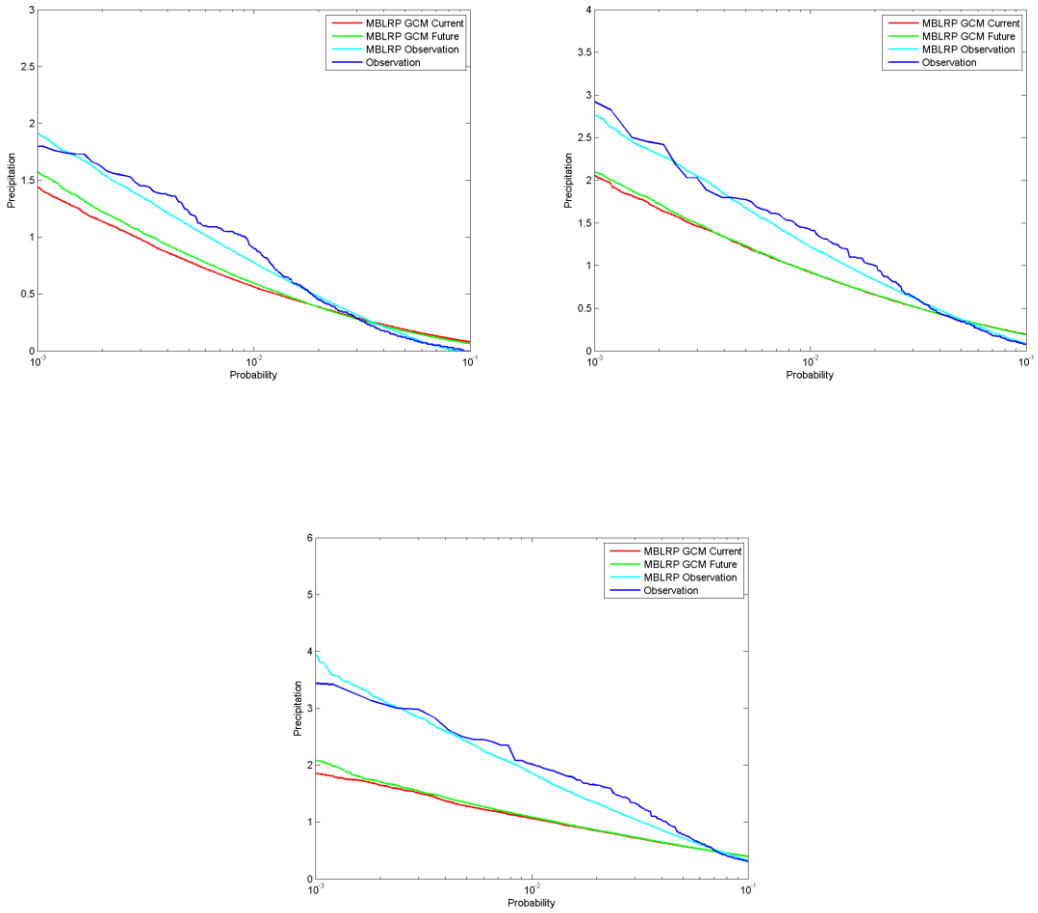

Duration curves of COOP: 414329 rainfall station for different accumulation levels' precipitation. From the top to bottom and left to right, 6-, 12-, and 24-hour levels.

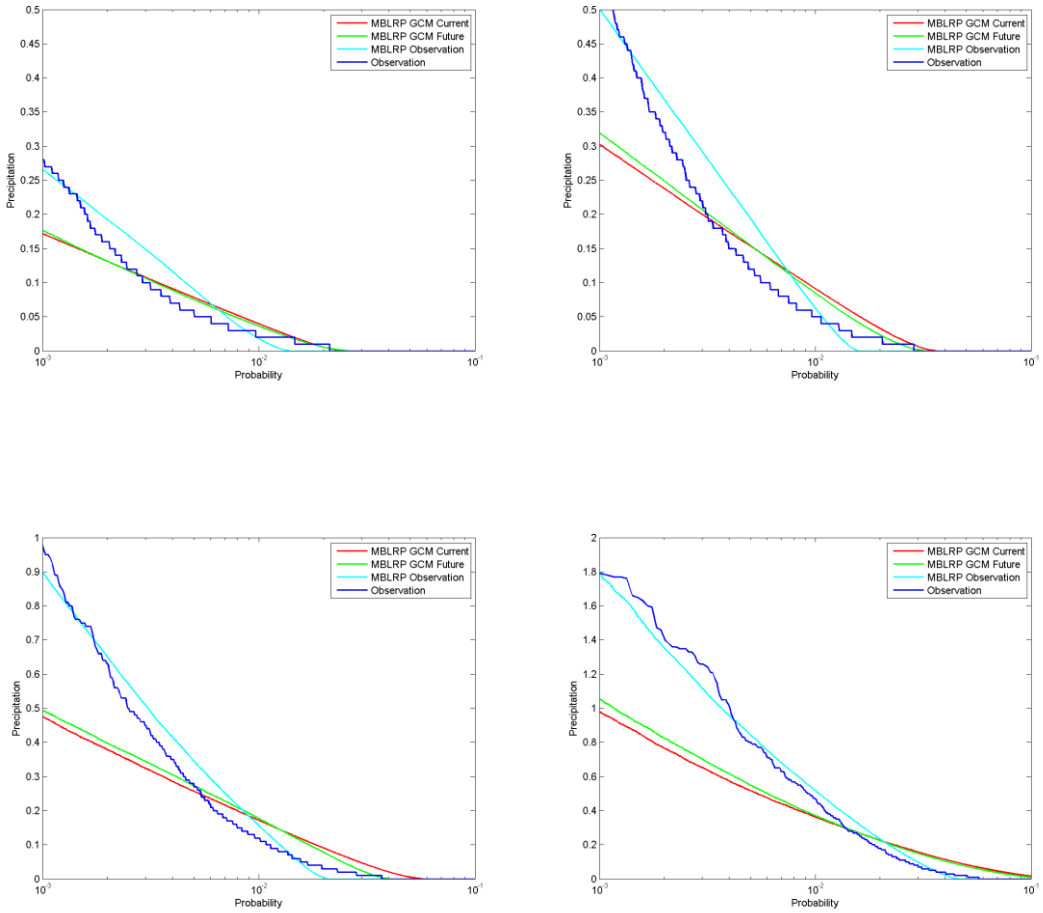

Duration curves of COOP: 417594 rainfall station for different accumulation levels' precipitation. From the top to bottom and left to right, 15-, 30-minute, 1-, and 3-hour levels.

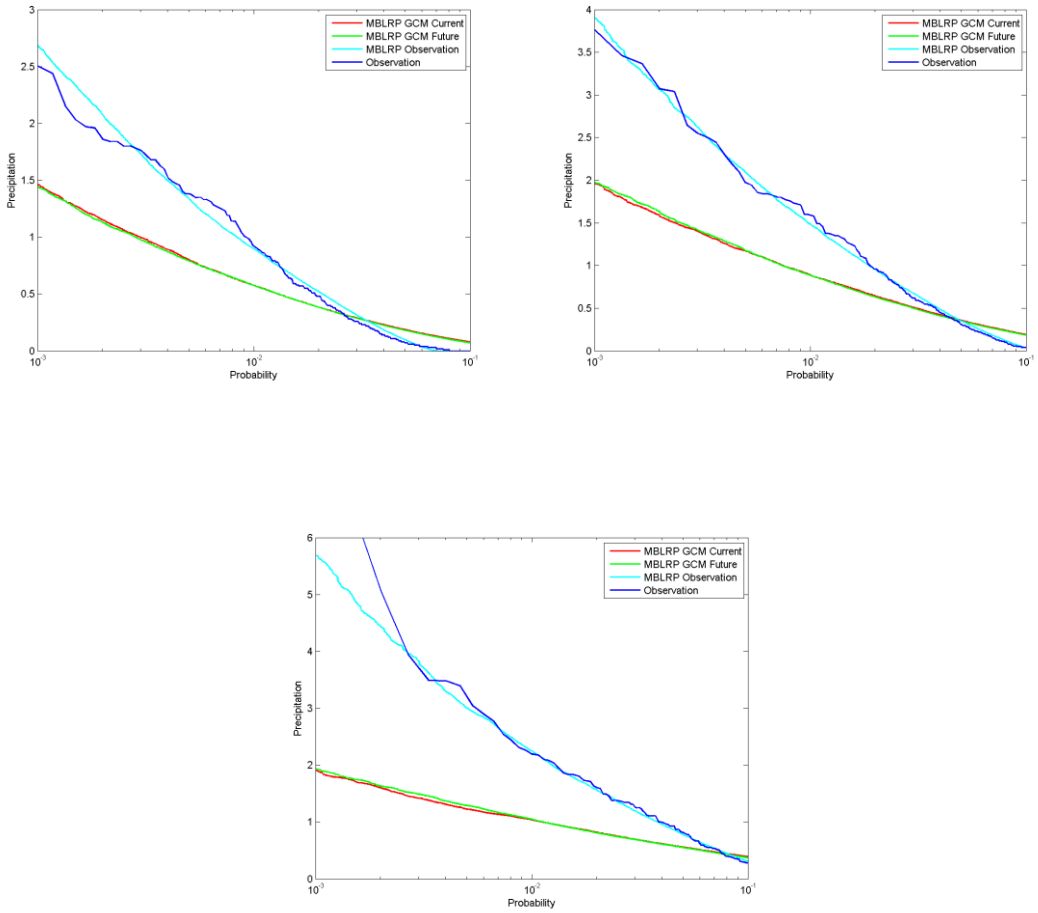

Duration curves of COOP: 417594 rainfall station for different accumulation levels' precipitation. From the top to bottom and left to right, 6-, 12-, and 24-hour levels.

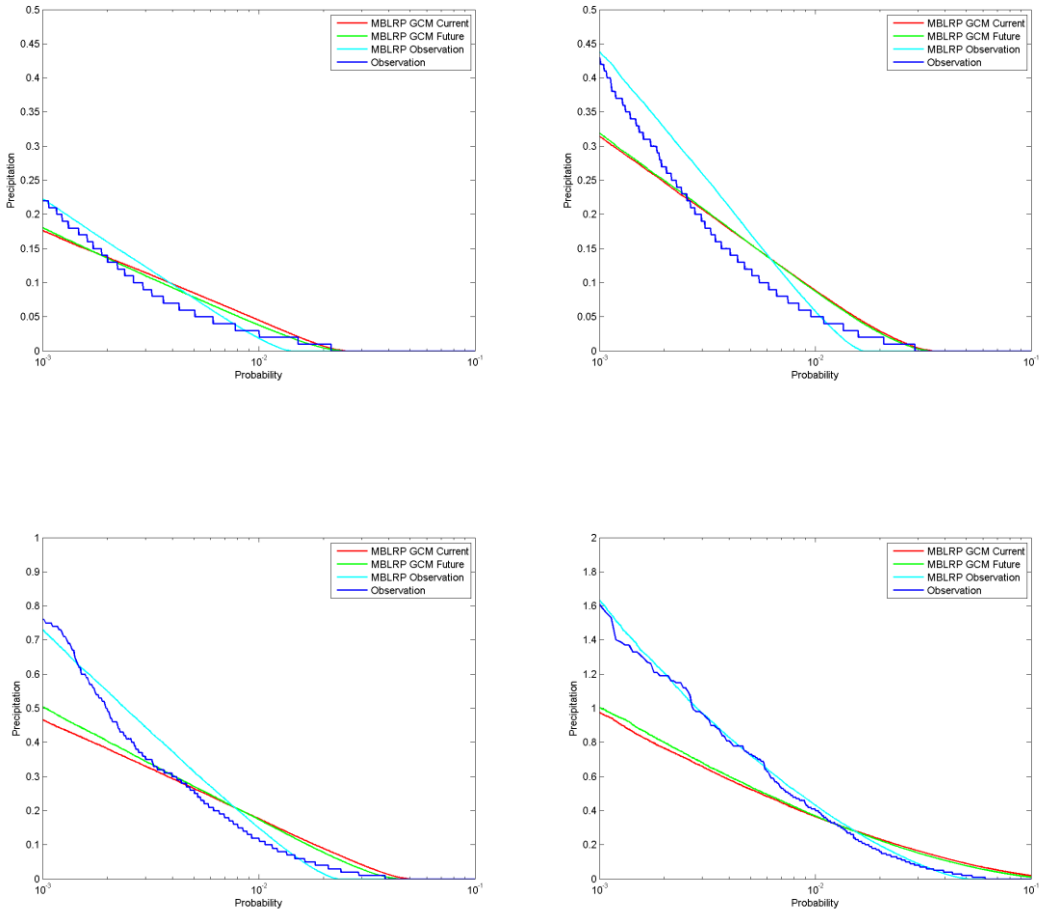

Duration curves of COOP: 418996 rainfall station for different accumulation levels' precipitation. From the top to bottom and left to right, 15-, 30-minute, 1-, and 3-hour levels.

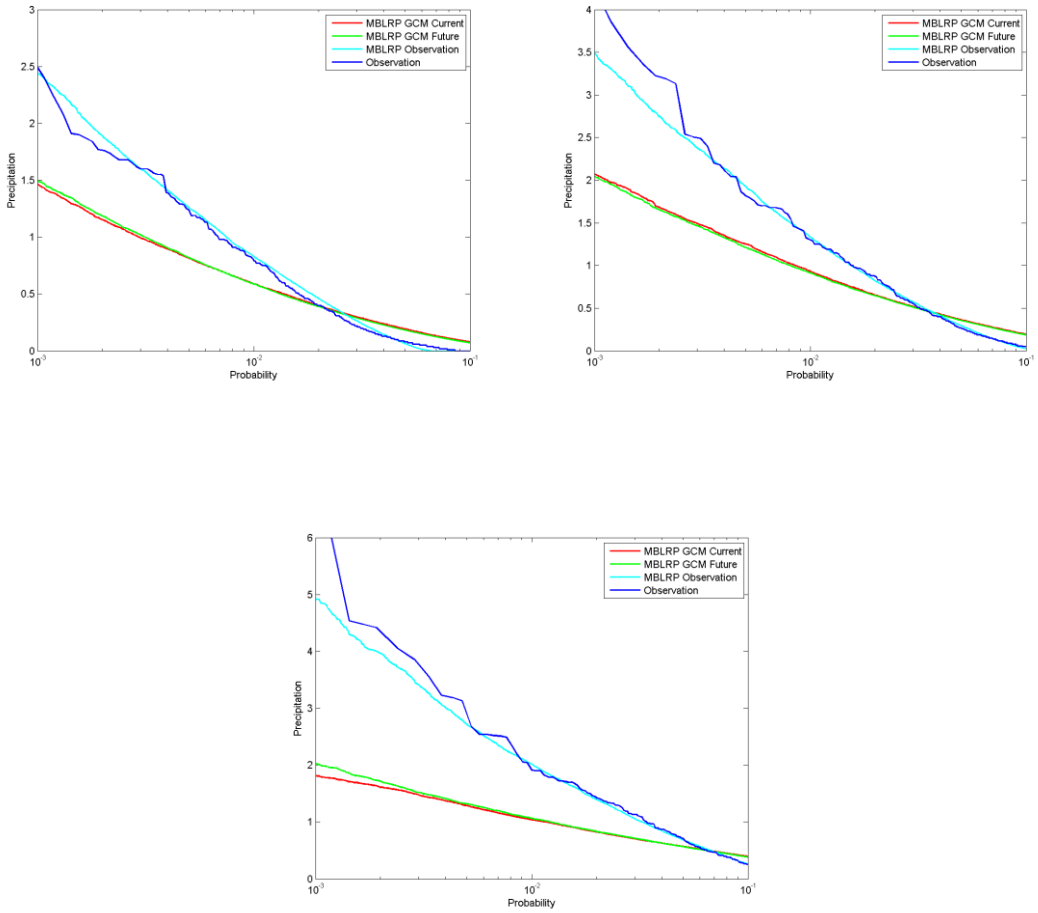

Duration curves of COOP: 418996 rainfall station for different accumulation levels' precipitation. From the top to bottom and left to right, 6-, 12-, and 24-hour levels.

Miroc-esm-chem.1 model:

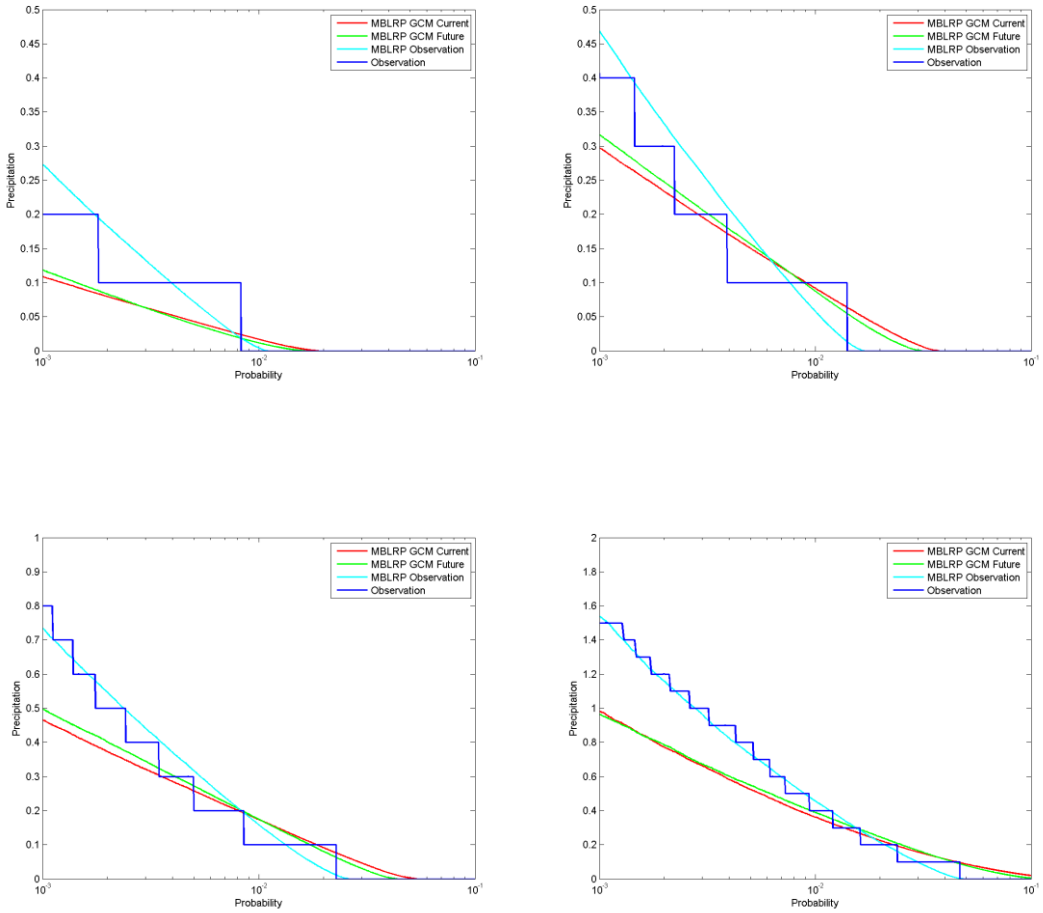

Duration curves of COOP: 411956 rainfall station for different accumulation levels' precipitation. From the top to bottom and left to right, 15-, 30-minute, 1-, and 3-hour levels.

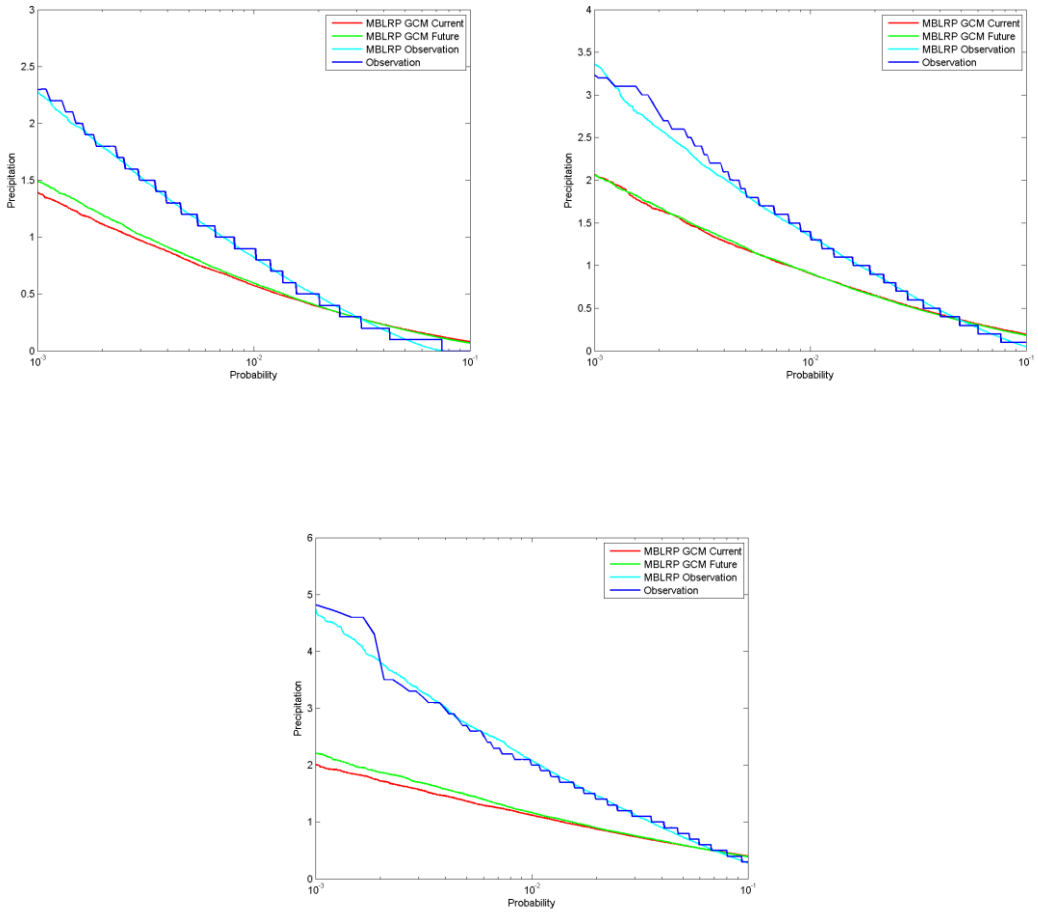

Duration curves of COOP: 411956 rainfall station for different accumulation levels' precipitation. From the top to bottom and left to right, 6-, 12-, and 24-hour levels.

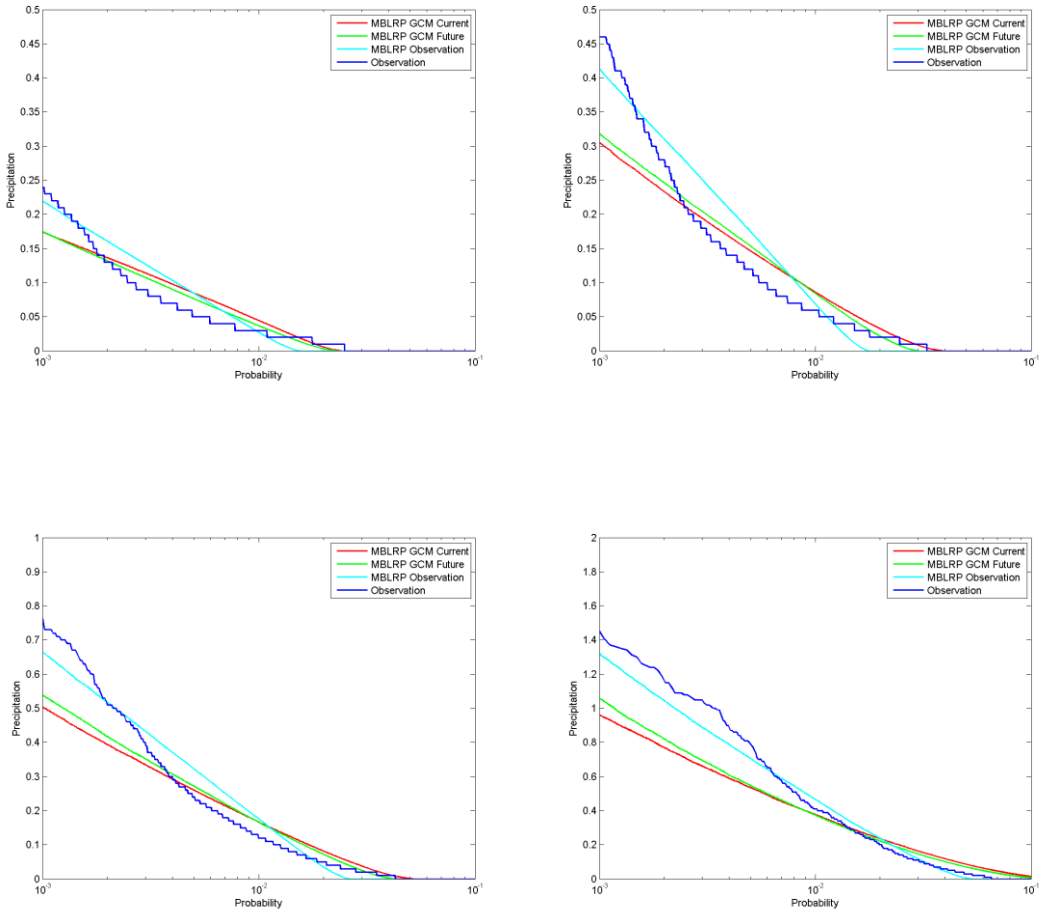

Duration curves of COOP: 412206 rainfall station for different accumulation levels' precipitation. From the top to bottom and left to right, 15-, 30-minute, 1-, and 3-hour levels.

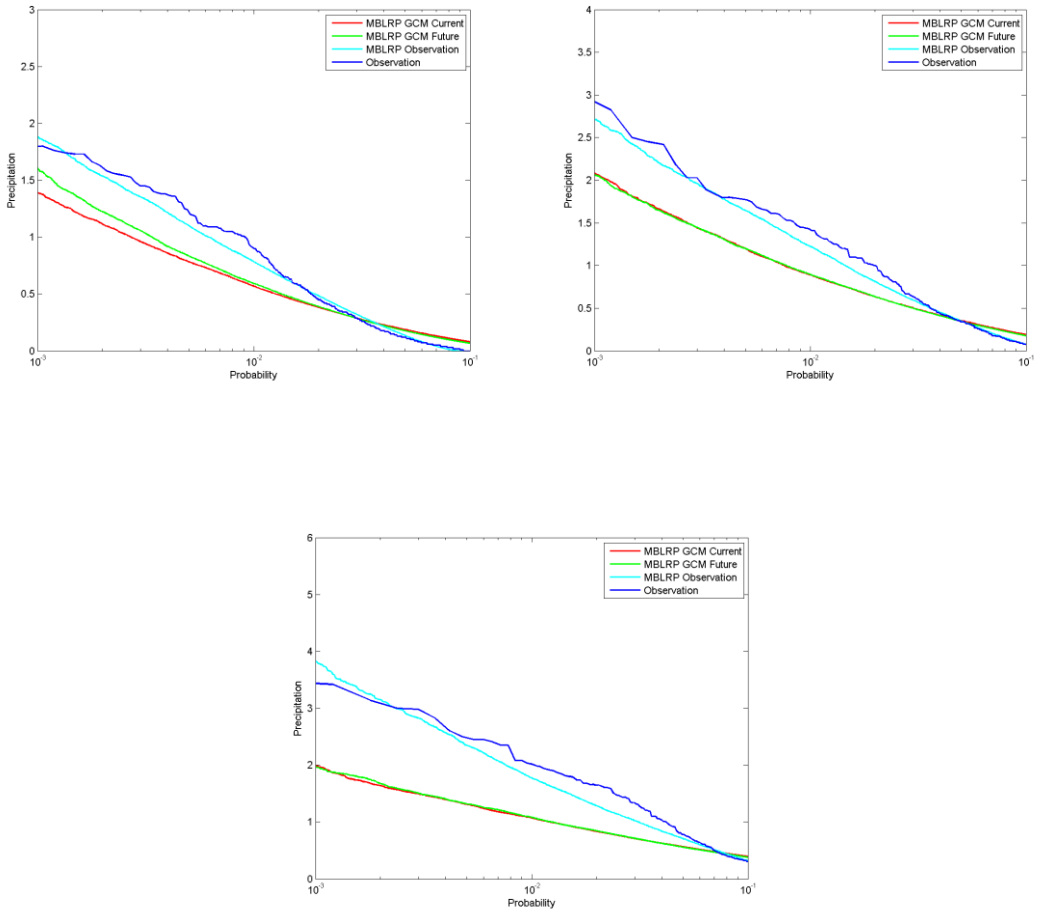

Duration curves of COOP: 412206 rainfall station for different accumulation levels' precipitation. From the top to bottom and left to right, 6-, 12-, and 24-hour levels.

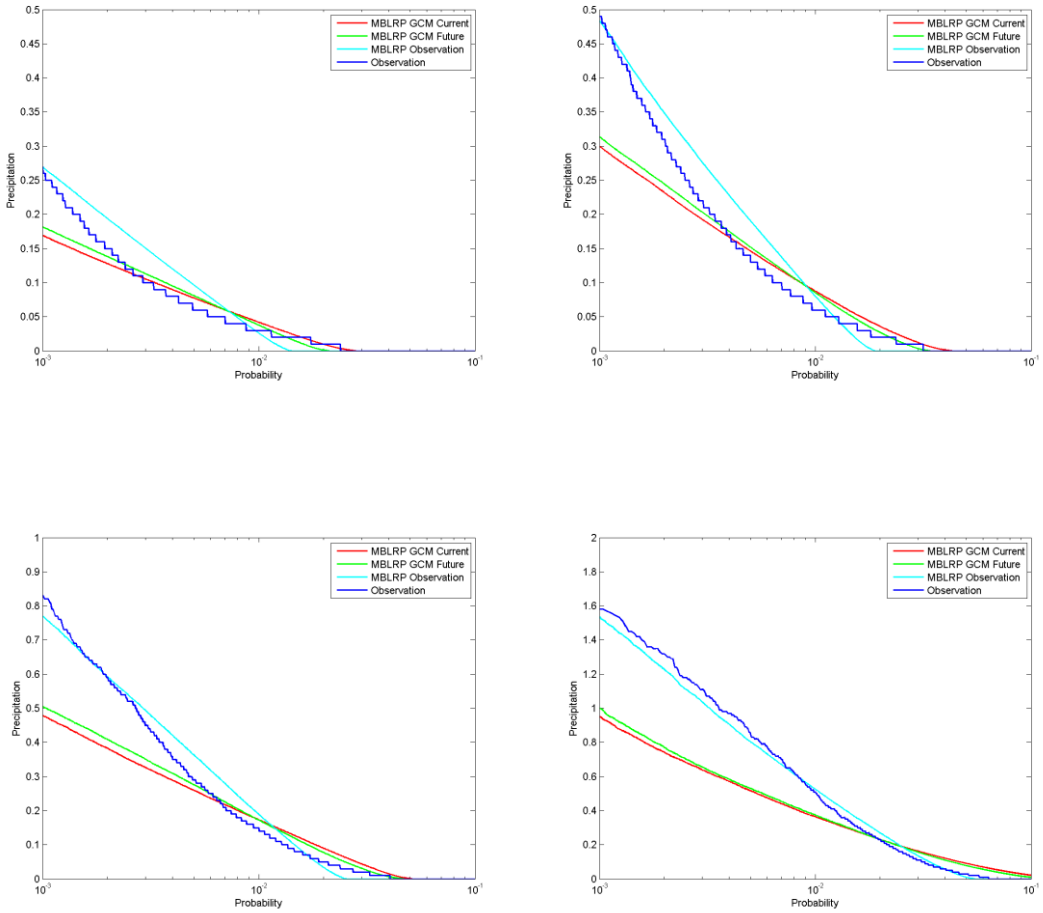

Duration curves of COOP: 414309 rainfall station for different accumulation levels' precipitation. From the top to bottom and left to right, 15-, 30-, 1-, and 3-hour levels.

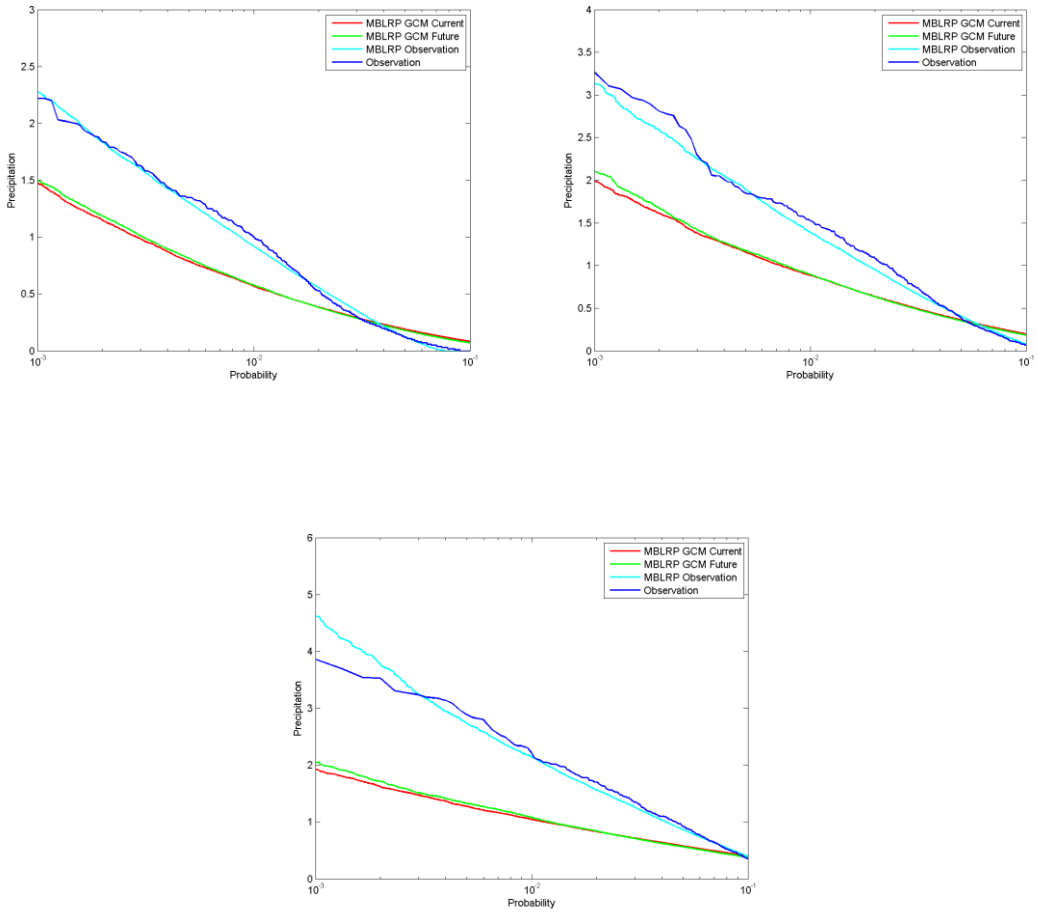

Duration curves of COOP: 414309 rainfall station for different accumulation levels' precipitation. From the top to bottom and left to right, 6-, 12-, and 24-hour levels.

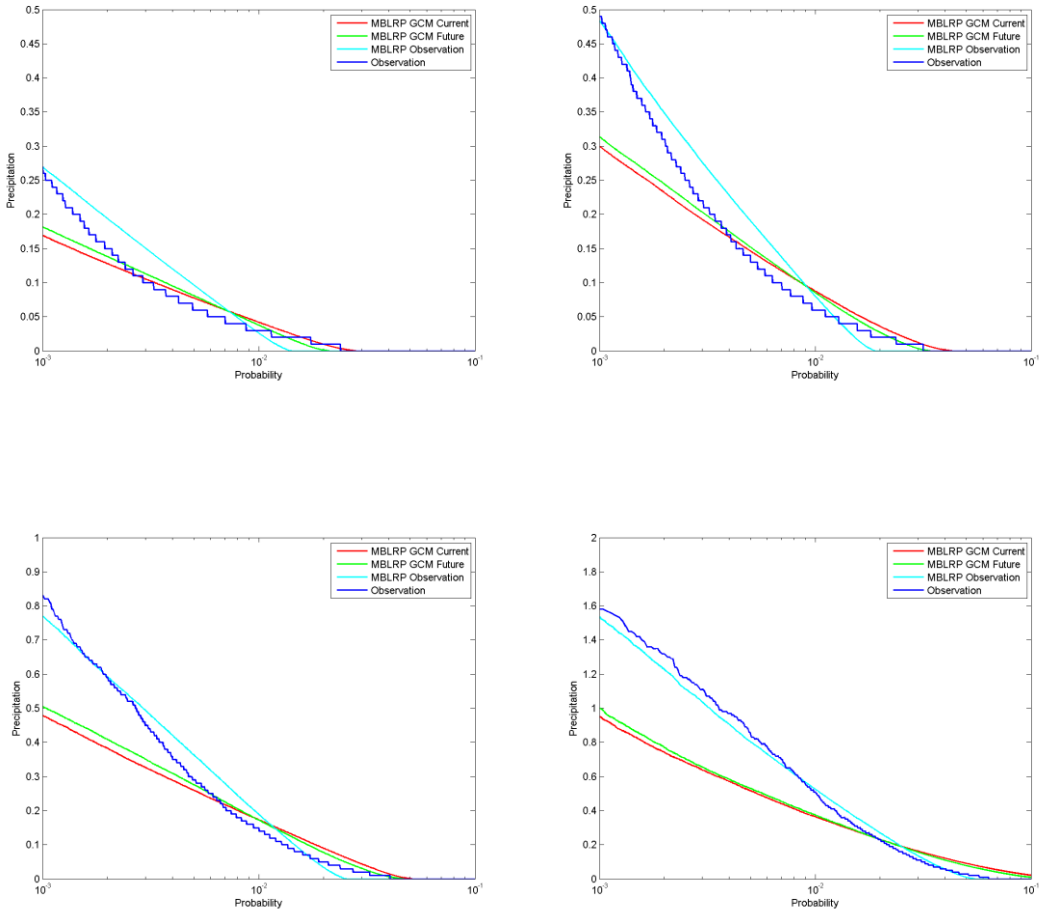

Duration curves of COOP: 414311 rainfall station for different accumulation levels' precipitation. From the top to bottom and left to right, 15-, 30-, 1-, and 3-hour levels.

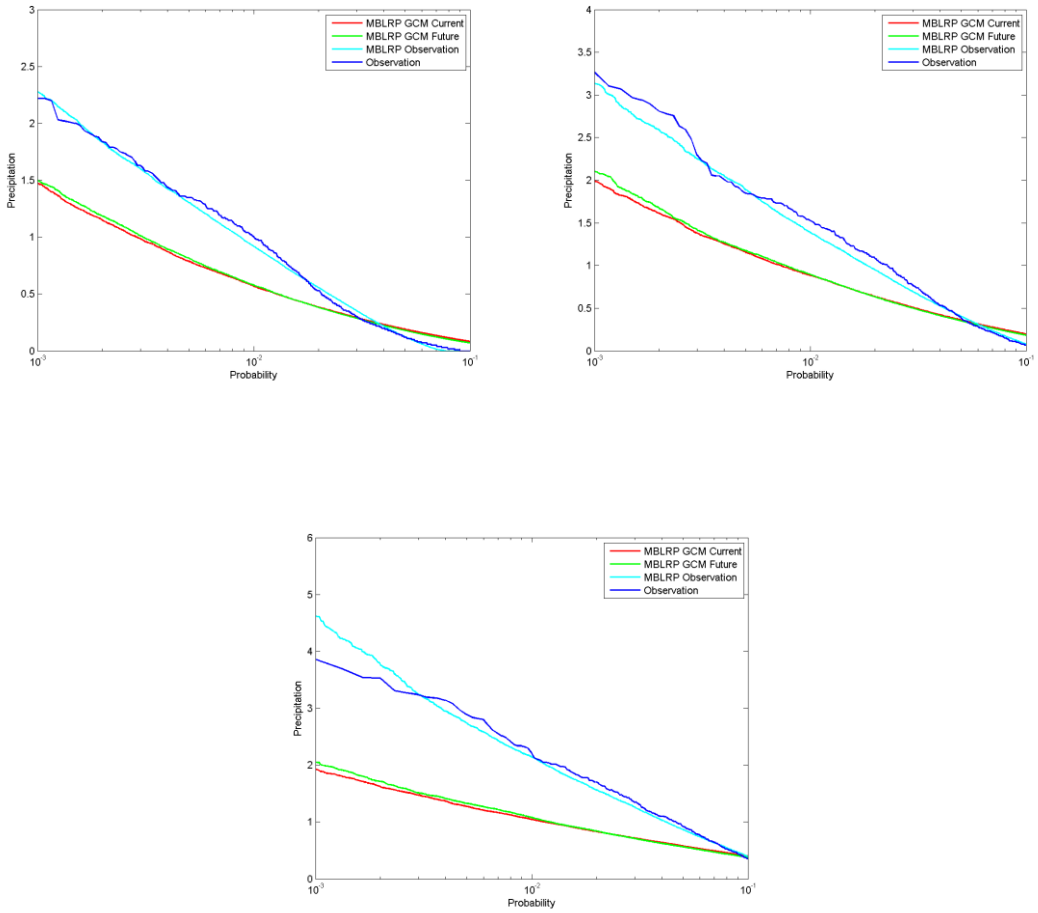

Duration curves of COOP: 414311 rainfall station for different accumulation levels' precipitation. From the top to bottom and left to right, 6-, 12-, and 24-hour levels.

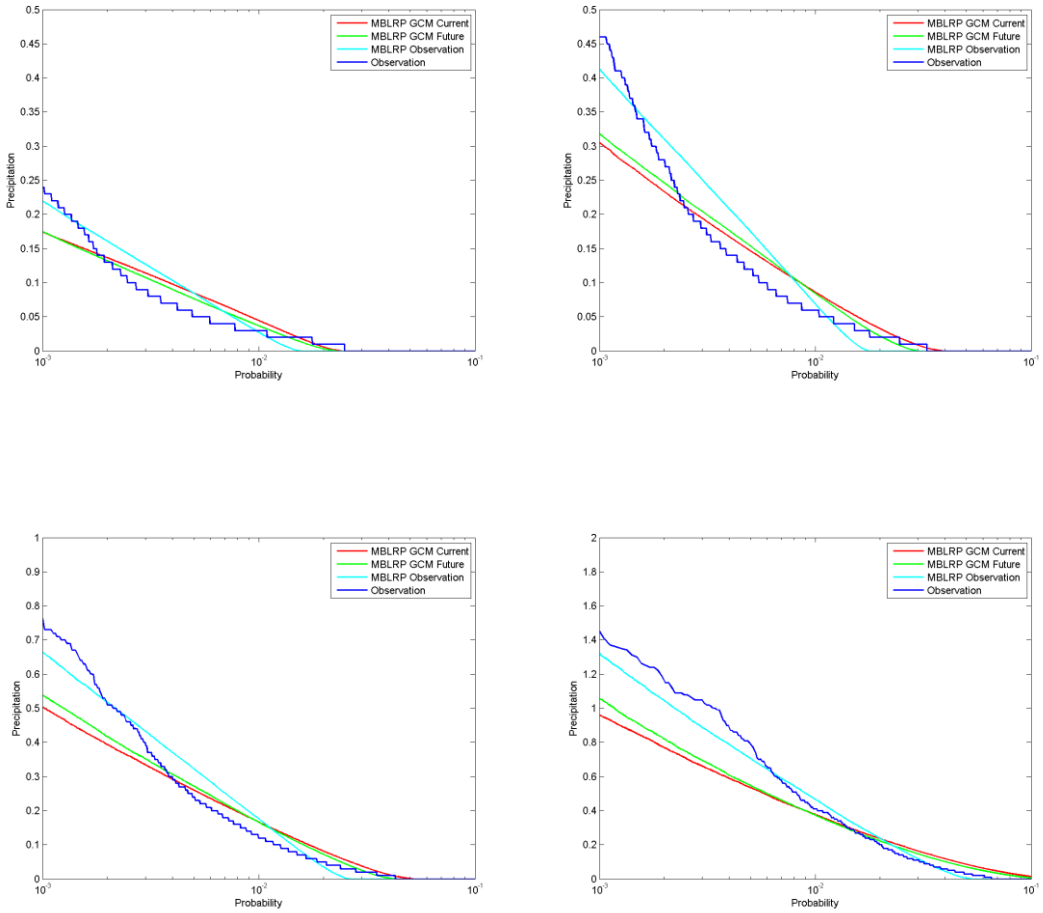

Duration curves of COOP: 414329 rainfall station for different accumulation levels' precipitation. From the top to bottom and left to right, 15-, 30-minute, 1-, and 3-hour levels.

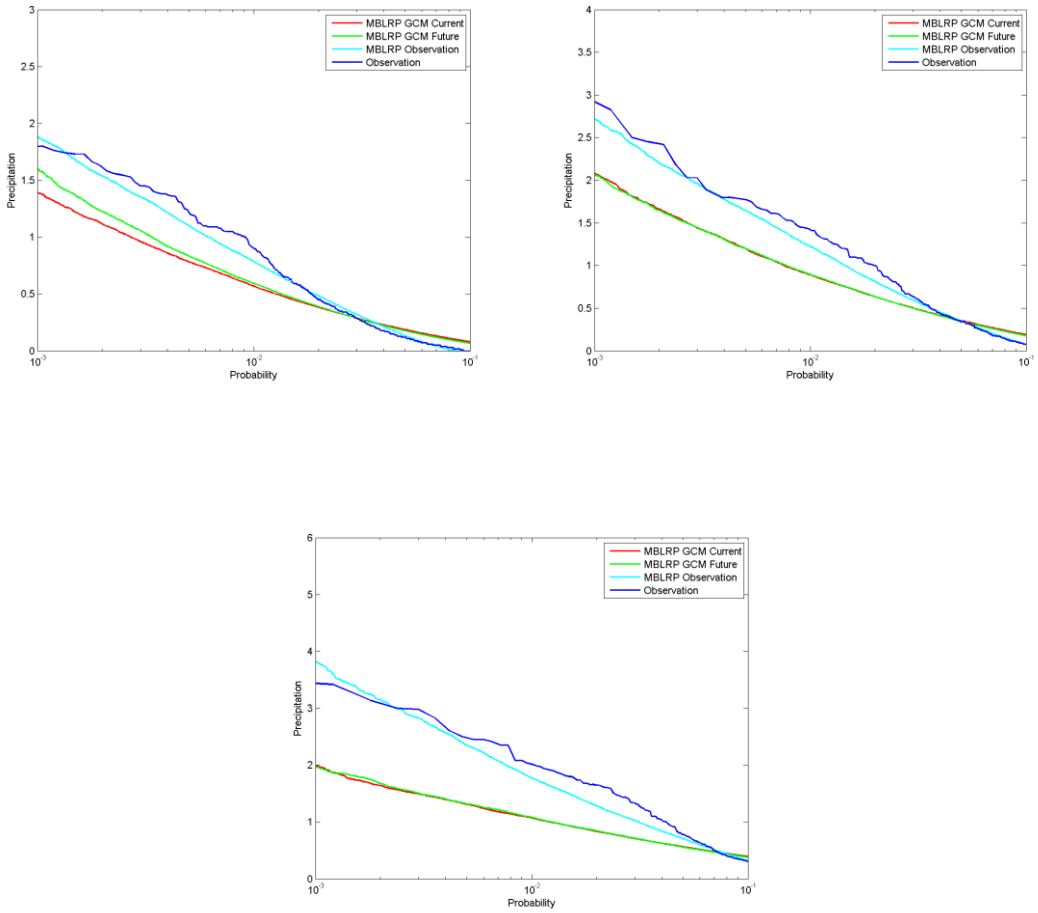

Duration curves of COOP: 414329 rainfall station for different accumulation levels' precipitation. From the top to bottom and left to right, 6-, 12-, and 24-hour levels.

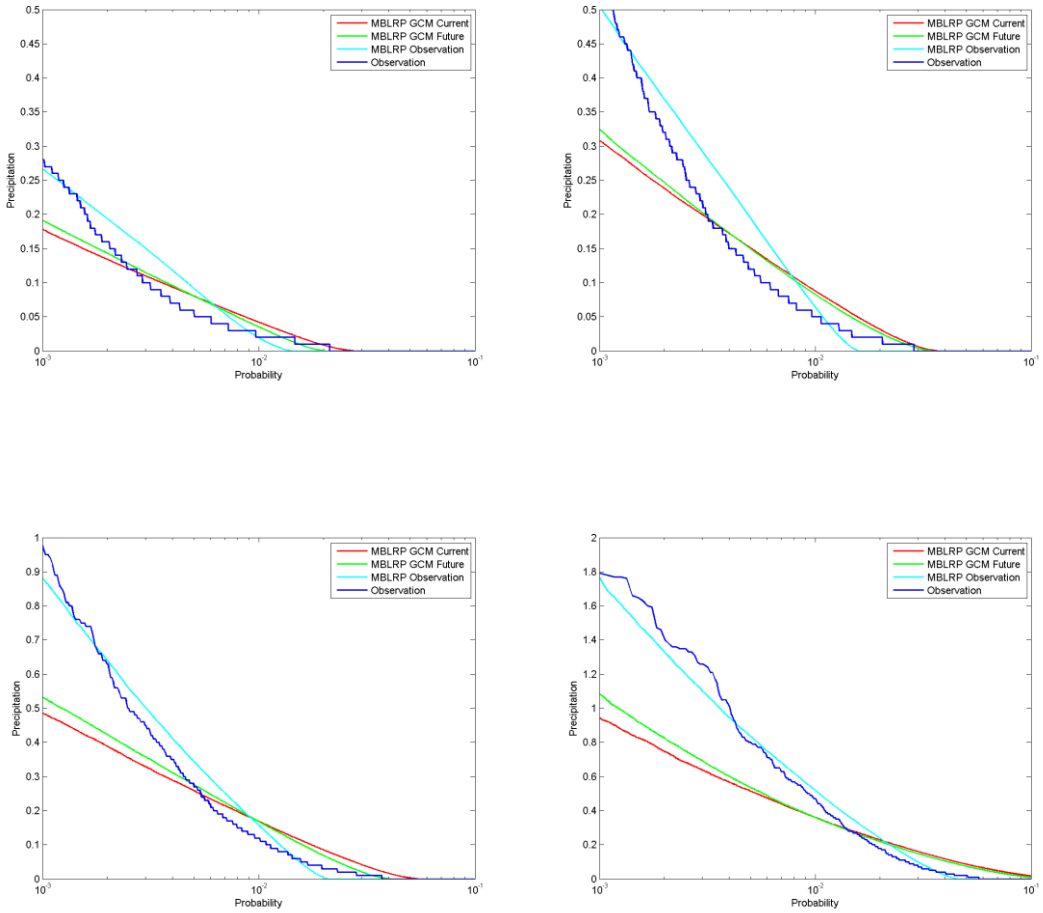

Duration curves of COOP: 417594 rainfall station for different accumulation levels' precipitation. From the top to bottom and left to right, 15-, 30-minute, 1-, and 3-hour levels.

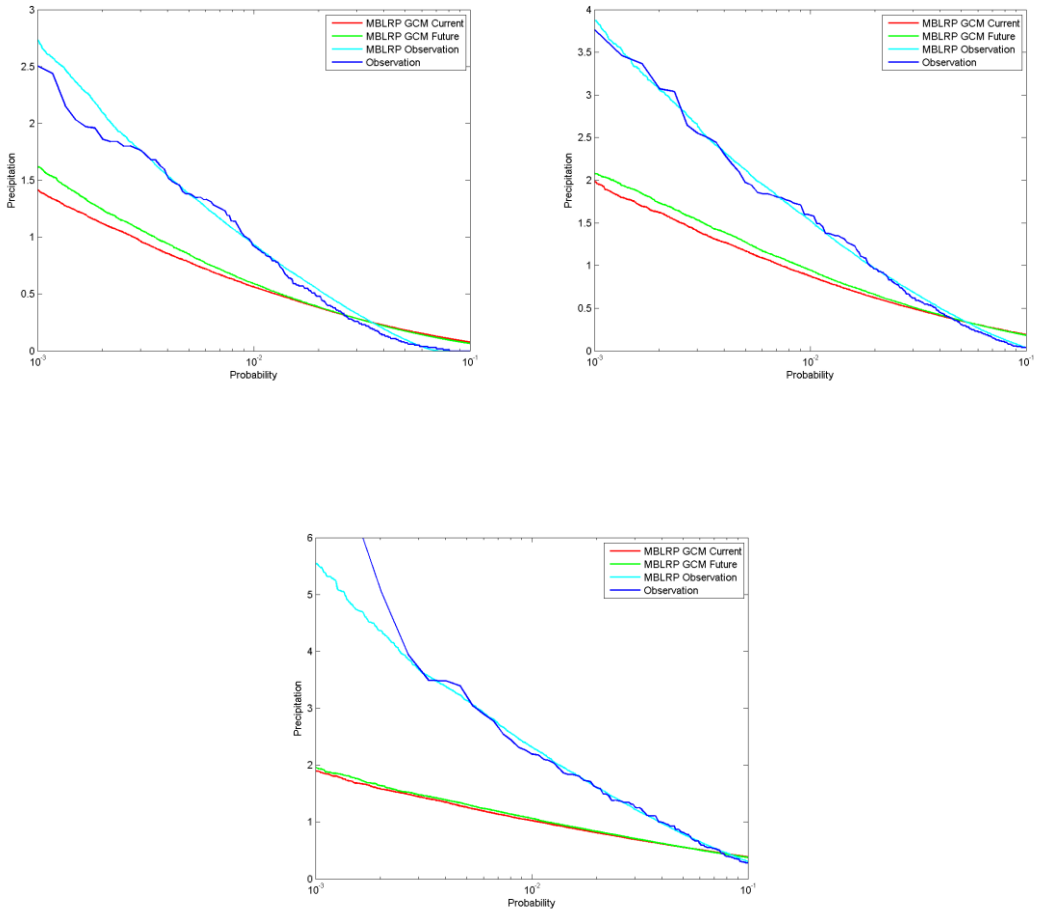

Duration curves of COOP: 417594 rainfall station for different accumulation levels' precipitation. From the top to bottom and left to right, 6-, 12-, and 24-hour levels.

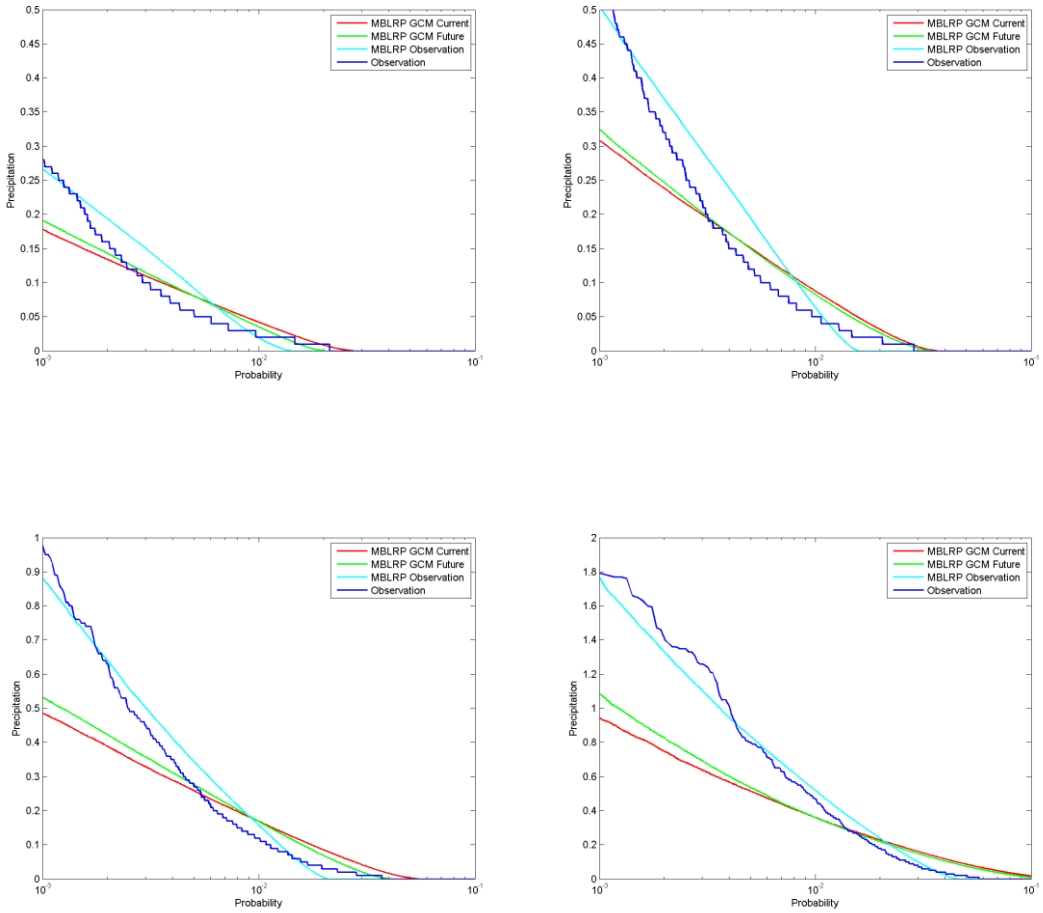

Duration curves of COOP: 418996 rainfall station for different accumulation levels' precipitation. From the top to bottom and left to right, 15-, 30-minute, 1-, and 3-hour levels.

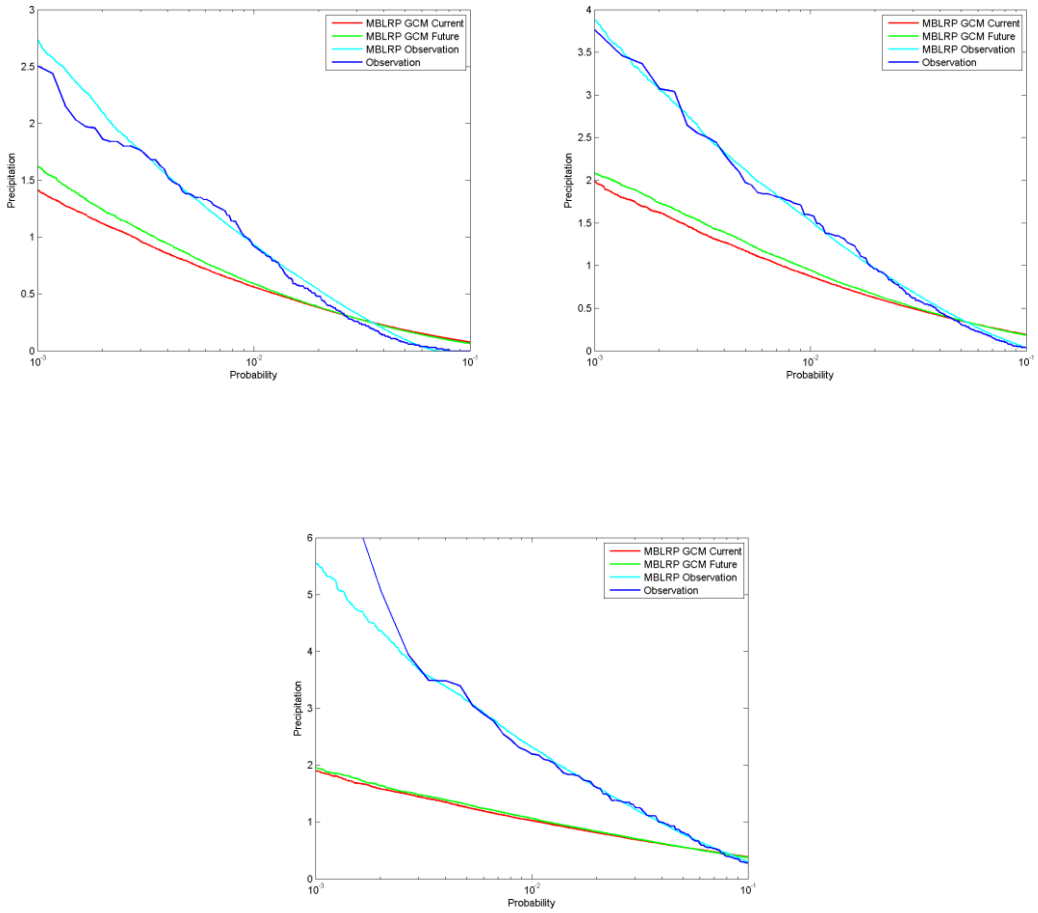

Duration curves of COOP: 418996 rainfall station for different accumulation levels' precipitation. From the top to bottom and left to right, 6-, 12-, and 24-hour levels.

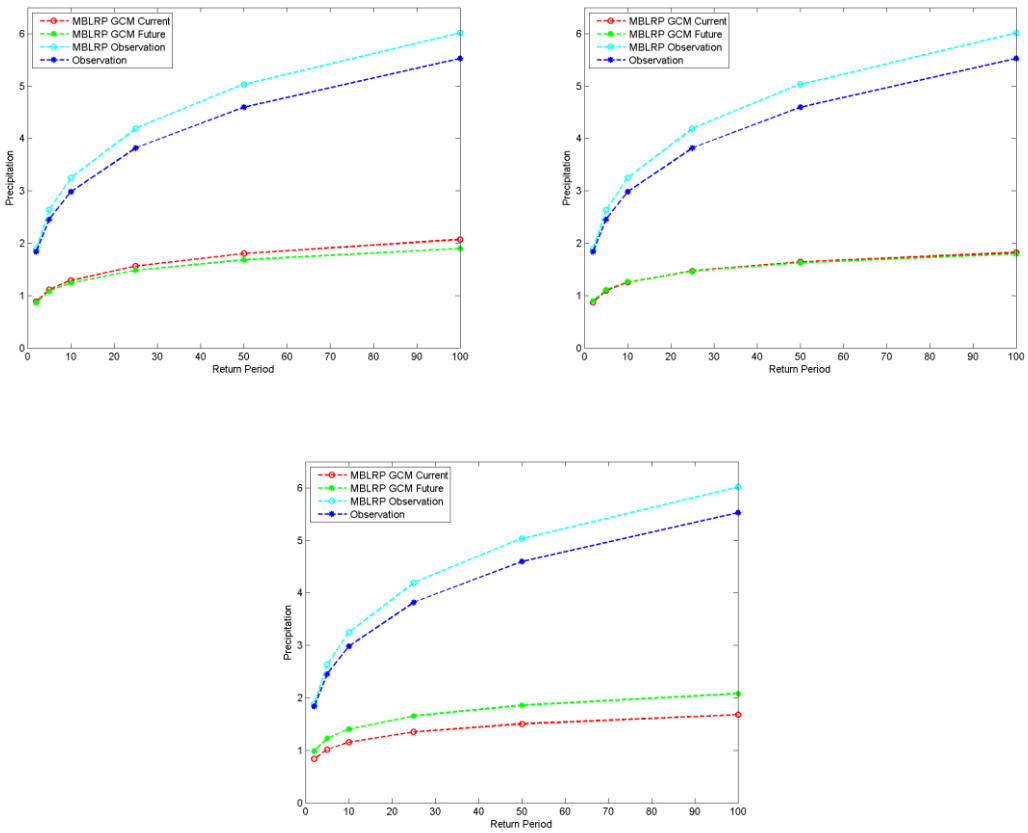

Annual hourly extreme precipitation for the return periods of 2-, 5-, 10-, 25-, 50-, and 100-years of Rainfall station 417594. From left to right, top to bottom, gfdl-cm 3.1 model, miroc-esm.1 model, and miroc-esm-chem.1 model.

APPENDIX C. USER INTERFACE OF MBLRP SIMULATOR

A user interface was developed in MATLAB code that allows users to generate a stochastic precipitation time series using the MBLRP method.

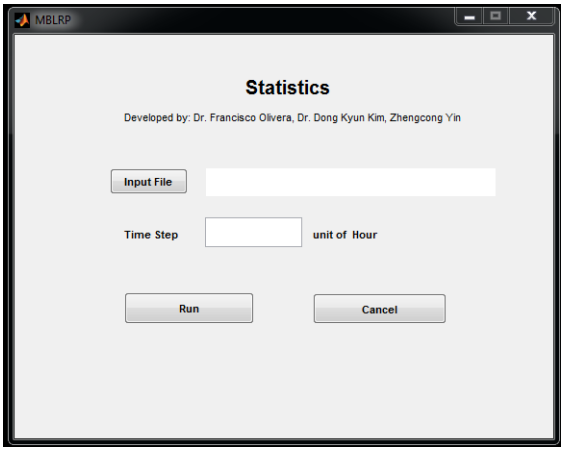

This interface allows users to calculate the statistics of a precipitation time series with a certain accumulation level. The input file must contain a precipitation time series. Users could input the expect accumulation level in the unit of hour to specify a certain accumulation level for the statistics. The output results are the mean, variance, probability of zero, and lag-1 autocorrelation coefficient of the input precipitation time series at a certain accumulation level specified by the user. By clicking “Run”, the statistics of the input precipitation time series for the expected accumulation level will be calculated and save as an Excel file at the same path as the input file.

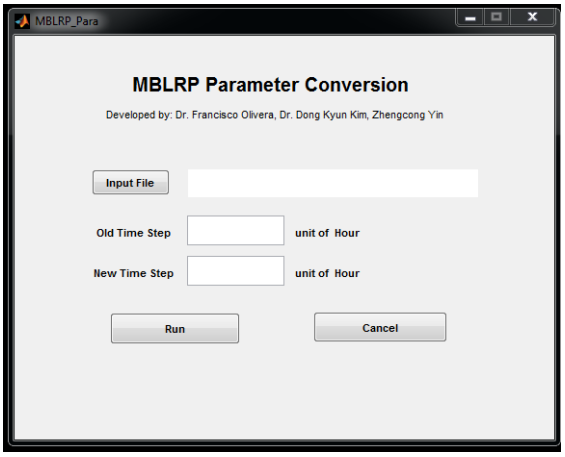

This user interface allows users to convert the MBLRP parameters to a certain accumulation level. In order to generate the stochastic precipitation time series at another accumulation level using the MBLRP method, the parameters need to be convert to the expected accumulation level. The "Input File" button allows users to input the parameters λ, ν, α, μ, ϕ, and κ. The old time step should equal the accumulation level of the input parameters. The new time step should equal the expected accumulation level. By clicking "Run", the parameters for the expected accumulation level will be calculated and saved as an Excel file at the same path as the input file.

This user interface allows users to generate a stochastic precipitation time series using the MBLRP model. With the "Input File" button, users can specify the file that contains a matrix of parameters required by the MBLRP model. In this matrix of parameters, each low represents a certain month. Each low contains six parameters in the following sequence: λ, ν, α, μ, ϕ, and κ. Time step allows users to set an accumulation level in the unit of hour for the output time series. By clicking "Run", the mean, variance, probability of zero, and lag-1 autocorrelation coefficient of the stochastic precipitation will be generated and saved as an Excel file at the same path as the input file. By default, the length of time series is 200 years. With this length, the statistics of the MLBRP precipitation have a good match with the observed precipitation.